

IN 321
146445

JPL Publication 88-12

MSAT-X Report 148

107 p

MSAT-X: A Technical Introduction and Status Report

Khaled Dessouky
Miles Sue

(NASA-CR-182921) MSAT-X: A TECHNICAL
INTRODUCTION AND STATUS REPORT (Jet
Propulsion Lab.) 107 p

N88-23933

CSCI 17B

Unclas
G3/32 0146445

April 15, 1988



National Aeronautics and
Space Administration

Jet Propulsion Laboratory
California Institute of Technology
Pasadena, California

1. Report No. 88-12	2. Government Accession No.	3. Recipient's Catalog No.	
4. Title and Subtitle MSAT-X: A Technical Introduction and Status Report		5. Report Date April 15, 1988	
		6. Performing Organization Code	
7. Author(s) Khaled Dessouky and Miles Sue		8. Performing Organization Report No.	
9. Performing Organization Name and Address JET PROPULSION LABORATORY California Institute of Technology 4800 Oak Grove Drive Pasadena, California 91109		10. Work Unit No.	
		11. Contract or Grant No. NAS7-918	
12. Sponsoring Agency Name and Address NATIONAL AERONAUTICS AND SPACE ADMINISTRATION Washington, D.C. 20546		13. Type of Report and Period Covered External Report JPL Publication	
		14. Sponsoring Agency Code RE4 BP 650-60-15-01-00	
15. Supplementary Notes			
16. Abstract NASA initiated the Mobile Satellite Experiment (MSAT-X) program at the Jet Propulsion Laboratory (JPL) to accelerate the introduction of a U.S. commercial Mobile Satellite System (MSS). Through MSAT-X, the identification, development, and demonstration of critical, high-risk MSS technologies have been performed. This document is intended as a technical introduction and status report for MSAT-X. It first introduces the concepts of an MSS and its unique challenges. It then delineates MSAT-X's role and objectives and subsequently focuses on its achievements. After outlining the MSS design philosophy adopted, it presents and analyzes the MSAT-X results and casts them in the broader context of an MSS. The current phase of MSAT-X has focused notably on the ground segment of MSS. The accomplishments in the four critical technology areas of vehicle antennas, modem and mobile terminal design, speech coding, and networking are presented. A concise evolutionary trace is incorporated in each area to elucidate the rationale leading to the current design choices. The findings in the area of propagation channel modeling are also summarized and their impact on system design discussed. To facilitate the assessment of the MSAT-X results, technology and subsystem recommendations are also included and integrated with a quantitative first-generation MSS design.			
17. Key Words (Selected by Author(s)) Communications; Electronics and Electrical Engineering		18. Distribution Statement Unclassified; unlimited	
19. Security Classif. (of this report) Unclassified	20. Security Classif. (of this page) Unclassified	21. No. of Pages	22. Price

MSAT-X: A Technical Introduction and Status Report

Khaled Dessouky
Miles Sue

April 15, 1988



National Aeronautics and
Space Administration

Jet Propulsion Laboratory
California Institute of Technology
Pasadena, California

The research described in this publication was carried out by the Jet Propulsion Laboratory, California Institute of Technology, under a contract with the National Aeronautics and Space Administration.

Reference herein to any specific commercial product, process, or service by trade name, trademark, manufacturer, or otherwise, does not constitute or imply its endorsement by the United States Government or the Jet Propulsion Laboratory, California Institute of Technology.

ABSTRACT

NASA initiated the Mobile Satellite Experiment (MSAT-X) program at the Jet Propulsion Laboratory (JPL) to accelerate the introduction of a U.S. commercial Mobile Satellite System (MSS). Through MSAT-X, the identification, development, and demonstration of critical, high-risk MSS technologies have been performed.

This document is intended as a technical introduction and status report for MSAT-X. It first introduces the concepts of an MSS and its unique challenges. It then delineates MSAT-X's role and objectives and subsequently focuses on its achievements. After outlining the MSS design philosophy adopted, it presents and analyzes the MSAT-X results and casts them in the broader context of an MSS.

The current phase of MSAT-X has focused notably on the ground segment of MSS. The accomplishments in the four critical technology areas of vehicle antennas, modem and mobile terminal design, speech coding, and networking are presented. A concise evolutionary trace is incorporated in each area to elucidate the rationale leading to the current design choices. The findings in the area of propagation channel modeling are also summarized and their impact on system design discussed.

To facilitate the assessment of the MSAT-X results, technology and subsystem recommendations are also included and integrated with a quantitative first-generation MSS design.

ACKNOWLEDGMENT

The work presented in this report is the result of the effort of many individuals involved in MSAT-X, both at JPL's and contractors' facilities. Without their dedication the progress reported would not have been possible. It is through the generous assistance of many colleagues on the MSAT-X team that this report itself has been made feasible. The authors would like to thank Dave Bell, Jeff Berner, Faramaz Davarian, Richard Emerson, Dariush Divsalar, John Huang, Vahraz Jamnejad, Tom Jedrey, Jim Parkyn, Ramin Sadr, Charles Wang, Robin Winkelstein, Ken Woo, and Tsun-Yee Yan, all at JPL.

Special thanks go to William Rafferty, who fostered the concept of an MSAT-X document and vigorously supported this effort. The many fruitful discussions the authors had with him have enhanced the presentation in this report.

CONTENTS

1.	INTRODUCTION	1-1
2.	MSS CONCEPT	2-1
3.	MSS SCARCE RESOURCES	3-1
3.1	EIRP	3-1
3.2	SPECTRUM	3-1
3.3	GEOSYNCHRONOUS ORBIT	3-2
4.	NASA'S APPROACH TO OVERCOMING MSS SCARCE RESOURCES	4-1
4.1	NASA'S CONCEPTUAL MSS DESIGN PHILOSOPHY	4-1
4.2	MSS SPACE SEGMENT EVOLUTION	4-3
4.3	MSAT-X, ITS OBJECTIVES, AND ITS RELATIONSHIP TO INDUSTRY	4-4
5.	TECHNOLOGY AREAS RESEARCHED UNDER MSAT-X	5-1
5.1	VEHICLE ANTENNAS	5-1
5.1.1	Challenging Objectives	5-1
5.1.2	Antenna Design Considerations	5-1
5.1.3	Salient Vehicle Antenna Requirements	5-4
5.1.4	Vehicle Antenna Designs	5-5
5.1.4.1	Mechanically Steered, Tilted Linear Array	5-5
5.1.4.2	Electronically Steered Phased Array Antenna	5-8
5.1.4.3	Planar Mechanically Steered Array	5-12
5.2	MODULATION, CODING, AND MOBILE TERMINAL DESIGN	5-12
5.2.1	Modulation/Coding	5-12
5.2.1.1	Minimum Shift Keying (MSK) and Gaussian MSK (GMSK)	5-13
5.2.1.2	Trellis-Coded Modulation/8-Phase Shift Keying (TCM/8PSK)	5-14
5.2.2	Mobile Terminal Design	5-18

5.3	SPEECH CODING	5-19
5.3.1	Background	5-20
5.3.2	Speech Compression Techniques Developed for MSAT-X . .	5-22
5.3.2.1	LPC-Based Compression Techniques	5-22
5.3.2.2	Speech Coding Techniques Developed at UCSB . .	5-23
5.3.2.3	Speech Coding Technique Developed by GIT . . .	5-24
5.4	NETWORKING	5-25
5.4.1	Perspective	5-25
5.4.2	I-AMAP	5-26
5.4.2.1	Channel Partitioning	5-27
5.4.2.2	Error Control, Packet Replication, and Packet Size	5-27
5.4.2.3	Request Channel Simulator	5-28
5.5	MOBILE SATELLITE CHANNEL MODELING	5-29
6.	RESULTS OF MSAT-X: RECOMMENDED TECHNOLOGY UTILIZATION FOR MSS . .	6-1
6.1	INTRODUCTION	6-1
6.2	BASIC MSS ARCHITECTURE	6-1
6.3	ON THE SPACE SEGMENT TO COMPLEMENT MSAT-X	6-3
6.4	TECHNOLOGY RECOMMENDATIONS FOR MSS	6-4
6.4.1	Mobile Terminal Technologies	6-5
6.4.1.1	Mobile Terminal Architecture	6-5
6.4.1.2	Speech Coding	6-6
6.4.1.3	Modulation/Coding	6-8
6.4.1.4	Transceiver Capabilities	6-9
6.4.1.5	Vehicle Antennas	6-10
6.4.2	Link Budgets	6-13
6.4.3	System Capacity	6-14
7.	REFERENCES	7-1

Tables

3.2.1	WARC 1987 Frequency Spectrum Allocations for Mobile Services	3-3
5.1.1	Estimated Cost Breakdown and Per Unit Cost for the MSAT-X Phased Array Mobile Antennas	5-32
5.1.2	Salient Characteristics of MGA Breadboards	5-33
6.4.1	Comparison of the Performances of TCM/D8PSK, DQPSK, and Differential GMSK (DGMSK) Under Typical MSS Link Conditions	6-16
6.4.2	Forward (Ground-to-Mobile) Link Budget for BER = 1×10^{-3}	6-17
6.4.3	Return (Mobile-to-Ground) Link Budget for BER = 1×10^{-3}	6-18

Figures

2.1	Mobile Satellite Network Concept	2-2
3.2.1	Frequency Spectrum Allocations by the FCC for Mobile Services	3-4
4.2.1	Example of Evolution of Multibeam Coverage	4-6
4.3.1	Areas of Concentration for MSAT-X Technology Development	4-6
5.1.1	A Typical Radiation Pattern Demonstrating the Adjacent Satellite Isolation Achievable by a Low-Gain Antenna	5-34
5.1.2	A Typical Radiation Pattern Demonstrating the Adjacent Satellite Isolation Achievable by a Medium-Gain Antenna With Taper	5-34
5.1.3	Mechanically Steered Linear Array Antenna Assembly	5-35
5.1.4	Schematic of Vehicle Antenna Pointing System Based on Single-Channel Monopulse Tracking	5-36
5.1.5	Elevation Pattern of Mechanically Steered Antenna	5-37

Figures (Contd)

5.1.6	Azimuth Pattern for Mechanically Steered Linear Array Antenna	5-38
5.1.7	Cross-Sectional View of the Phased Array Antenna	5-38
5.1.8	Triangular Lattice Pattern of Phased Array Antennas	5-39
5.1.9	Stacked Dual Resonant Microstrip Element Developed by Ball Aerospace Corporation	5-39
5.1.10	Stripline-Fed Crossed-Slot Radiator Developed by Teledyne Ryan Electronics	5-40
5.1.11	Typical Elevation Radiation Pattern of TRE Phased Array Antenna	5-41
5.1.12	Typical Elevation Pattern Showing Axial Ratios for TRE Phased Array Antenna	5-41
5.1.13	Typical Azimuth Radiation Pattern of TRE Phased Array Antenna	5-42
5.1.14	Typical Azimuth Pattern Showing Axial Ratios for TRE Phased Array Antenna	5-42
5.2.1	A Worst-Case Interference Scenario in MSS	5-43
5.2.2	Adjacent Channel Interference for GMSK	5-44
5.2.3	System Block Diagram for Coherent TCM/8PSK	5-45
5.2.4	Performance of Rate 2/3, 16-State Trellis- Coded 8PSK Modulation (TCM/8PSK) Over Rician Fading Channel With CSI (Ideal Coherent Detection) and Interleaving	5-46
5.2.5	Two Versions of the Tone Calibrated Technique (TCT): (a) TCT Spectrum With Single Tone (b) DTCT Spectrum	5-46 5-46
5.2.6	Block Diagram of Trellis-Coded MDPSK System	5-47
5.2.7	Simulation Results for Bit Error Rate Performance of Rate 2/3, 16-State Trellis- Coded 8DPSK (TCM/D8PSK)	5-48
5.2.8	Comparison of TCM/D8PSK With Coherent TCM/8PSK (Using DTCT With Noisy Pilot) at UHF and L-Band	5-48

Figures (Contd)

5.2.9	Eye Diagram of Root Raised-Cosine Pulse Shaping With 100% Excess Bandwidth	5-49
5.2.10	Mobile Terminal Block Diagram	5-49
5.3.1	Model of LPC Speech Coders	5-50
5.3.2	VAPC Functional Block Diagram	5-50
5.3.3	Block Diagram of VXC Speech Coder	5-51
5.3.4	LSP Quantization System Concept Developed by GIT for the SEV	5-51
5.4.1	An Illustration of Channel Partitioning at Two Instants of Time: (a) This Partition Supports 25 Voice Calls per Minute and 3600 Data Messages per Minute (b) This Partition Supports 4 Voice Calls per Minute and 6600 Messages per Minute	5-52 5-52
5.4.2	Number of Request Channels (N_r) and Data Channels (N_d) Versus Data Message Arrival Rate	5-52
5.4.3	Number of Voice Channels (N_v) and Total Number of Channels (N) Versus Message Arrival Rate (Ω_d)	5-53
5.4.4	Average End-to-End Delay Versus Packet Size When Arrival Rate = 65 Messages/s	5-54
5.4.5	Average End-to-End Delay Versus Closed-End Traffic for Various Packet Sizes (Total Message Length = 4096 bits)	5-54
5.4.6	Block Diagram of the Simulator for the Request Channel of MSAT-X	5-55
5.5.1	Cumulative Signal Level Distributions for Various Geographic Locations and Elevation Angles	5-56
5.5.2	Predicted Peak-to-Peak Power Variation as a Function of Channel Bandwidth	5-57
6.3.1	Multibeam Coverage of CONUS by First- Generation MSS Satellite	6-19

SECTION 1.

INTRODUCTION

This document is intended as a technical introduction and status report for the Mobile Satellite Experiment (MSAT-X). It introduces the reader to the Mobile Satellite System (MSS) concept, introduces MSAT-X and identifies its role, briefly presents the accomplishments of MSAT-X, and reports on the results and their impact on future mobile satellite systems.

These goals are achieved in this document through the performance of four tasks. First, the concepts of an MSS are introduced. Second, after the unique challenges of such a system are identified, NASA's approach to overcoming these challenges is presented, and thereupon the MSAT-X effort is placed in the proper perspective. Third, the different components of the MSAT-X effort undertaken under the leadership of the Jet Propulsion Laboratory (JPL) are presented. This then sets the stage for performing the fourth and final task of assessing the system concepts and technology developed in a first-generation MSS context. Recommendations derived from that assessment highlight the contributions of NASA and JPL to achieving the goal of bringing about an early realization of a technically sound and economically viable MSS. This is the ultimate goal of MSAT-X and, more generally, of NASA's communications program, which aims to preserve the U.S.'s leadership in space communications.

Because of the high-level nature of this document, the emphasis in the presentation is not on fine detail--rather, the intent is to reveal as many as possible of the technical issues in MSAT-X, report the salient results, and identify their impact on MSS. In a parallel effort, a more detailed and technically exact document is currently being prepared. Many of the significant points that are not addressed here are addressed in that document, which is referred to in the text as SYSDOC [Jet Propulsion Laboratory, in preparation]. Further information can be found also in the many references cited in the present document. It is worth noting that in choosing the references, the emphasis has been on those articles that provide the reader with overviews of the technical issues addressed. These sources, in turn, provide more references that guide the specialist to the fully detailed technical information.

This section is followed by the introduction of the MSS concept in Section 2. Section 3 contains a clear identification of the challenges that have to be conquered before an MSS becomes a reality. These challenges are to overcome the scarce resources peculiar to the difficult environment in which the MSS will operate. Section 4 then explains NASA's approach to overcoming these challenges, and from there introduces NASA's MSAT-X program, its objectives, and the premise and philosophy upon which it is based. Section 4 also points out the relationship between MSAT-X and the MSS industry, embodied at present in the consortium of MSS applicants. This perspective is needed for the proper appreciation of the implications of Sections 5 and 6. Section 5 contains five subsections, each introducing one of the MSS ground segment technology areas researched under MSAT-X. This sets the stage for Section 6, which draws upon the results described in Section 5 to present JPL's recommendations for MSS ground segment technology utilization. The recommendations are directed not only at each technology area, but also at creating a cohesive effective ground segment. Inasmuch as the ground segment is a part of an overall MSS system architecture, consideration of the space segment and overall system issues is necessary. Realistic space segment assumptions are made, and the ground segment is quantitatively tied to the space segment through link budgets and system capacity results.

SECTION 2

MSS CONCEPT

An MSS is a satellite-based communication network that provides voice and data communications to mobile users over a vast geographical area. The relay satellite, or satellites, in geosynchronous orbit at a height of 22,000 miles permits an extremely large coverage array. The type of service provided augments, and complements, the land mobile or cellular terrestrial systems, which are generally more economical in localized urban areas.

A variety of services have been proposed for MSS by its potential commercial operators. The services envisioned include two-way voice, two-way interactive data communication, and one-way data as in dispatch operations, position determination, or data base query.

The MSS network concept is depicted in Figure 2.1. At the heart of the system is the Network Management Center (NMC). It performs such functions as answering requests for channel assignment, setting up call routes, billing, and generally overseeing the network's operation. Other entities on the ground include the gateways and base stations. The gateways are terminals that provide an interface between the MSS and other networks such as the Public Switched Telephone Networks (PSTN). The base stations are not necessarily connected to other networks and are normally centers for dispatch operations.

The two other key elements in MSS are the mobile terminal and the satellite. The mobile unit operates in a hostile environment where multipath from terrain exists together with shadowing from trees or obstacles. A minimum mobile terminal consists of the radio, antenna, and user interface (as will be explained later). This equipment is constrained to being low in cost and small in size; both are necessary features if the system is to have the wide customer acceptance needed for its economic viability. The satellite, on the other hand, by its dedicated design, is limited by the feasible technology and evolves in steps or generations. As new technology becomes available, and the spacecraft evolves accordingly, the spacecraft becomes capable of supporting an MSS network with growing needs.

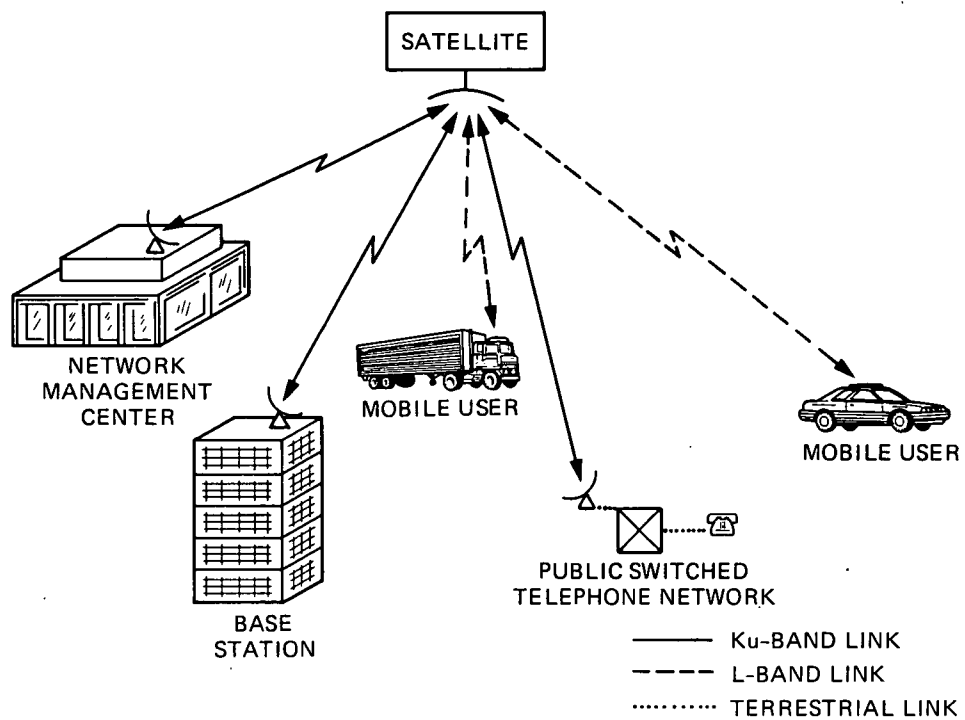


Figure 2.1. Mobile Satellite Network Concept

SECTION 3

MSS SCARCE RESOURCES

A number of studies undertaken by NASA have revealed that a growing MSS will have to overcome scarcity in three critical areas, viz., spacecraft EIRP, spectrum, and orbital slots. Although this is not unique to MSS, some of the problems and solutions are unique because of the specific nature of MSS.

3.1 EIRP

A critical MSS communications link is the forward link between the satellite and the mobile terminal. The small, possibly unsteered mobile antenna on the vehicle has relatively low directivity and can be susceptible to multipath. In addition, shadowing by trees and other obstructions can severely attenuate the signal. Hence, the space segment will have to make up part of the deficiencies in the link power budget by transmitting higher EIRP.

A mobile satellite system generally favors a single-channel-per-carrier (SCPC) architecture. As will be explained in Section 4.1, frequency division multiple access (FDMA) is the multi-access scheme of choice under the severe spectrum limitations described below and the requirement for simple mobile terminals operating in a hostile fading environment. This, coupled with the large geographical distances between the users, leads to an SCPC design. The SCPC operation exacerbates the spacecraft-transmitted radio frequency (RF) power problem. To limit intermodulation distortion in the spacecraft transmitter, the high-power amplifier will have to operate in the linear region at a reduced efficiency. For a fully operational MSS with thousands of users, the power requirement on the spacecraft would be very large. Thus, it is of great importance to devise power-efficient technologies to minimize the power-per-channel requirement in the MSS.

3.2 SPECTRUM

The potential frequency spectrum available for the MSS in the U.S. is severely limited. The Federal Communications Commission (FCC) has allocated the frequency spectrum shown in Figure 3.2.1 to a combination of

mobile satellite services. MSS will operate as co-primary with the Aeronautical Mobile Satellite Service (AMSS-R) in the bands 1549.5 - 1558.5 and 1651 - 1660 MHz, and as secondary to the aeronautical mobile satellite service in the bands 1545 - 1549.5 and 1646.5 - 1651 MHz. On the international level, the frequency assignment issue was recently addressed by the 1987 World Radio Administrative Conference (WARC). The allocations are shown in Table 3.2.1. Although the United States and Canada took reservations on the WARC provisions, it appears that, on the international level, the spectrum allocation for MSS will be even more restrictive than within North America. It is therefore evident that efficient utilization of the limited available spectrum, within the constraints placed by the other scarce resources, is paramount.

3.3 GEOSYNCHRONOUS ORBIT

Due to the requirement that the mobile antenna be small and relatively inexpensive, high directivity, comparable to fixed satellite systems, is not possible. An omni antenna would illuminate the entire geosynchronous arc over the contiguous United States (CONUS). This, unless spread spectrum is used, would preclude the possibility of employing orbit reuse (using more than one satellite operating in the same frequency band to increase system capacity). For either low- or medium-gain antennas, antennas that rely only on low axial ratios to provide polarization isolation as a primary means of orbit reuse are not possible. Hence, pattern discrimination and polarization isolation are needed to permit orbit reuse. One of the design goals for a medium-gain antenna would then be to provide sufficient inter-satellite isolation for multiple satellite operation. The inherent directivity creates a challenging design problem to meet the required tracking of the satellite while the vehicle moves.

Table 3.2.1. WARC 1987 Frequency Spectrum Allocations for Mobile Services

Downlink (MHz)	Allocation
1530 - 1533	Coequal primary MSS and maritime mobile satellite services (MMSS)
1533 - 1544	MSS secondary to MMSS (limited to nonspeech low-bit-rate data)
1545 - 1555	Aircraft-to-ground mobile telephone with restrictions
1555 - 1559	<u>Exclusive</u> primary MSS
Uplink (MHz)	Allocation
1626.5 - 1631.5	MSS secondary to MMSS
1631.5 - 1634.5	Coequal primary MSS and MMSS
1634.5 - 1645.5	MSS secondary to MMSS
1646.5 - 1656.5	Ground-to-aircraft mobile telephone with restrictions
1656.5 - 1660.0	<u>Exclusive</u> primary MSS
1660.0 - 1660.5	MSS coequal primary with radio astronomy

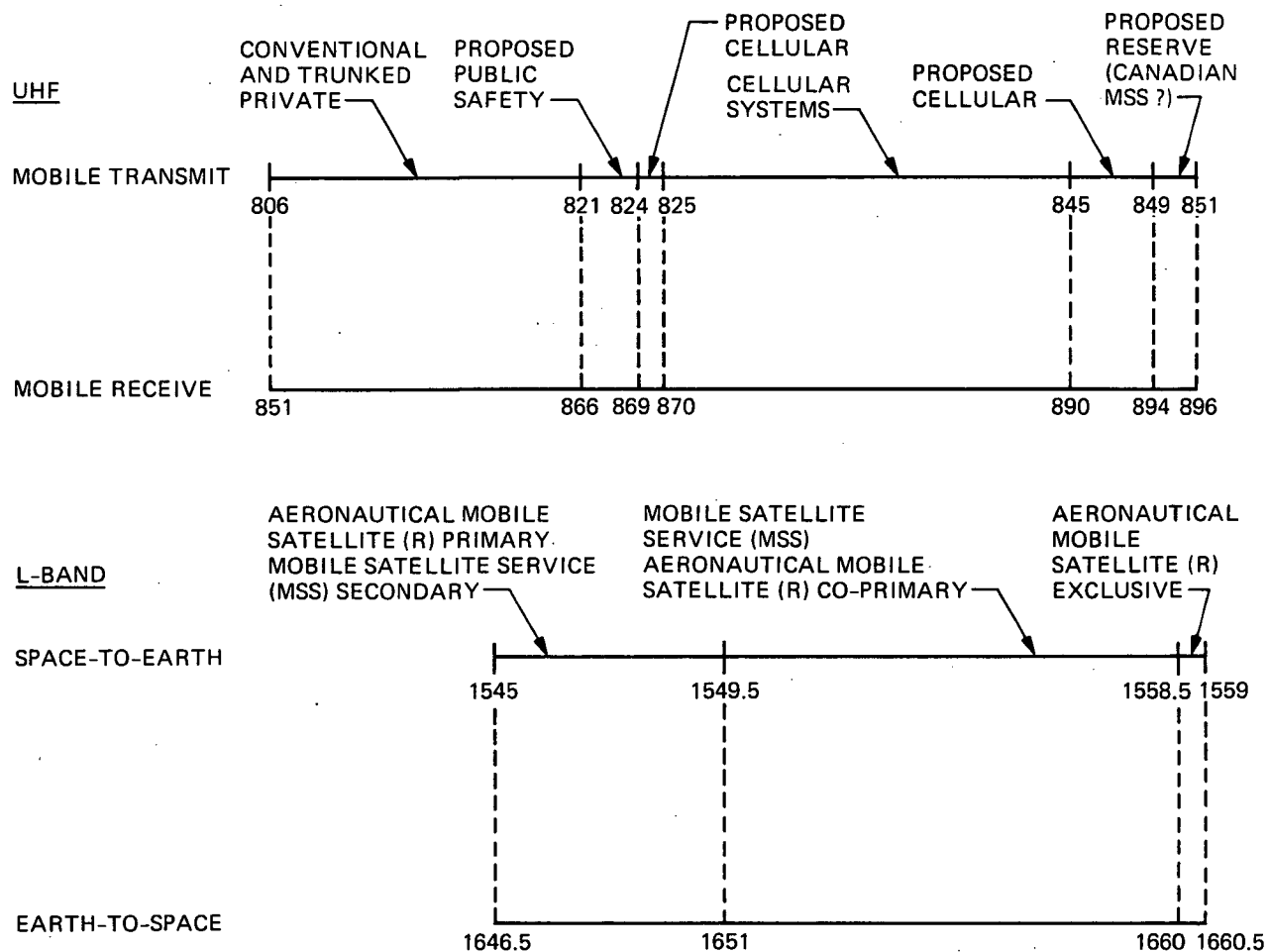


Figure 3.2.1. Frequency Spectrum Allocations by the FCC for Mobile Services

SECTION 4

NASA'S APPROACH TO OVERCOMING MSS SCARCE RESOURCES

Since the 1970s, the U.S.'s national policy, as evidenced by presidential directives such as PD42, has aimed at bolstering the role played by NASA in the field of satellite communications. In response, NASA's communications program has been directed at maintaining the U.S.'s position in the increasingly competitive satellite communication market. In this spirit, NASA launched the MSAT-X program to support the U.S. industry in developing new concepts and the high-risk technologies that would enable the realization of a commercial MSS.

Since the MSS can be conveniently divided into a space segment and a ground segment, NASA structured different program phases to develop the two segments. It was also clear that the ground segment requirements would have a significant impact on all aspects of the MSS. Consequently, the ground segment has received the greatest amount of research and development to date. The development strategy reflected a broad conceptual MSS design philosophy that NASA had formulated in the early eighties. This design philosophy influenced the ensuing development through implicit assumptions about how an efficient MSS could be put together to overcome its scarce resources. The envisioned system concept will be explained in the next subsection. This is followed by two subsections to outline the roles of the space and ground segments, and their development effort, in the overall MSS picture.

4.1 NASA'S CONCEPTUAL MSS DESIGN PHILOSOPHY

In this document, "system design philosophy" means the broad approach to creating an MSS concept that overcomes the scarce resources of bandwidth, power, and orbit. The system concept envisioned by NASA is based on an FDMA scheme combined with bent-pipe spacecraft that utilize multibeam technology to effect frequency reuse. The FDMA efficiently packs as many channels as possible in the limited spectrum of Figure 3.2.1, or any given part thereof (consistent with the isolation requirements of the multibeam scenario). Since, even with efficient modulation and speech representation, the ratio of the overall available bandwidth to a single channel bandwidth is

too small to support the number of users expected in a full system, frequency reuse is essential to complement the FDMA scheme.

The choice of FDMA and frequency reuse through satellite multibeam technology evolved from JPL in-house and NASA-contractor studies that evaluated a variety of preliminary MSS concepts and foreseen market trends, demands, and requirements [Naderi, 1982; TRW, 1983; and General Electric Corporation, 1983]. The merits of such a choice may not be immediately obvious when compared with other alternative concepts based on code division multiple access (CDMA) or time division multiple access (TDMA). There are, however, strong arguments to be made against those alternate choices, particularly under the circumstances that have been associated with the evolution of MSS throughout the eighties (such as the regulatory climate).

A CDMA system would, firstly, be hampered by the limited bandwidth available. Its key design parameters and performance relate directly to the spreading (contiguous) bandwidth available. Thus, in an uncertain regulatory climate, with the possibility of being allowed less than the expected bandwidth, predicted CDMA performance would be questionable. Although adding users to the CDMA system would be possible within a certain ceiling, it is contended that CDMA is not as flexible as FDMA in accommodating unexpected growth in the future. This is because of the high impact of the CDMA parameters on the user equipment. For example, a change in the basic spreading parameters may be unfeasible because of the need to upgrade the user terminals.

The above factors have steered NASA away from CDMA. Nevertheless, discounting CDMA completely as a basis for a network architecture should be based on a thorough system trade-off study.

TDMA is arguably a less desirable choice. First, TDMA is not well-suited to the low burst rates envisioned for MSS user terminals. If MSS were configured for high burst rates, this would lead to high peak power requirements and most likely to more expensive terminal hardware--a strong drawback. Low burst rates, on the other hand, require long frames and lead to long delays. Equally important, in a fading and shadowing environment, TDMA

would be vulnerable to frequent loss of synchronization. Moreover, the higher bit rates of TDMA would create even more demanding synchronization requirements, with resulting network and user terminal complications.

Although the technology developed for MSS is strongly influenced by the FDMA/multibeam scheme, critical technologies such as vehicle antennas and speech coding are largely independent, and essential in any conceivable MSS architecture. It should also be kept in mind that NASA's goal has been to assist the industry in developing new concepts and high-risk technologies rather than in actually implementing a specific system. This philosophy has been reflected in NASA's efforts, as will become clearer in the following two subsections.

4.2 MSS SPACE SEGMENT EVOLUTION

As outlined above, the MSS envisioned by NASA relies on multibeam spacecraft technology. The reliance, however, is in response to the potential need to expand the capacity of future systems. Hence, it allows for the time necessary to develop generations of more advanced spacecraft multibeam antennas. As larger spacecraft antennas with more beams become available, an MSS network with increasing capacity can be supported.

A first-generation MSS spacecraft would be based on the current technology of communication satellites. Such a first-generation satellite would probably have an antenna diameter of less than 5 meters. This would allow launch via the space shuttle without the need for new, high-risk deployable antenna technology. Such an antenna would only have a limited multibeam capacity. Later-generation satellites would have larger antenna diameters and a considerably higher multibeam capacity. These antennas would be large enough to resolve the EIRP problem, and have enough beams to enable sufficient frequency reuse to resolve the bandwidth problem. A schematic illustration giving an example for the evolution of the multibeam coverage is given in Figure 4.2.1.

Early studies have been performed to investigate the feasibility of the MSS using multibeam technology. Unfortunately, the studies were performed for an MSS using UHF rather than L-band, as now is the case. These early

results have been presented in [Naderi, 1982] and later in [Sue et al., 1985]. Because the MSS concept has evolved since those early days, the numbers quoted are no longer relevant, but the analysis serves to illustrate the scope of the problem. The sizes of the antennas would be smaller at L-band and consequently easier to build, at least from a structural standpoint.

A fair amount of work under the guidance of NASA and JPL has already been accomplished in the area of large antennas. A summary of these activities is given in [Naderi et al., 1984], together with the appropriate references. Looking towards the future, a later-generation antenna will probably be a large, flexible, and asymmetric structure posing challenging problems to control system designers. NASA, with its Space Station capability, will have a unique facility to experiment with the assembly of large structures in space.

4.3 MSAT-X, ITS OBJECTIVES, AND ITS RELATIONSHIP TO INDUSTRY

The mobile satellite experiment (MSAT-X) is the framework within which NASA has been developing critical ground segment technologies, and it has been organized as a research and development task at JPL. Its present goals are the development and demonstration of advanced ground segment technologies for first-generation mobile satellite systems, the objective being the acceleration of the implementation of MSS through timely infusion to the industry of critical high-risk technologies. The ground segment technologies all aim at overcoming the scarce resources of power, bandwidth, and orbit. Figure 4.3.1 depicts the technology areas related to the resolution of the scarcity of each of the three resources. Validation of the developed technology by a set of experiments is also a goal for MSAT-X. In addition to validating the newly developed equipment, these tests will aid NASA's and JPL's effort to assist government agencies in determining the usefulness of MSS services to their mobile operations.

Since the MSAT-X task has been defined as a technology development task (as opposed to the development of a specific end-to-end network), system requirements have basically taken the form of requirements for the individual technology development areas. Of course, the different requirements reflect a

consistent end-to-end definition that utilizes FDMA/multibeam spacecraft architecture. Yet, because the detailed network architecture in an operational MSS of the future depends on the networking philosophy of the network operator, the requirements at this stage have been maintained as requirements for the technology areas, each contributing its share to the overall efficiency and viability of the overall system.

The FCC has determined that only one MSS is feasible for the first generation of mobile satellite service. This is a reflection of the scarcity of resources that a successful MSS has to conquer and the present state-of-the-art in mobile communications. As a result of the FCC's ruling, a single U.S. consortium (the American Mobile Satellite Consortium [AMSC]) has been formed of all MSS industry applicants. At present there are eight members in the consortium. The members have differing opinions on a variety of technical issues pertaining to the MSS architecture. These views reflect differing technical opinions or business orientations. Differences notwithstanding, the members will have to agree on a single system architecture. That architecture may then contain a variety of technically feasible options whose ultimate viability will probably depend on market forces and technology maturity.

One of MSAT-X's goals is to make available the system concepts and technology needed to steer the consortium towards making the decisions that, it is hoped, will ultimately lead to early realization of the most viable MSS. JPL, as an arm of NASA, an impartial government agency, and as a leading technology research center, is in a unique position to assume this responsibility. Through concrete and demonstrated results of MSAT-X, this positive and highly visible role of NASA/JPL should be a major factor in achieving the ultimate goal of maintaining the U.S.'s leadership in space communications.

Concrete and demonstrated results rest on calculated, executed, and disseminated work. The following sections will attempt to provide a concise presentation of this work. It should be kept in mind that the presentation is mainly concerned with the MSAT-X effort; it will not deal with decisions made within the consortium so far.

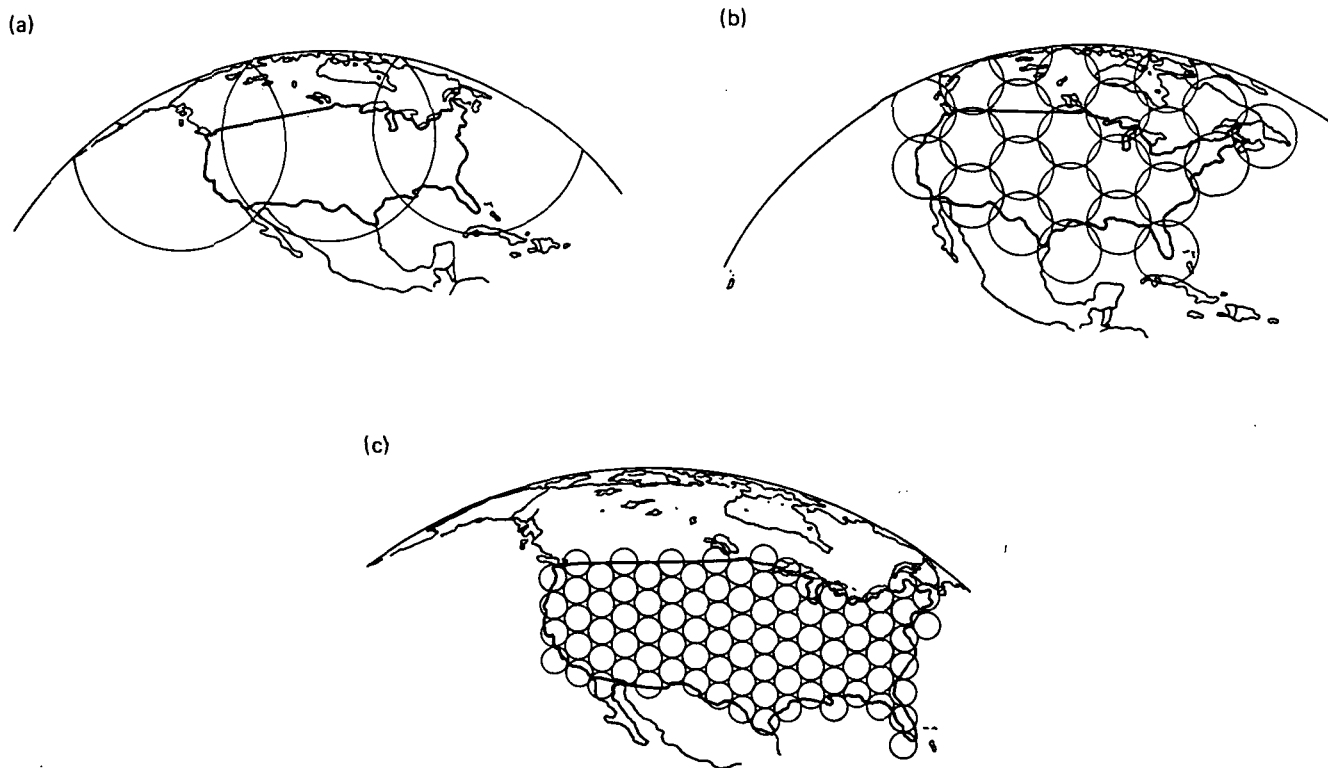


Figure 4.2.1. Example of Evolution of Multibeam Coverage

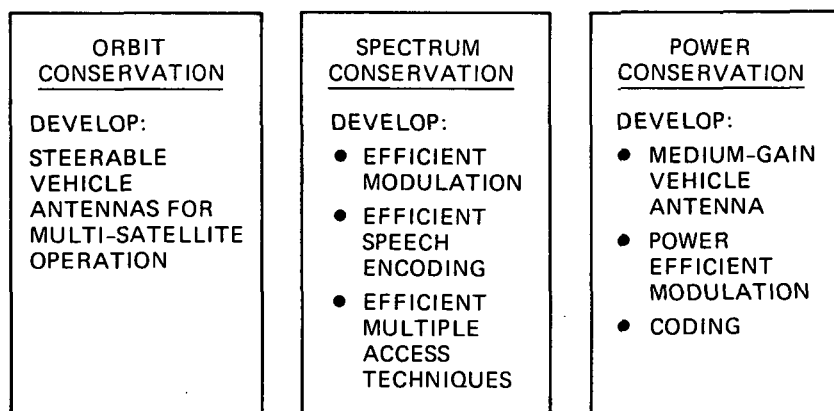


Figure 4.3.1. Areas of Concentration for MSAT-X Technology Development

SECTION 5

TECHNOLOGY AREAS RESEARCHED UNDER MSAT-X

In the following sections the different research performed and technologies developed under MSAT-X are described. The design principles, salient characteristics, and performances obtained are presented for each technology area. It is not the purpose here to be exact--rather, the intent is to give a presentation that touches on the different technical issues, which relate to the reader the work undertaken within MSAT-X, and which form the background needed for MSS system-level decision making. (A more complete presentation is given in [SYSDOC].) The results reported here (in Section 5) are considered and compared from a broader MSS system-level point of view in Section 6.

5.1 VEHICLE ANTENNAS

5.1.1 Challenging Objectives

As was illustrated in Figure 4.3.1, the vehicle antenna is a major consideration in the areas of power and orbit conservation. It was realized from the outset that the vehicle antenna will be a very critical technology. The reasons are essentially the small-size and low-cost requirements that have been placed on the vehicle antenna and that are crucial for the economic viability of an MSS. The challenges are to simultaneously: (1) provide as high an antenna gain as possible, (2) provide sufficient directivity to enable orbit reuse, (3) minimize the physical dimensions and preferably make the antenna conformal to the vehicle, (4) reduce the effects of multipath at low elevation angles, and (5) be capable of rapidly acquiring and then tracking the satellite despite the adverse operating environment (vehicle motion, multipath, and shadowing). All of the foregoing requirements have to be achieved through a low-cost, reliable antenna.

5.1.2 Antenna Design Considerations

Two broad categories of antennas have been considered: very-low-cost, low-gain (omni-type) antennas (LGAs) and directive medium-gain antennas

(MGAs). The LGAs may provide up to about 4 dB of gain at 20° elevation from the horizon. Invariably, they have very wide beams covering essentially all the orbit above CONUS. MGAs, on the other hand, have higher gains (8 to 12 dB at 20° elevation) and considerably more directivity than LGAs. Because of the MGAs' directivity, they need a satellite acquisition and tracking capability. This contributes significantly to their cost and causes them to be considerably more expensive than LGAs.

Because of MSS capacity considerations, one of the most important factors affecting the mobile antenna design is the need for orbit reuse. To enable orbit reuse, the mobile antenna must provide sufficient adjacent satellite discrimination. Apart from frequency discrimination, which is wasteful of precious MSS bandwidth, adjacent satellite discrimination can be obtained through spatial (pattern) discrimination and/or polarization discrimination. Either one or a combination of both could be used, depending on the antenna characteristics and the amount of discrimination required. Generally, 20 to 25 dB discrimination will be sufficient for mobile satellite systems employing digital modulations. To achieve the needed discrimination, polarization discrimination alone is not sufficient in MSS. This is in part due to the inability to achieve good circular polarization at low elevation angles with antennas mounted on conducting vehicle rooftops. Moreover, since the elevation angle varies from about 20° to 60° over CONUS, at or below the Brewster angle the sense of polarization reverses upon reflection from the ground or obstacles, making polarization discrimination very limited. Figures 5.1.1 and 5.1.2 [Huang, 1987a] show a typical cross-polarized pattern in relation to a typical co-polarized pattern for an LGA and an MGA. Polarization discrimination, if employed, must be combined with pattern discrimination.

The amount of pattern discrimination is directly related to the size of the mobile antenna. An LGA is compact in size, but obviously offers little or no spatial discrimination. On the other extreme, a high-gain antenna (HGA) would be large and require a pointing capability that would make it very expensive. Hence, because of their size and cost, HGAs are unsuitable for the mobile application. Motivated by the need to effect orbit reuse as well as to alleviate the spacecraft power burden, and to work within the cost

and size constraints of MSS, the research and development effort in MSAT-X has recently concentrated on MGAs.

The concentration on MGAs in MSAT-X does not mean that LGAs have been discarded. In spite of their major drawbacks (having low gain, having low directivity, and offering less immunity to multipath, particularly at low elevation angles, because of their wide azimuthal beamwidths), LGAs are cheap and simple, and therefore continue to be of interest to MSS designers. LGAs have been studied at JPL during the early stages of MSAT-X, and several breadboard units have been developed. The results can be found in [Woo, 1982; Woo, 1984; and Naderi et al., 1984] or [SYSDOC, Section 2]. The problems stemming from the utilization of LGAs on the vehicle are addressed from an MSS overall system perspective in Section 6.4.1.

A major effort to study, develop, and demonstrate MGAs was undertaken under the leadership of JPL. After detailed conceptual studies by contractors with experience in antenna manufacturing [Ball Aerospace Corporation, 1984; Cubic Corporation, 1984; and SYSDOC, Section 2.2], three types of MGAs were selected for development: a low-profile mechanically steered linear array, a conformal electronically steered phased array, and a planar mechanically steered array. The intent was basically twofold, to provide the maximum reasonable number of options to the industry and eventually the system user, and to maintain a certain amount of diversification, since the technology involved is high risk and may lead to disappointing results when implemented. The mechanically steered, tilted linear array breadboard was developed mostly in-lab at JPL. The others are being developed by contractors. All the breadboards are currently undergoing testing in realistic conditions to determine their full characteristics. The detailed requirements, characteristics, and performance of the different antennas are discussed in [SYSDOC, Section 2]. In what follows we summarize the key technical features and performance characteristics. This will then set the stage for the technology recommendations for MSS given in Section 6.

5.1.3 Salient Vehicle Antenna Requirements

Detailed requirements for the different medium-gain vehicle antennas are given in [SYSDOC, Section 2]. The references therein give the complete specifications. Here we mention the most important requirements to prepare for the antenna descriptions to follow and for subsequent comparisons.

The RF requirements for the mechanically steered, tilted linear array and electronic phased array are basically the same. The design goals call for a minimum gain of 10 dBic over elevation angles of 20° to 60° from the horizon (the real engineering challenge is to achieve it at 20°); a minimum of 20-dB adjacent satellite isolation for 30° to 40° satellite spacing; a 6-dB roll-off from 20° to 0° elevation to reject multipath fading, which can be severe near the horizon. For the planar mechanical array the requirements are the same except that a 12-dBic minimum gain is specified.

There are also detailed requirements on insertion losses (see, for example, [SYSDOC] and the references cited therein). From a system standpoint, the contribution of these losses to the ratio of the antenna's gain to its effective noise temperature (G/T) is the major concern. The G/T is a critical antenna performance measure. It determines the vehicle antenna's receiving performance, which is on the most critically power-starved and vulnerable link from the satellite to the mobile terminal. G/T values for MGAs that are significantly higher (by 5 dB or more) than for LGAs are imperative for MGAs' viability, and important for MSS as a whole. Simple LGAs, like the drooping dipole, can readily achieve G/T values of -20 dB/K at 20° elevation (with a receiving system of 1.8-dB noise figure [NF]). Hence, G/T values of -15 dB/K or higher (at 20°) need to be demonstrated with the MGAs.

As for the pointing subsystem, requirements are somewhat different for the mechanical and electronic antennas. The acquisition time is 10 s for the phased array and 15 s for the mechanical arrays. Both antenna types are required to track the satellite with 2° or less error despite possible vehicle rotation at a rate of up to $45^\circ/\text{s}$.

5.1.4 Vehicle Antenna Designs

In the following sections the different antenna types are described. Their design principles, characteristics, and performance are presented. The results are compared in Section 6 from an MSS standpoint.

5.1.4.1 Mechanically Steered, Tilted Linear Array

5.1.4.1.1 Antenna System Design. Tilted linear arrays containing 4, 6, and 8 elements have a broad elevation beamwidth (typically 65°) and a narrow azimuth beamwidth about 25° , 19° , and 13° , respectively. Because of the narrow azimuthal beam, tracking in the azimuthal direction is required. To point the beam at the desired range of elevation angles, the array is tilted approximately 45° . Preliminary investigations indicated that the minimum gain and adjacent satellite isolation requirements can be met by an array containing only 4 elements. Consequently, a proof-of-concept breadboard tilted linear array antenna system using 4 elements and including the pointing subsystem was developed by JPL [Jamnejad, 1988a and 1988b]. It was demonstrated successfully in the first of a sequence of Pilot Field Experiments (PiFEx) [Jet Propulsion Laboratory, 1988]. The principal objective of this experiment was to evaluate the antenna's performance, particularly the performance of its pointing system developed at JPL. This objective was met, as discussed further in the following subsection.

The antenna contains the radiating elements, which are four square microstrip patches, stripline combiners, and an antenna pointing system, which includes an angular rate sensor, stepper motor, drive assembly, motor controller, hybrid coupler, phase modulator, and monopulse receiver. The whole assembly is covered by a radome. The antenna assembly is shown in Figure 5.1.3. The rate sensor, motor controller, motor, and drive assembly are placed on the fixed base-plate of the antenna, while the antenna array, sum/difference hybrid, coupler, and phase modulator are placed on a rotating circular platform, which is stacked on top of the fixed platform. The breadboard has a 20-in. diameter, and a 9-in. height, which will be reduced to 5 in. in later versions. This may involve the use of a "pancake" motor

assembly or the relocation of the pointing electronics behind, rather than under, the array.

5.1.4.1.2 Pointing Subsystem. Antenna pointing is accomplished using a closed-loop pseudo-monopulse system aided by an open-loop system. The open-loop system includes an angular rate sensor which enables initial antenna pointing and maintains pointing during signal fades by providing an inertial reference [Bell and Naderi, 1986; Jammejad, 1988a and 1988b; and Berner and Winkelstein, 1988].

The closed-loop system requires a satellite-transmitted signal or pilot as a reference for tracking. Signals from two subarrays (adjacent halves) are passed through a hybrid coupler to form the sum and difference signals. The difference signal is then modulated by a squarewave signal and added to the sum channel to form a composite signal. The composite signal is then routed to the receiver, where the error signal is detected. After filtering, the error signal is fed to a stepper motor, closing the servo tracking loop. The motor edge-drives the rotating antenna platform. Figure 5.1.4 gives a schematic block diagram of the pointing system [Jammejad, 1988a].

Field tests have demonstrated that the antenna/pointing system can successfully acquire and track a satellite-transmitted signal in an actual mobile environment, i.e., in the presence of fading, shadowing, and vehicle motion [Berner, 1987, and Berner and Winkelstein, 1988]. Acquisition is performed within the specified 15 s, and the pointing system tracks the satellite within 2° of error. This requirement is met when the vehicle is turning at 45°/s [Jammejad, 1988a, and Berner and Winkelstein, 1988].

The pointing algorithm is currently implemented on a personal computer for the field tests. The entire algorithm is suitable for implementation on a single circuit board.

In a multibeam, frequency-reuse mobile satellite system, the satellite transmits a number of pilot signals, each having a distinct frequency, to facilitate antenna pointing and perform other functions. The tracking system must perform spatial (in the azimuth direction) and frequency

acquisitions in order to lock onto the desired pilot signal. The task of pilot frequency acquisition is assigned to the transceiver, which interacts with the antenna under the supervision of the mobile terminal processor. For the mechanical antennas the rotation is sufficiently slow that it allows for frequency scanning during a single rotation. Frequency scanning could be repeated at a number of angular positions determined by the dwell time necessary for pilot acquisition. The dwell time per pilot has been shown through analysis to be 40 ms [Winkelstein, 1987]. Since the antenna takes 9.6 s per rotation, frequency scanning can be repeated at up to 60 positions in an MSS with four pilot frequencies.

5.1.4.1.3 Antenna Performance and Cost. The antenna is tilted with respect to the ground plane to provide elevation coverage from 20° to 60°. The minimum gain demonstrated in the coverage range is 10 dBic and the maximum gain is about 12 dBic. Elevation and azimuth radiation patterns are shown in Figures 5.1.5 and 5.1.6 [Jamejad, 1988b]. Preliminary results indicate that the adjacent satellite requirement is met, as are the pointing requirements as outlined above.

As mentioned earlier, a critical performance measure that determines the efficacy of this type of antenna is G/T, the ratio of its gain to effective noise temperature. G/T plays a major role in determining the performance of the critical forward downlink (the link from the satellite to the mobile terminal), and as such, it has a significant impact on the design of the satellite communications payload. The contributors to the antenna temperature are the sky temperature, which is basically fixed; the ground temperature as seen by the antenna, which is generally lower for a more directive antenna; and finally, the internal temperature due to the circuitry inside the antenna. For MGAs a major contributor to the effective antenna temperature is the internal component. Preliminary tests have been performed recently at JPL to obtain values for the G/T (and its components) for the proof-of-concept antenna (and other antennas as well). G/T values around -15.3 dB/K have been obtained [Bell et al., 1988]. It should be kept in mind that the proof-of-concept antenna is not a refined production prototype and therefore yields a conservatively low G/T.

The mechanically steered linear array antenna concept with its good performance, but nonconformal shape, is expected to become available for a manufacturing cost of \$600 at a production level of 10,000 units per year over a five-year period.

5.1.4.2 Electronically Steered Phased Array Antenna. Phased array antenna development was initiated in 1984 through a number of study contracts. In the early phase of the development, various concepts and designs were examined. These have evolved into the breadboard designs presently under consideration. The evolution up to the present status is traced in [SYSDOC, Section 2.2]. Here we present and compare the breadboards recently delivered by Ball Aerospace and Teledyne Ryan Electronics (TRE). (Each contractor has delivered two breadboard units.) A more detailed presentation is given in [SYSDOC].

5.1.4.2.1 Array Design. Figure 5.1.7 [Huang, 1987a] depicts a cross-sectional view of the antenna. The planar array contains a radiator layer, a hybrid layer, a phase shifter and power divider layer, and a supporting structure layer.

In the two designs the radiator layer contains 19 radiating elements, which are arranged in a triangular lattice to maximize the resulting gain and avoid grating lobe formulation (Figure 5.1.8). The radiating elements are implemented using microstrip or stripline technologies. In the Ball Aerospace design, the radiating elements are dual resonant, stacked, 0.5-in.-thick circular microstrip elements. The 3-dB beamwidth of a single element is about 90°. In the Teledyne design, a stripline, cross-slot radiator is employed, with a 3-dB beamwidth of approximately 140° [Huang, 1987a]. The microstrip element, due to its narrower beamwidth, may have a lower gain at a low elevation angle than the stripline radiator. However, the microstrip element is mostly composed of low-cost foam material, in contrast to the stripline radiator, which requires higher-cost dielectric material. Figures 5.1.9 and 5.1.10 [Huang, 1987a] show the microstrip and stripline designs, respectively.

The hybrid layer contains the hybrid circuits that generate the orthogonal phases to create circular polarization. The hybrids of the TRE antenna are of stripline design. In Ball's design, the hybrid is a microstrip design etched on the same layer as the radiator.

The phase shifter and power divider layer contains 18 3-bit phase shifters and a 19-way power divider. The two contractors employ different designs for the phase shifters. Ball Aerospace uses a hybrid reflection/loaded-line design for the phase shifters, while Teledyne employs switched-line diode phase shifters. Ball's hybrid design requires 6 diodes per phase shifter, has about a 1.5-dB insertion loss, and purportedly has a 20° maximum phase error (see Section 5.1.4.2.3). TRE's switched-line design requires 12 diodes per phase shifter, achieves a 1.3-dB insertion loss, and an 11° maximum phase error. The phase shifters and the 19-way power dividers are implemented on a microstrip board [Huang, 1987a].

5.1.4.2.2 Beam Pointing Technique. The mobile operating environment and the directive beam of the 19-element phased array antenna necessitate the use of a beam-pointing mechanism. This pointing mechanism performs the tasks of satellite acquisition and tracking in the presence of multipath fading and changing vehicle orientation. Tracking and acquisition are accomplished using an open-loop angular rate sensor in combination with a closed-loop sequential lobing technique. Initial acquisition of the satellite is accomplished by a full azimuth and limited elevation search for maximum signal strength of a transmitted pilot. (Two elevation positions are used due to the narrower beamwidth of the phased array in the elevation plane.) The open loop is used to establish the initial reference in azimuth. Once the satellite is acquired, the closed-loop system begins to perform azimuth tracking with an occasional elevation search. An occasional elevation search is sufficient because the change of elevation angle is slow. During fading outages, the beam pointing system relies on information derived from the open-loop system to maintain its pointing at the satellite [Huang, 1987a].

The open-loop subsystem is basically the same as for the mechanical antenna. It is equipped with a crystal or quartz-type angular rate sensor

[Bell and Naderi, 1986]. Designs using a mechanical gyro and compass have been investigated and determined unsuitable for mobile applications because of accuracy, cost, or reliability considerations.

Because azimuthal scanning is fast for the phased array, faster than what would allow for simultaneous pilot acquisition, in a frequency reuse system, in which several pilots are used, the entire azimuth is scanned at one frequency, then repeated for others. The acquisition time, then, is a function of the product of the number of pilot signals and the number of beam positions. The number of pilot signals is determined by the number of the frequency reuse factor, and the number of beam positions is the number of positions that the beam must be rotated through in order to complete one 360° rotation in azimuth. Analysis has shown that for a system using four pilot signals and 50 beam positions, the pointing system can acquire the pilot in 8 s with a probability greater than 99% at a 35 dB-Hz carrier-to-noise ratio [Winkelstein, 1987].

5.1.4.2.3 Antenna Characteristics and Cost. The phased array antenna breadboards delivered by both contractors are conformal and can be easily mounted on the top of a passenger car. The TRE antenna, including a radome, is 0.7 in. in height and 20.7 in. in diameter. Ball's breadboard, on the other hand, is 1.3 in. by 24 in. The maximum gain is 12 to 13 dB and occurs at close to 60° elevation. The minimum gain for both antennas occurs at a 20° elevation angle. For Teledyne's antenna, the average gain (over eight azimuth positions) is 9.9 dBic at 1545 MHz (receive) and 8.2 dBic at 1660 MHz (transmit). For Ball's antenna, the average gain at 20° is 8.2 dBic at 1545 MHz and 8.1 dBic at 1660 MHz. Complete patterns covering the three-dimensional field of view are being obtained. Typical radiation and axial ratio patterns in elevation and azimuth planes are shown in Figures 5.1.11 through 5.1.14. The 3-dB beamwidth is about 25° in azimuth and about 35° in elevation.

As with the mechanical antenna, the G/T for the phased array is a critical parameter. This is even more true here because of the potentially high resistive internal loss resulting from the numerous diodes, power dividers, etc. Preliminary G/T tests for the phased arrays have yielded G/T values of about -15.4 dB/K for TRE's and -16.7 dB/K for Ball's.

From the preliminary data available, the 20-dB adjacent satellite isolation is expected to be met 81% of the time by the Teledyne antenna, but only 38%, on the average, by the Ball antenna. Multipath rejection, represented by the 6-dB roll-off, is, in general, achieved. However, backlobe levels that are higher than specification have been observed at certain points. These high levels can be detrimental to inter-satellite isolation, multipath rejection, and equivalent antenna temperature.

As for the performance of the pointing subsystem, acquisition for a single pilot frequency takes about 2.5 s. The estimated tracking error is 5° on either side of the boresight, of which the 3-bit phase shifter quantization accounts for 2° and the remainder is due to pattern asymmetry, receiver noise, etc. During tracking, the sequential lobing pointing algorithm imparts unwanted amplitude modulation (AM) and phase modulation (PM) on the received data channel signal. The specification calls for the peak-to-peak AM to not exceed 1 dB and the PM to not exceed 10° . Ongoing tests indicate that both antennas exhibit about 1.5 dB of AM. TRE's antenna also exhibits about 15° of PM, while Ball's antenna creates an obviously unacceptable 37° of PM. It is not clear at this time whether Ball's poor phase performance is due to design limitations or implementation problems.

Last, and certainly not least, is the cost consideration for this type of antenna. Unfortunately, the cost for conformity is not small. The manufacturing costs have been estimated by Teledyne and Ball to be \$1848 and \$1610 for their respective units, based on a production level of 10,000 units per year over a five-year period. The cost breakdown for the two antennas is given in Table 5.1.1 [Huang, 1987b]. It can be concluded that further research is needed to reduce the cost of the dielectric material.

The salient characteristics of the phased array antennas (as well as of the mechanically steered, tilted linear array) are summarized in Table 5.1.2.

Due to its superior RF performance and smaller size, the Teledyne antenna has been preferred by JPL and has been viewed as the more likely candidate for further phased array development. A final decision will be made

after more comprehensive field testing is performed by JPL. Antenna G/T, reliability, and performance repeatability (from one unit to the second) will be taken into account.

5.1.4.3 Planar Mechanically Steered Array. This antenna type is a compromise between the conformal, yet expensive, phased array and the cheapest MGA, the nonconformal mechanical tilted array. Due to its expected moderate cost (\$900 to \$1000 manufacturing cost) and its nearly conformal shape (1.5-in. thickness), it remains a very viable MGA candidate. JPL has recently awarded a one-year contract to TRE to develop two breadboard units.

A minimum gain of 12 dBic is specified. At 12 dB all inter-satellite and multipath rejection requirements are expected to be met. The biggest challenge for this antenna is in the drive mechanism, particularly the low-profile motor and rotary joints.

Progress for the planar mechanical array will be reported in later versions of this document.

5.2 MODULATION, CODING, AND MOBILE TERMINAL DESIGN

5.2.1 Modulation/Coding

Modulation and coding play a key role in meeting the challenging power and spectrum requirements in MSS. A considerable amount of research and development effort has been performed at JPL with the aim of identifying, implementing, and demonstrating a modulation/coding scheme well-suited to the MSS application. The mobile environment requires a scheme that is bandwidth- and power-efficient and robust (to fading, shadowing, frequency uncertainties due to motion and hardware, etc.), and that lends itself to easy implementation at a reasonable cost.

The modulation and coding candidates regarded as most promising have changed with the evolution and maturity of the MSS concept and the other technologies developed for it. The choices have also been strongly influenced by the regulatory decisions affecting MSS. The FDM structure of the network,

combined with the desire to transmit 4800-bps near-toll-quality voice, has led to the selection of 5 kHz as the basic channel bandwidth. This has been a major factor influencing the choice of a modulation/coding scheme. The evolution of the modulation/coding in MSAT-X is discussed in detail in [SYSDOC]. In what follows we outline the progression of modulation schemes considered to put the present candidate in the proper perspective and prepare for the recommendations given in Section 6.

5.2.1.1 Minimum Shift Keying (MSK) and Gaussian MSK (GMSK). In the early stages of MSAT-X, when a data rate of 2400 bps in a 5-kHz channel was envisioned, MSK and then GMSK were considered. MSK is a form of continuous phase frequency shift keying (CPFSK) that has a modulation index of 0.5. Because MSK maintains a phase continuity during bit transitions, its spectral sidelobes fall off more rapidly than in phase shifted keying (PSK) or quadri-phase shifted keying (QPSK). This is, of course, of major importance in controlling adjacent channel interference in the FDMA network. MSK was considered for mobile applications in the early phase of the research because of its relative spectral and power efficiencies. The focus was later shifted to baseband filtered MSK to reduce adjacent channel interference.

Interference in the mobile satellite environment can be severe. A mobile satellite system is likely to employ multibeam frequency reuse technology and orbit reuse in order to maximize the spectral utility. Such a system is often interference limited. A number of potential interference sources are identified in Figure 5.2.1 [Sue et al., 1985]. Gaussian baseband filtered minimum shift keying (GMSK) is spectrally more efficient than MSK, but at the expense of a somewhat higher power requirement (received E_b/N_0 for the same data rate). By varying the baseband filter parameter, adjacent channel interference can be significantly reduced. Figure 5.2.2 [Murota and Hirade, 1981] shows the adjacent channel interference as a function of the normalized channel separation ($f_s T$) for selected baseband filter parameter values ($B_b T$). As shown in the figure, with $B_b T = 0.5$ and $f_s T = 1.5$, the adjacent interference can be 10 dB lower than that for MSK. A separation equal to 1.5 times the bit rate, which, at 2400 bps, corresponds to 3600 Hz, would reduce adjacent channel interference to about 40 dB. With 5-kHz channel

spacing, this would still leave ample margin to accommodate other frequency errors.

To demonstrate the practicality of MSK-type modulation in the mobile environment, a practical two-bit differential MSK (DMSK) receiver was built [Davarian et al., 1985]. This receiver could also test GMSK by including the appropriate Gaussian filtering along the chain. The receiver demonstrated robust operation in the Rician fading environment and exhibited a lower error floor than its coherent counterpart [Davarian et al., 1985].

5.2.1.2 Trellis-Coded Modulation/8-Phase Shift Keying (TCM/8PSK). As the voice coding requirement was reshaped to 4800 bps, a more efficient modulation/coding was sought. The scheme had to provide the needed bandwidth containment without sacrificing power efficiency. Research at JPL arrived at a combined modulation/coding scheme as the solution to this challenging task of squeezing 4800 bps in a 5-kHz bandwidth while maintaining power efficiency. Trellis-coded modulation (TCM), combined with MPSK, was investigated, and a 16-state rate 2/3 TCM with an 8PSK scheme was adopted [Divsalar and Simon, 1986]. (A comparison of the relevant aspects of the different modulation schemes is provided later, in the recommendations of Section 6.)

TCM is an approach that combines modulation and coding. Traditionally, coding and modulation have been treated separately and independently optimized. In TCM, the difference is that modulation and coding are combined as a single entity in system optimization. In so doing, a significant improvement is obtained. In the combination, the 8PSK signaling offers the needed spectral efficiency, while trellis coding matched to it provides performance improvement, which offsets the power penalty that would be paid in a more traditional scheme such as MSK.

Since a form of TCM/MPSK is the present candidate, we will present some of its salient features in the following subsections. Again, a detailed technical presentation will be found in [SYSDOC].

Research focused first on coherently detected TCM/MPSK, in which phase information was assumed to be extracted by using some form of pilot-aided technique (more on that shortly). Figure 5.2.3 shows a general block diagram for a coherent end-to-end TCM system using MPSK [Divsalar and Simon, 1986]. Input bits representing data or the coded speech are first encoded by a rate $n/(n+1)$ trellis encoder. The encoded output symbols are block interleaved by an interleaver to ameliorate the effects of the bursty multipath channel. The symbols at the output of the interleaver are then mapped into the MPSK signal space using the set partitioning method [Ungerboeck, 1982]. To limit spectral occupancy and minimize intersymbol interference, the in-phase and quadrature components of the MPSK signal are pulse-shaped. To allow coherent detection, one or two pilot tones are inserted into a data-free portion of the allocated transmit channel spectrum. At the receiver, the in-phase and quadrature signal components are coherently demodulated using the extracted pilot tone (or tones), quantized, block deinterleaved, and decoded by a trellis decoder.

Various TCM schemes were investigated with symmetrical and non-symmetrical signal sets. The most suitable candidate, as stated earlier, was found to be rate $2/3$, 16-state TCM with symmetric 8PSK modulation and interleaving.

Interleaving is essential to randomize burst errors induced by the fading channel. Software simulation was used to obtain the optimum interleaver parameters, subject to the maximum processing delay requirement for voice [Divsalar and Simon, 1986]. This delay requirement was placed at 60 ms or less. At 4800 bps, and for rate $2/3$ TCM/8PSK (2400 sps), the optimized interleaver length was found to be 128 symbols (of 8PSK) with a depth of 16 and span of 8 symbols. This interleaver length corresponds to about 53 ms. The bit error performance of this scheme, assuming ideal coherent detection, is shown in Figure 5.2.4 [Divsalar and Simon, 1986]. As the figure indicates, TCM provides about 3-dB improvement over uncoded QPSK, while maintaining the same spectral efficiency. (Further comparisons, such as for the case of a noisy reference, will be given shortly and in Section 6.)

To perform coherent demodulation, for TCM or otherwise, carrier phase information is needed. Due to their feedback configuration, Costas loop type schemes for carrier recovery are well-known to be unsuitable for use on fading channels. Hence, research has considered a variety of schemes belonging to the class of tone calibration techniques (TCTs) to effect carrier phase recovery. In one such technique, a pilot signal is inserted into the data spectrum. The problem with this is that the power in the data spectrum near the pilot constitutes self-noise and consequently degrades its detection. One way to avoid this problem is to create a notch in the data spectrum for the pilot tone. There are basically two variations of TCT: single- and dual-tone TCT (Figure 5.2.5 [Rafferty and Divsalar, 1988]). The single-tone TCT involves creating a notch in the spectrum (which may expand the bandwidth, if some form of spectral coding, such as Manchester coding, is used) and inserting a tone in the gap in the middle. On the other hand, the dual-tone TCT (DTCT) is generally simpler to implement and less wasteful of bandwidth. Yet the performance of the DTCT is inferior to that of the single-tone TCT by more than 3 dB, because of the squaring loss implicit in the carrier recovery process. Another variation is a scheme referred to as transparent tone in band (TTIB) [McGeehan and Bateman, 1984]. In this scheme, bandwidth is saved relative to single-tone TCT by splitting the data spectrum rather than expanding it. Unfortunately, to date no practical means of reconstituting the split spectrum without distorting the data has been found (see, for example, [Rensselaer Polytechnic Institute, 1988]). Therefore, DTCT is the prime candidate if coherent detection is used.

Although TCT or DTCT can mitigate the effects of multipath fading, they cause a decrease in the allowed data bandwidth in addition to the power penalty. At UHF, 200 Hz are needed to accommodate each pilot. The 200 Hz are needed to account for Doppler spread as well as for other frequency uncertainties. (Doppler spread is a phenomenon associated with the mobile satellite channel caused by multipath fading. A carrier transmitted over this channel is spread by an amount equal to the Doppler frequency of the mobile vehicle.) The required pilot bandwidth became a critical issue as the regulatory process forced the abandonment of UHF in favor of L-band. At L-band, the bandwidth needed to handle a pilot would be about 400 Hz, due to the roughly doubled Doppler spread. This bandwidth not only reduces the bandwidth available for

data transmission, but also increases the noise power in the notch(es) and degrades pilot detection. To compensate for the increased noise bandwidth, one would have to more than double the power in the pilot signal, making TCT unattractive.

Differential detection is well-suited to the fading channel because it requires phase stability over a short time interval (basically two symbols). Figure 5.2.6 shows the block diagram for a multilevel trellis-coded differential phase-shift keying (MDPSK) system [Simon and Divsalar, 1987]. The performance of the TCM 8PSK with differential detection (TCM/D8PSK) is shown in Figure 5.2.7 for the cases with 10-dB fading (i.e., $k = 10$ dB, where k is the direct line-of-sight to multipath ratio), no fading, with interleaving, and without interleaving. As indicated, an average E_b/N_o of 9.5 dB is sufficient to achieve a bit error rate of 1.0×10^{-3} for $k = 10$ dB with interleaving. In comparison with the performance of idealized coherent TCM/8PSK in Figure 5.2.4 (where no degradation is assumed due to the implicit DTCT), TCM/D8PSK requires about 2.5 dB more signal power for the same BER. However, it is very important to note that DTCT detection is inferior to ideal detection. This is a natural consequence of the noise surrounding the pilots, specifically that observed within the band needed to accommodate the possible Doppler spreading. To place the actual performance of DTCT in perspective, a comparison of differential versus coherent DTCT detection of TCM/8PSK in the fading environment is shown in Figure 5.2.8. As can be easily seen, DTCT is slightly better than differential detection at UHF, but worse by about 2 dB at L-band.

From the results just presented it is concluded that differential detection is the viable option for the present setting in L-band. Consequently, differential detection of 16-state rate 2/3 TCM/8PSK (TCM/D8PSK) with interleaving is the baseline at present.

One of the important features of the modem in MSAT-X is the built-in ability to estimate phase errors induced by Doppler or residual frequency uncertainties. The large components of frequency errors in the network are corrected at the NMC (see Section 6.4.1.4). The precompensated pilot is tracked by the transceiver and used to set the local oscillator. The

remaining Doppler due to vehicle motion and residual frequency errors can be up to 200 Hz. Consistent with differential detection, an open-loop Doppler estimation and correction scheme was developed for the D8PSK demodulator [Simon and Divsalar, 1988]. The scheme exploits the fact that the phase shift observed over half a channel symbol is due to Doppler and not to data modulation. Further, with the proper processing, the unwanted phase shift can be mostly removed. For the modulation in MSAT-X, the presence of the two ISI free points at $T_s/4$ and $3T_s/4$ in the 100% root raised-cosine case (Figure 5.2.9) is crucial to the operation of the Doppler estimation. (Samples with independent noises can be extracted there. See [Simon and Divsalar, 1988] for the theoretical details.)

Modem breadboard implementation at JPL is in its final stages of development [Jedrey and Lay, 1987]. Lab testing using the channel simulator (Sections 6 and 5.6) has been recently accomplished. Modem performance within 1 dB of theory was demonstrated for both the AWGN and fading channels [Jedrey et al., 1988]. This is a significant result in favor of the present modulation/coding baseline design. Field testing of the mobile terminal breadboard will take place soon.

5.2.2 Mobile Terminal Design

Although a considerable amount of effort went into furthering the state of the art in modulation/coding research, the modem is but one of the ingredients of the mobile terminal. Research and development effort was also undertaken to arrive at the best architecture for the mobile terminal. For MSAT-X the goal has been to develop a structure that satisfies two objectives: First, the architecture had to be modular and flexible to support the technology validation experiments, and second, the breadboard transceiver should utilize techniques that a final user mobile terminal design could take advantage of.

The mobile terminal structure given in the block diagram of Figure 5.2.10 was arrived at [Cheetham, 1987]. The modular design is evident. The terminal processor plays a central role in controlling the operation of the mobile terminal. It controls the interfaces among the different subsystems,

such as the speech coder, modem, and transceiver, and also contains the logic to control the execution of the antenna pointing algorithms and implement the networking protocol. Details pertaining to the terminal processor can be found in [Cheetham, 1987, and SYSDOC]. The terminal processor was developed at JPL and is currently part of the experimental setup for technology validation.

Proper design of the transceiver is crucial in the MSS link. The performance of the receiver is inseparable from that of the receiving vehicle antenna. The overall G/T is a critical factor in selecting a particular terminal/antenna design option. This has major implications for the overall MSS architecture. In particular, it strongly influences the satellite design through the higher EIRP required to offset a lower receiving terminal G/T. A higher EIRP implies a larger satellite and possibly high-risk satellite development.

The transceiver/antenna interface has been validated in the experiments conducted by JPL. Effort to refine the transceiver design is also under way at JPL to demonstrate the desired G/T in the neighborhood of -15 dB/K. The transceiver performs other functions that are also vital to the proper operation of the mobile link. The functions of Doppler estimation and correction, and frequency calibration of the inexpensive local oscillator to a network reference, are integral components in the operation of the ground terminal and the network. Research and development effort in this area is continuing.

5.3 SPEECH CODING

Voice communication is an essential ingredient of MSS. The challenge in MSAT-X has been to devise and develop voice compression algorithms that operate at a low rate commensurate with the narrow channel bandwidth requirement of MSS. For the purposes of MSAT-X, this bandwidth is taken to be 5 kHz for all channels.

5.3.1 Background

Both analog voice and digital voice have been considered for mobile applications. Analog voice includes those techniques using frequency modulation (FM), single sideband modulation (SSB), and amplitude companded single sideband modulation (ACSB). FM voice has been widely employed by terrestrial systems, but it is spectrally inefficient compared to ACSB and SSB. Digital voice is compatible with digital modulation techniques, and, with the introduction of advanced digital signal processing hardware, it has emerged as an approach with considerable promise in the MSS application. The technology development program has focused on digital voice.

The objective in MSAT-X has been to develop a "near-toll-quality," low-rate, real-time speech coding system, which, when coupled with power- and bandwidth-efficient modulation/coding, can provide a quality voice service within the tight bandwidth constraints of MSS. "Near-toll-quality" here is intended to mean a natural-sounding, intelligible voice with good speaker identification, that is free of processor-induced anomalies (such as bleeps). As the name implies, it is a quality that approaches that of a long-distance telephone call. The goal is to achieve this quality with a real-time coder and handset-type of user equipment.

Speech compression techniques can be divided into two broad categories: the techniques of waveform coding, and those of source coding [Flanagan et al., 1979]. Hybrids have also emerged. Waveform coding aims at representing an analog waveform with a digital representation that, when decoded, would produce a replica as close as possible to the original waveform. Source coding techniques, on the other hand, aim at modeling the human voice-producing mechanism. Waveform coding results in high-quality, natural-sounding speech with robustness to background noise. Unfortunately, it requires high data rates (16 kbps - 64 kbps). In 1984, high-quality (broadcast commentary quality) speech was attained at 64 kbps using companded PCM. At present, the CCIR is adopting a version of differential PCM (DPCM) at 32 kbps as the standard for toll-quality speech. Currently it is also possible to get high-quality speech at 16 kbps.

A prominent source coding approach is Linear Predictive Coding (LPC), which uses linear filtering theory to model the vocal tract. LPC has been used in the past to produce fairly low quality speech at low data rates. For example, the Department of Defense standard at 2400 bps is the LPC-10 vocoder. Its voice suffers from a lack of naturalness, has a synthetic quality, and results in some loss of speaker recognizability. It is not considered suitable for general public use. LPC-based techniques have also tended to be more vulnerable to background environment noise than waveform coding techniques are.

Since synthetic quality results at 2400 bps, it is evident that a higher data rate will be needed in MSS. Since, on the other hand, the channel bandwidth is limited to 5 kHz, and multiple bps/Hz modulation schemes are inconsistent with power, complexity, and cost constraints of MSS, the goal for the speech rate has been set at 4800 bps. The challenge in MSAT-X, therefore, has since been to develop a speech coding system that operates at 4800 bps, meets the quality objective, is simple enough to be implemented in a mobile terminal for real-time operations (with less than 50-ms delay), and is robust in the mobile environment, where the speech is corrupted by vehicle noise, and the communication channel is impaired by multipath fading and shadowing.

In late 1984, JPL awarded a three-year contract to each of two academic institutions to research and develop the speech coder breadboards. The contracts had three phases: concept identification, algorithm development, and hardware implementation.

The University of California, Santa Barbara (UCSB), developed two algorithms, called Vector Excitation Coding (VXC) and Vector Adaptive Predictive Coding (VAPC). The Georgia Institute of Technology (GIT) developed a Self-Excited Vocoder (SEV). Recently both contracts were amended to include the development of three robust pre-prototype units that can be used in field testing.

In what follows we briefly present the different speech coding techniques and equipment under development.

5.3.2 Speech Compression Techniques Developed for MSAT-X

The basic framework within which the different algorithms operate is as follows. The input speech is sampled at 8 kHz with 12-bit resolution. The sampled speech is divided into frames of approximately 20 ms. A compression algorithm is used so that the number of bits of information transmitted per frame may not exceed the aggregate rate of 4800 bps. In addition, it is necessary to allocate some of the bits in each frame for functions such as frame synchronization and error detection.

The speech compression techniques developed by both contractors are based on the classical LPC compression technique and are generalizations of it wherein waveform coding is used in combination with LPC to achieve natural-sounding speech.

5.3.2.1 LPC-Based Compression Techniques. LPC speech coders can be modeled as in Figure 5.3.1. The core of these coders is the so-called analysis-synthesis model. The speech analyzer consists of a short-term predictor and a long-term predictor. The parameters of the long- and short-term predictors can be determined by LPC analysis of the speech waveform. The long-term predictor is concerned with modeling the pitch in the voice, while the short-term predictor is for tracking the short-term waveform variations in the speech. The speech synthesizer in the encoder also contains the long-term and short-term predictors. A coded excitation signal or residual is injected into the speech synthesizer to generate the coded speech. The optimal code is obtained using an analysis-by-synthesis procedure, which chooses an excitation sequence from an ensemble of possible excitation sequences, subject to the criterion of minimizing the resultant perceptually weighted distance between the coded speech and the original speech. Different LPC-based techniques vary in the means by which the excitation sequence is selected. The address of the selected codevector is transmitted to the synthesizer in the decoder, which reconstructs an approximation of the original vector by mapping the codevector from its stored codebook or by generating the output sequence based on a fixed model.

5.3.2.2 Speech Coding Techniques Developed at UCSB. Using the vector quantization (VQ) technique, UCSB has developed two speech coding schemes: vector adaptive predictive coding (VAPC) and vector excitation coding with pulse excitation (VXC).

5.3.2.2.1 VAPC. In principle, the VAPC scheme works as follows. A sampled speech waveform is first filtered by a long-term predictor (pitch predictor) to remove the long-term redundancy due to pitch quasi-periodicity. It is also filtered by a short-term predictor, which is, in effect, a whitening filter, to produce the so-called "residual" sequence. The predictor parameters are computed, vector-quantized, and transmitted to the decoder once every voice frame, which is 22.5 ms. The residual is then divided into nine vectors, each representing a 2.5-ms segment of the residual waveform. These vectors are quantized by a gain-adaptive vector quantizer. The gain and the VQ index of the codevectors, which is selected from the VQ codebook (which contains 128 codevectors, each of dimension 20), are then sent to the receiver. The speech is reconstructed at the receiver by using the short-term and long-term predictors, which are excited by the quantized residual. The speech signal is further enhanced by postfiltering. Figure 5.3.2 shows the VAPC functional block diagram.

5.3.2.2.2 VXC. The second coder developed by UCSB employs a codebook excitation scheme. The VXC functional block diagram is shown in Figure 5.3.3 [Chen et al., 1987]. This technique employs the classical LPC model. Notable contributions to this technique have been the development of algorithms for small codebooks used in modeling the excitation sequence, and the reduction of computational complexity for real-time coder operation.

5.3.2.2.3 VAPC and VXC Predicted Performance. The performance of both VAPC and VXC operating in the presence of white noise and truck noise has been predicted by simulation. Results have indicated that the two techniques can reproduce speech with fairly good intelligibility and quality even in the presence of truck noise and at low SNR (6 dB) [Chen et al., 1987]. UCSB reports that, compared to the original speech, the decoded speech is slightly muffled, but the overall quality and intelligibility are improved due to the noise suppression effect. Laboratory versions of the vocoders have been

demonstrated by UCSB in March 1987. Speech intelligibility and naturalness were achieved, but the overall speech quality could not be considered near-toll-quality. The speech quality is expected to improve with recent and continuing refinements.

UCSB has recently delivered a stand-alone single-board VAPC/VXC Voice Compression Unit (VCU), which is based on three AT&T DSP-32 digital signal processors. (A change in EPROMs effects the switch from one scheme to another.) A critical evaluation will include laboratory listening tests, testing of the vocoder with the hardware simulator, and testing of the vocoder as a part of the end-to-end link to be demonstrated in the field.

5.3.2.3 Speech Coding Technique Developed by GIT. After considering a wide variety of algorithms, GIT selected a form of extended Self-Excited Vocoder (SEV) for real-time implementation. An SEV can be considered to be similar to a Code-Excited Linear Predictive Coder (CELPC) or a Multi-Pulse Linear Predictive Coder (MPLPC) with the exception that the current excitation signal for the SEV is also determined from the excitation signal's own past history. Actually, the excitation sequence in this technique is a hybrid of codebook excitation and the excitation used in previous speech frames.

Because the SEV determines the current excitation signal by utilizing the excitation signal's past history, fewer bits are needed for the coding of the excitation function. To encode and quantize the short-term filter coefficients, SEV employs the quantized line spectrum pair (LSP) for bit rate reduction. The concept is depicted in Figure 5.3.4 [GIT, 1987]. The details can be found in the reference cited and [SYSDOC]. Extensive simulation has indicated that the relatively simple SEV can achieve speech quality similar to that of more complex vocoders.

GIT has delivered a VCU that consists of a PC/AT chassis with the Intel IPAX/286 mother board, a DSP-32 board, a TMS 320C25 board, and an I/O board. The I/O board is used mainly to interface with the terminal processor and the handset. The speech decoding and analog-to-digital (A/D) and D/A conversion is performed on the TMS 320C25 board. The speech encoding is performed on the DSP-32 board, which has three DSP-32 processors. The

remainder of the hardware is used as a development system. This hardware is obviously considerably larger than that of the UCSB vocoder; this is attributed to the fact that it is a developmental system that is not intended by GIT to be a stand-alone vocoder. This is more convenient for the development work performed by GIT, but makes the hardware inconvenient to integrate with the remainder of the mobile terminal.

Preliminary listening tests have indicated that the speech obtained is generally intelligible and natural-sounding, but of only fair quality. As with the UCSB vocoder, thorough testing will be performed by JPL, both in the lab and in the field. These tests will determine the exact qualities of the speech obtained.

5.4 NETWORKING

5.4.1 Perspective

Networking concepts in MSAT-X reflect the uniqueness of its requirements and operating environment. The networking concepts are also directly coupled to the basic system design philosophy arrived at by NASA and discussed in Section 4.1.

It became evident early in the MSAT-X program that novel networking approaches had to be developed. The challenge in the protocol design arises from the integrated voice and data services that a mobile satellite system provides. Voice and data services have different characteristics in terms of message duration, message arrival rate, acceptable delay, and blocking probability. The available networking protocols were not suitable or adaptable to MSAT-X [Signatron, 1985]. The protocols that integrated voice and data utilized TDMA as a general rule. Broadcast-type protocols would have been impractical in an FDM system. Other schemes were simply not applicable due to the low-cost constraint on the mobile terminal.

In 1983 an adaptive multiple access protocol (AMAP) was developed at JPL for the data messages in MSAT-X. From this evolved, in 1984, the

integrated adaptive multiple access protocol (I-AMAP) that integrated voice and data services.

5.4.2 I-AMAP

In I-AMAP the channels (of equal bandwidth or capacity) are divided into information and request channels. The information channels are further divided into open-end and closed-end channels. The open-end channels (open connection duration) are used for voice or long file transfers, while the closed-end channels (specified connection duration) are used for usual data channels. I-AMAP adaptively varies the mix of request, open-end, and closed-end channels to suit the demands placed on the network. The protocol treats the open-end links according to a blocked calls cleared strategy with the main objective of minimizing the blocking probability. For closed-end data links, the objective is to minimize the end-to-end delay.

In the 1984 time frame, I-AMAP was designed to use pure ALOHA for reservations. Subsequently, a feasibility and software sizing contract was awarded to Signatron Corporation. Improvements to I-AMAP that involve minor or moderate extra cost were suggested in a study by Signatron. These included using modified slotted ALOHA, integrating data into available voice channels, and prioritizing the voice and data messages. The first recommendation, viz., slotted ALOHA, relies on slot-time definition, a task for which inexpensive solutions were found [Signatron, 1985, and Emerson, 1985]. Slotted ALOHA became (and still is) the baseline in I-AMAP. The second suggestion, i.e., integrating data into available voice channels, was not pursued. The third suggestion, i.e., prioritizing voice and data messages, will be incorporated into I-AMAP in the future. The Signatron study gave detailed signaling handshakes, software builds with time and cost estimates, and estimates of the needed computation power in the NMC. Because of the predicted cost (\$3.6 million over 24 months) and NASA's budget constraints, detailed software development was relegated to future MSS operators, each with his specific system architecture.

Concurrent with and subsequent to the Signatron study, several of the key design details for I-AMAP were established by JPL, e.g., the

recommendation of slotted ALOHA with binary exponential backoff. The technical details of I-AMAP are given in [SYSDOC] and the references cited therein. Here we only highlight some of the salient features and results.

5.4.2.1 Channel Partitioning. The adaptive partitioning of the channels in I-AMAP is illustrated in Figure 5.4.1: (a) shows the channel partition at one instant of time, and (b) shows the channel partition at another instant of time as the traffic mix changes [Yan and Naderi, 1986]. Figures 5.4.2 and 5.4.3 show the partitioning of channels as a function of the message arrival rate for a fixed average message delay (1.75 s) and blocking probability (2%) [Yan and Wang, 1985]. The required number of request channels and the number of closed-end channels as a function of the data message arrival rate are shown in the first figure, while the total number of channels and the number of open-end channels are shown in the second figure. For example, at a message arrival rate of 100 messages per second for data and 0.1 for voice, the channels of a 97-channel system will be partitioned as follows: 35 request channels, 46 data channels, and 16 voice channels. By monitoring the message/call arrival rates, the utilization of resources can be maximized by dynamically adjusting the channel partitioning.

5.4.2.2 Error Control, Packet Replication, and Packet Size. Analysis at JPL also arrived at optimal error control design, packet replication strategy, and packet length (all in the sense of minimizing the end-to-end delay). Error control is effected by means of an inner forward error correction (FEC) code, and an outer cyclic redundancy check (CRC) for packet error detection. The FEC in the baseline is the rate 2/3 16-state trellis code combined with the D8PSK and interleaving. (See Section 5.2.) The CRC is used in conjunction with a selective automatic retransmission request (ARQ) algorithm [Wang and Yan, 1987a]. All successfully received packets, excluding voice packets, will be acknowledged within a predetermined period of time. Packets received with errors will be negatively acknowledged and subsequently retransmitted. The method of packet retransmission varies according to the type of channel connection. In an open-end connection, in which the channel is assigned to the user until it is relinquished, packet retransmission takes place over the same assigned channel and immediately after the receipt of the negative acknowledgment. In a closed-end connection, retransmission occurs after the

completion of the transaction that is in progress, and generally over a different channel, for which the user must make a separate connection request and successfully obtain an assignment.

Request packets that are not positively acknowledged within a specific time period will be assumed to have been lost or received with errors and will be treated as negatively acknowledged packets.

Multiple transmission of the acknowledgment and assignment packets reduces the probability of their retransmissions and can minimize message delay. Computer simulation has shown that packet replication (two copies inclusive) significantly lowers the average end-to-end delay, as indicated in Figure 5.4.4 [Wang and Yan, 1987a]. This figure shows the average delay as a function of the packet sizes with and without packet replication. As indicated, for the range of packet sizes considered, packet replication reduces the average delay significantly. Figure 5.4.4 is based on a message length of 4096 bits and an arrival rate of 65 messages per second. From this figure it is also evident that for a given message size, message arrival rate, and channel performance, the end-to-end message delay is affected by the packet size. Figure 5.4.5 provides additional information on the message delay as a function of the message arrival rate. As seen from these figures, a packet size between 256 and 512 bits is optimal in the sense of minimizing the delay during busy traffic hours [Wang and Yan, 1987a].

5.4.2.3 Request Channel Simulator. Recently, with the parameters of I-AMAP established mostly through analysis, the focus has shifted to developing and implementing a simulator for networking purposes. The simulator is concerned particularly with the request channel, because of its vulnerability, and is currently close to being complete. Its objectives are to validate the results derived through analysis (which always contains some idealized assumptions) in a realistic simulated fading channel environment, to refine the the parameters of the request channel, and to test new potentially useful protocols. The simulator is shown in the block diagram of Figure 5.4.6 [Wang and Yan, 1987b] and is discussed also in [SYSDOC]. Along the line of investigating other protocols, an in-house effort at present is investigating tree algorithms that have been developed in the eighties and that promise higher capacities than

slotted ALOHA, while being stable, unlike slotted ALOHA. Tree algorithms will also be tested on the request channel simulator.

5.5 MOBILE SATELLITE CHANNEL MODELING

In the strict sense of the phrase, propagation modeling is not a technology development. Nevertheless, the development of new and effective techniques to model the MSS propagation environment is essential to the prediction of the MSS's performance. This, in turn, has a significant impact on the development of the MSS subsystems. Since the MSAT-X program's inception, a joint effort under NASA's MSAT-X and propagation programs has been dedicated to developing the necessary propagation models and an indispensable channel simulation capability.

Important propagation parameters for MSAT-X include signal attenuation, fading rate, depth and duration, and Doppler spread. The statistics of these parameters are needed for a variety of MSS terrains, e.g., unobstructed flatland, forested areas, hilly areas, and areas with buildings and other man-made structures. Some estimates of these parameters can be obtained through analysis based on simplified assumptions. Yet the most effective method to obtain reliable data is through propagation experiments, since the propagation characteristics are a function of the mobile environment, including antenna patterns, elevation angles, and vehicle speed. Propagation experiments were performed that utilized stratospheric balloons, helicopters, remotely piloted drones, and high, fixed towers. These tests were funded by MSAT-X and the propagation program in support of MSAT-X. A large body of data has been gathered and is being analyzed.

The experiments, the data, and the results are discussed in detail in [SYSDOC] and the references cited therein. For the system-level presentation, it suffices to mention some of the most salient results. The signal attenuation statistics are given in the curves of Figure 5.5.1 [Vogel and Goldhirsh, 1987]. (The references cited in the figure can be found in [Bostian, 1987]. It should be noted that curves A and B were results of experiments funded by another program.) In summary, they show that at L-band,

the following fade depths (attenuations) are exceeded 1% of the time: (a) 1.4 dB for an unobstructed path, (b) 5.5 dB at a 45° elevation in multipath (canyon) terrain, (c) 7.6 dB at a 30° elevation in multipath terrain, and (d) at least 8 dB worse in wooded flat areas than in multipath terrain! These results are extremely significant. First, they indicate that foliage shadowing is the dominant cause of degradation. Second, they indicate that serious attenuation can result from multipath alone, without even shadowing. In general, these results indicate worse effects due to propagation than had been thought initially. As a result they have a significant impact on the development of the technologies in MSAT-X. This will be addressed again in Section 6.

Computer simulation and analysis to augment and explain the results of the propagation experiment have also been performed. Although the measurements are yet to be fully analyzed, some results have been applied to software channel simulators that model the propagation of radio waves, simulate terrain blockage effects, and estimate link performance [Divsalar, 1985, and Bostian, 1987]. The analytical effort has included modeling scatterers, the effects of the distance to the scatterer, and tree complexity modeling. Tree complexity modeling, for example, aims at furnishing a tree attenuation model that assesses the effect of tree complexity on signal attenuation. A tree can be modeled as a two-dimensional figure consisting of a number of finite opaque strips that are canted together to approximate the trunk and branches of a real tree [Vogel and Hong, 1987]. By varying the number of branches, different attenuations levels are predicted. Results of the correct order of magnitude have been obtained.

A significant result that has come out of the scattering modeling effort pertains to MSS in general, and predicts the channel bandwidth restriction that results from propagation in the MSS environment [Vogel and Hong, 1987, and SYSDOC]. As can be inferred from Figure 5.5.2, the bandwidth of the channel, as measured by a specified amount of envelope peak-to-peak variation, is restricted to few tens of kilohertz (depending on the average fading depth). This result supports the choice of an FDMA system by making the broad assertion that wide band signals, such as TDMA and CDMA, are less suitable for transmission on MSS channels than signals in an FDMA scheme are.

To facilitate the development of the MSAT-X hardware, improve the efficiency of testing the new technology, and facilitate in general the study of the effects of propagation anomalies on communication system performance, a flexible hardware channel simulator was developed at JPL [Salmasi et al., 1984, and Davarian, 1987]. The results of the propagation experiments, e.g., fade statistics, are being included in the channel simulator for realistic in-lab testing. This will precede the full-scale field experiments of the end-to-end MSAT-X breadboard system.

Table 5.1.1. Estimated Cost Breakdown and Per Unit Cost for the MSAT Phased Array Mobile Antennas^a

	Percentage of Total Cost (A + B)	
	Ball	Teledyne
A. <u>Material/Parts</u>		
Dielectric Circuit Boards		
- Radiator and Hybrid Layers	18.9	19.9
- Phase Shifter Layer	3.4	2.5
Phase Shifter Components		
- Pin Diodes	26.9	11.5
- Resistors	0.1	0.8
- Capacitors, Chokes, Etc.	1.4	7.5
Open-Loop Pointing Sensor	11.5	13.7
Electronics		
- Microprocessor	23.0	4.3
- Peripheries		14.8
Mechanical Structures and Radome	3.1	1.6
Cables, Connectors, Etc.	2.3	1.1
Subtotal	90.6	77.7
B. <u>Assembly/Labor</u>		
Radiators and Hybrids	6.2	12.5
Phase Shifter Layer		4.6
Electronics	1.7	1.7
Mechanical Structures and Radome	1.5	2.8
Antenna Integration		0.7
Subtotal	9.4	22.3
C. <u>Total Manufacturer's Cost</u>		
(A + B)	\$1610	\$1848

^aThe production quantity is 10,000 units annually for a five-year period.

Table 5.1.2. Salient Characteristics of MGA Breadboards

	JPL Mechanically Tilted Linear Array	TRE Phased Array	Ball Aerospace Phased Array
Average ^a Received Gain (1545 MHz), dBi			
20° Elevation	10.0	9.9	8.2
40° Elevation	11.5	11.3	11.6
60° Elevation	10.0	12.8	11.5
Average ^a Transmit Gain (1660 MHz), dBi			
20° Elevation	10.0	7.8	8.1
40° Elevation	12.0	10.1	11.4
60° Elevation	10.0	12.2	12.4
Average ^a Receive System G/T at 20° (including NF = 0.86 Mobile Terminal [MT] Receiver), dB/K	-15.2	-15.4	-16.7
Acquisition Time, s	15	<10	<10
Interference to Data Channel During Tracking			
AM, dB (peak-to-peak)	Negligible	1.5	1.5
PM, ° (peak-to-peak maximum)	Negligible	15	37
Size (height x diameter), in.	9.0 ^b x 20.0	0.7 x 20.7	1.3 x 24.0
Manufacturing Cost (estimated), \$	600	1848	1610

^aAveraging gains over eight azimuth beam positions.

^bHeight of mechanical linear array is to be reduced to 4.5 in.

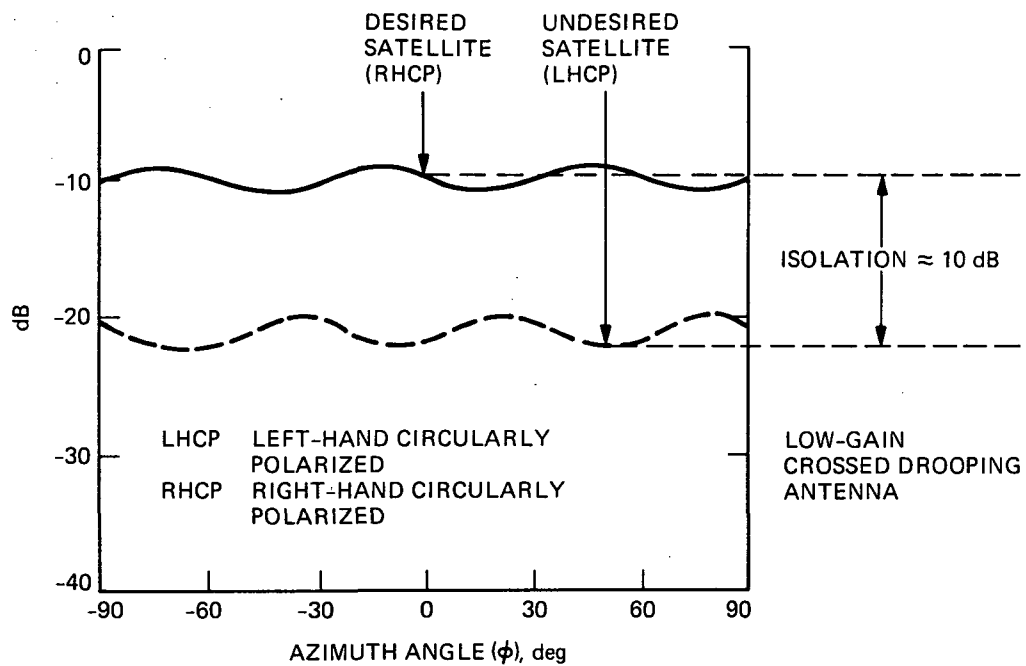


Figure 5.1.1. A Typical Radiation Pattern Demonstrating the Adjacent Satellite Isolation Achievable by a Low-Gain Antenna

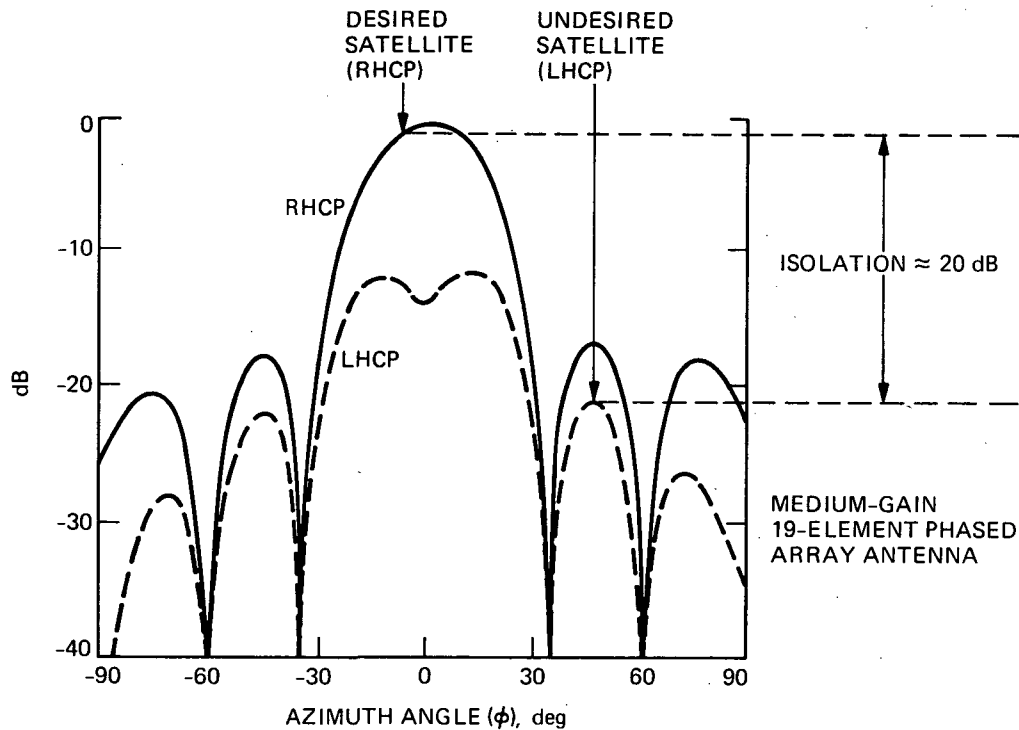
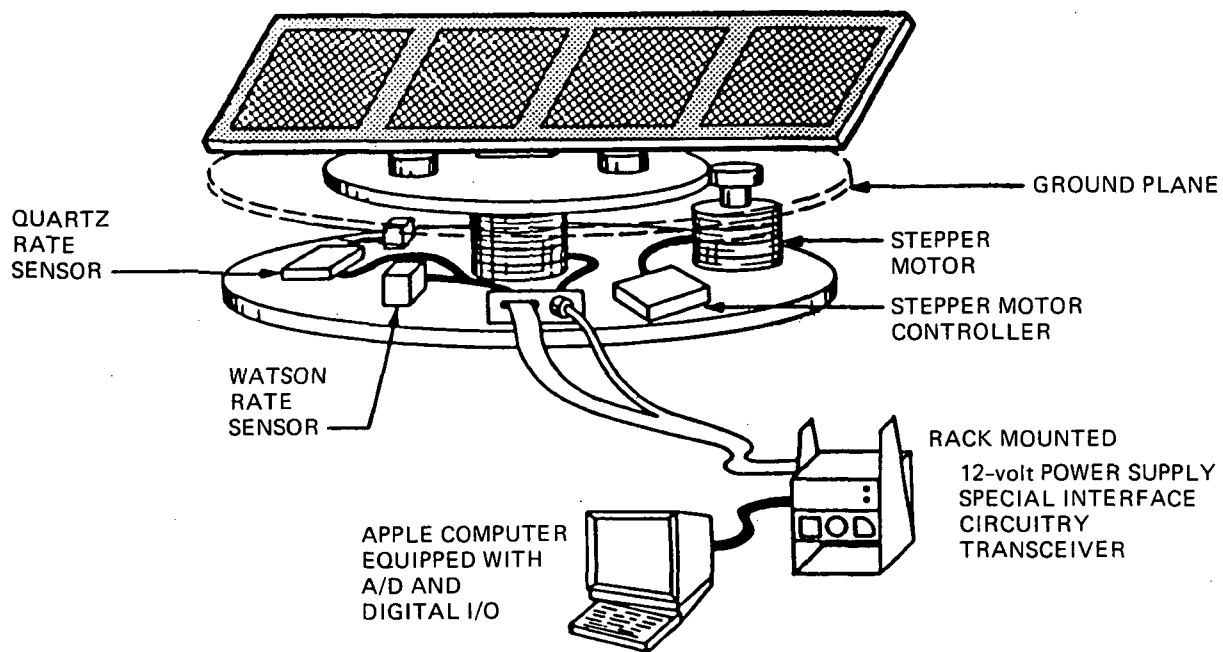


Figure 5.1.2. A Typical Radiation Pattern Demonstrating the Adjacent Satellite Isolation Achievable by a Medium-Gain Antenna With Taper



ANTENNA SUBSYSTEMS

RF ARRAY AND FEED
 STEERABLE PLATFORM
 CONTROL/SUPPORT ELECTRONICS
 Δ CHANNEL DEMODULATION/FADING CORRECTION CIRCUITRY
 APPLE POINTING CONTROL COMPUTER

Figure 5.1.3. Mechanically Steered Linear Array Antenna Assembly

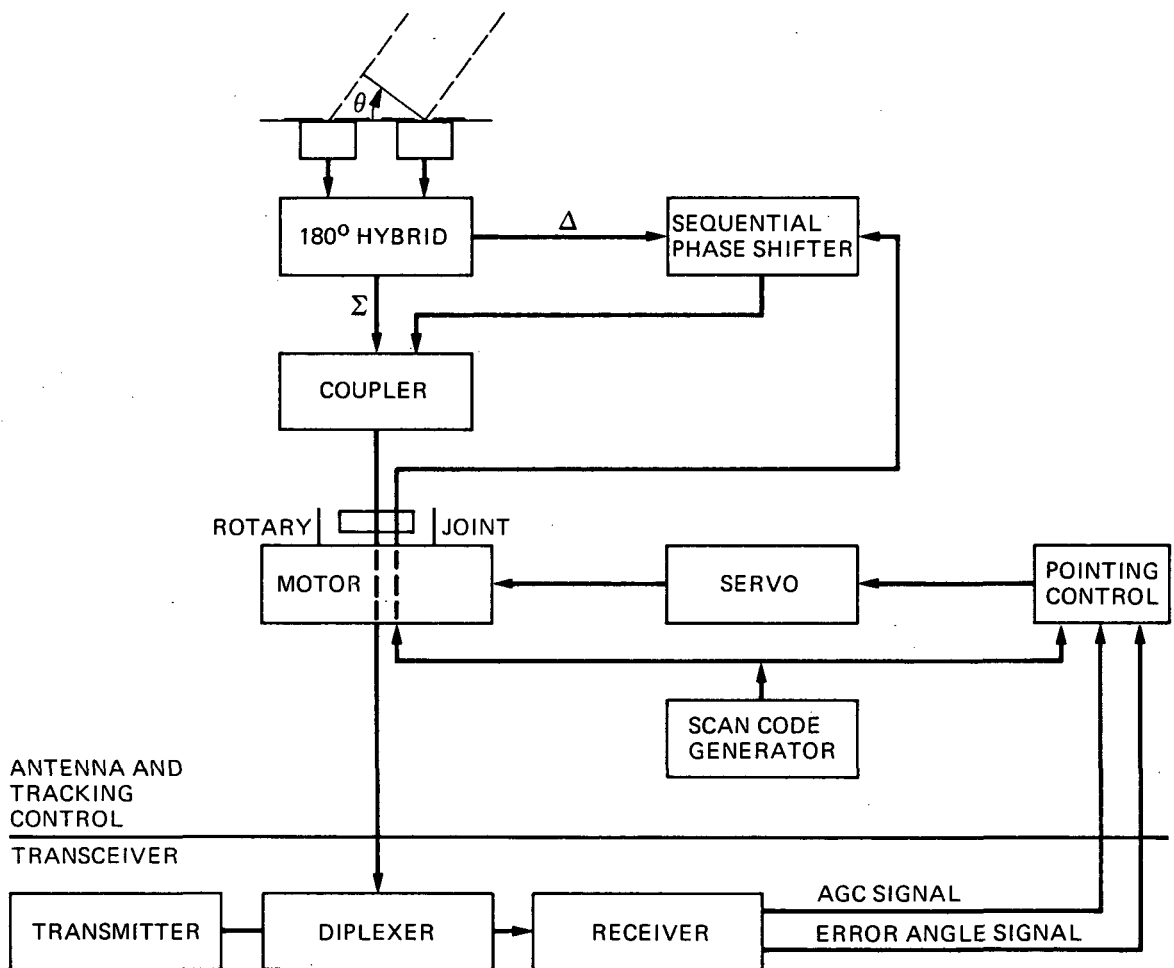
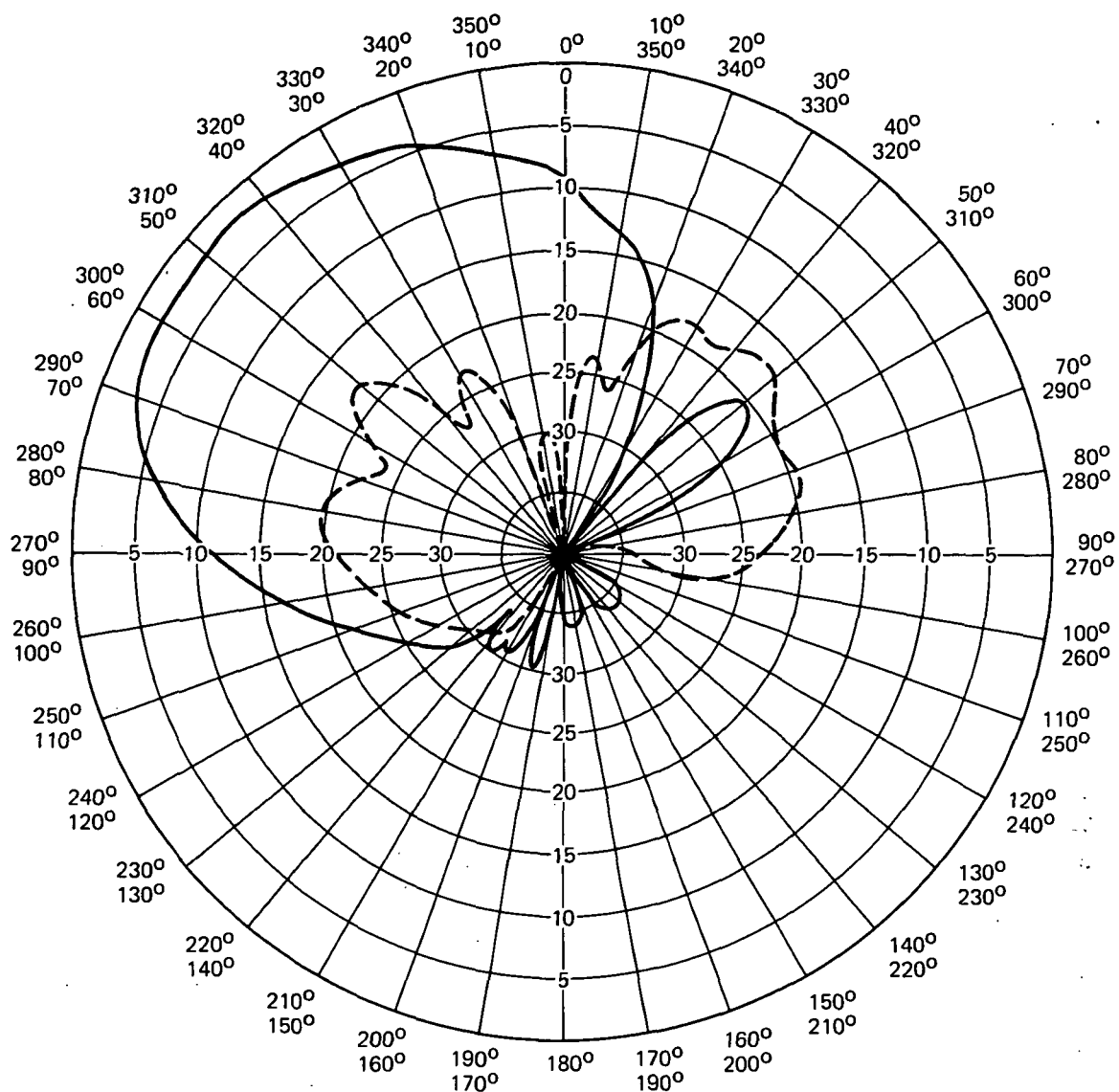
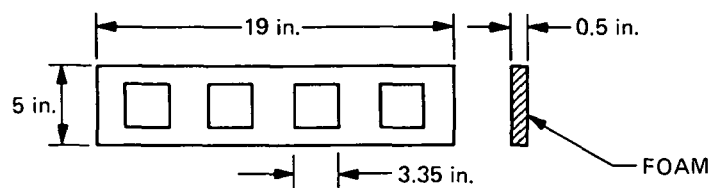


Figure 5.1.4. Schematic of Vehicle Antenna Pointing System Based on Single-Channel Monopulse Tracking



— CO-POLARIZATION
 - - - CROSS-POLARIZATION



ARRAY DIMENSIONS

ELEVATION PATTERN
 AT 1600 MHz
 MAXIMUM GAIN
 ≈ 12 dBic

GROUND PLANE
 DIMENSIONS: 48 in. x 56 in.
 ARRAY TILT ANGLE: 45°

Figure 5.1.5. Elevation Pattern of Mechanically Steered Antenna

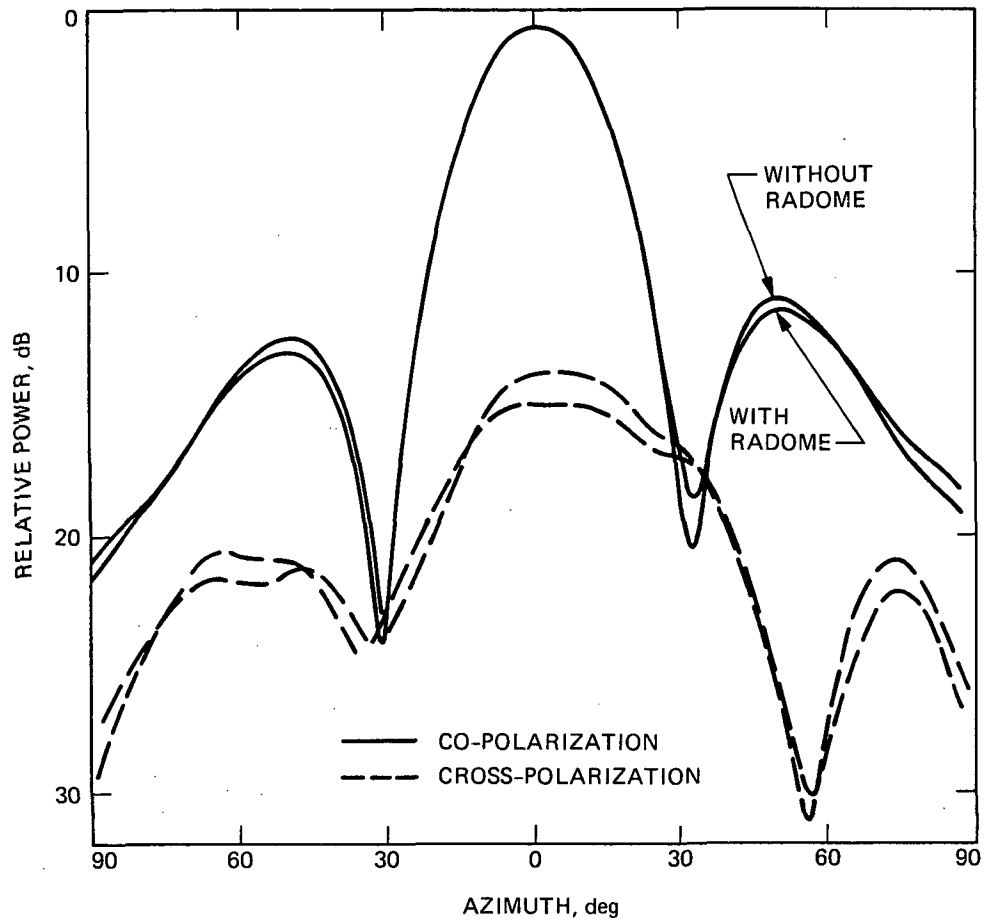


Figure 5.1.6. Azimuth Pattern for Mechanically Steered Linear Array Antenna

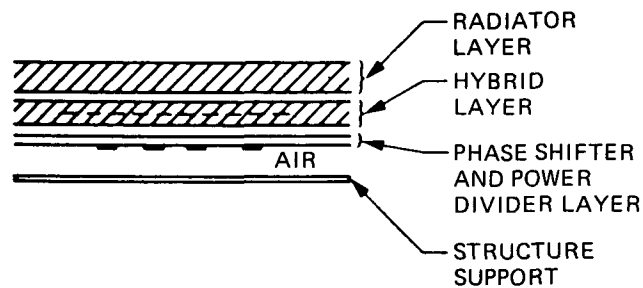


Figure 5.1.7. Cross-Sectional View of the Phased Array Antenna

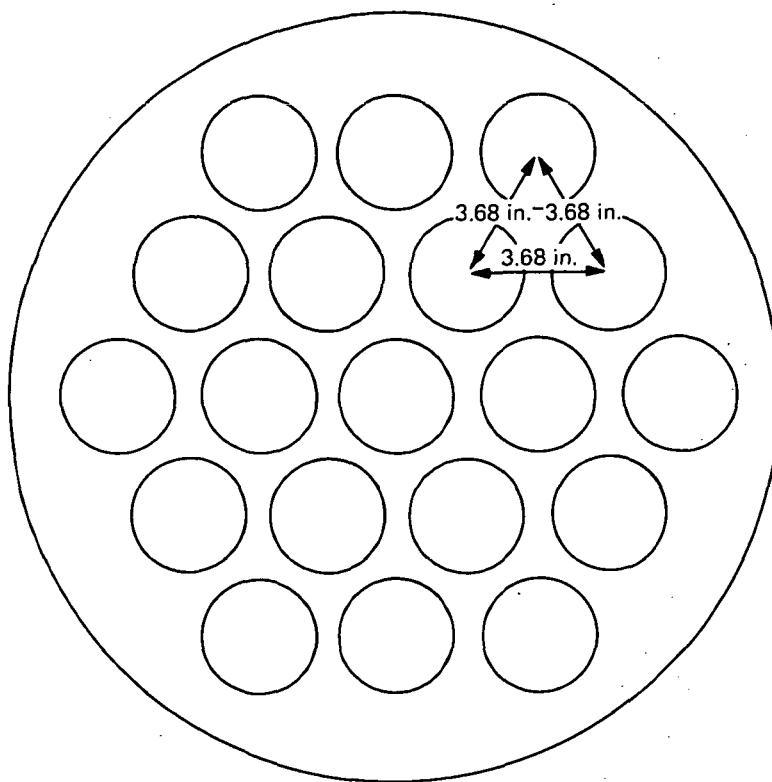


Figure 5.1.8. Triangular Lattice Pattern of Phased Array Antennas

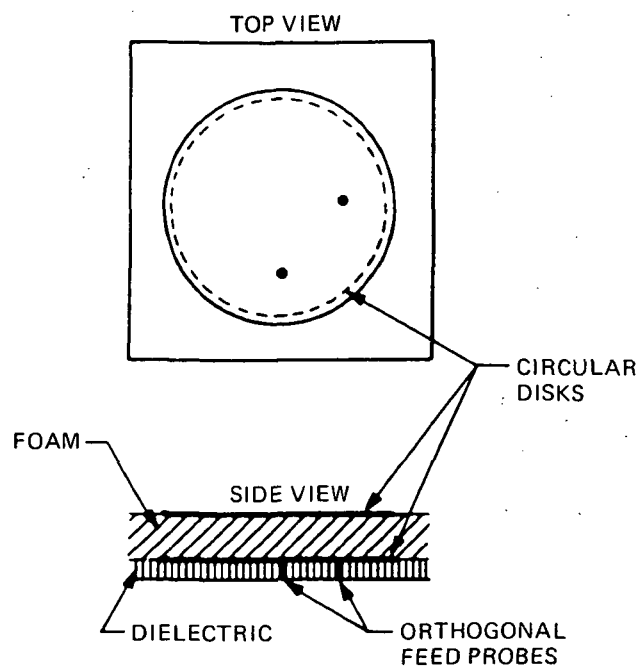


Figure 5.1.9. Stacked Dual Resonant Microstrip Element Developed by Ball Aerospace Corporation

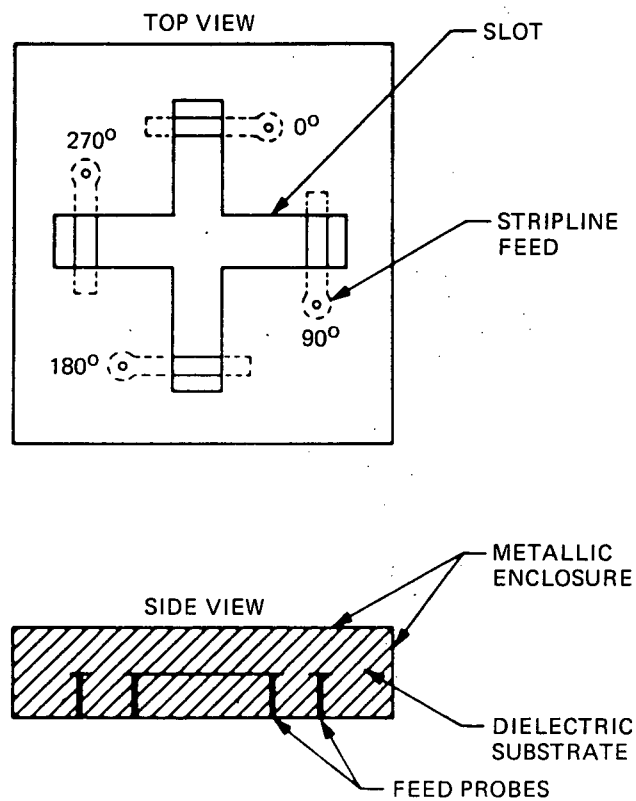


Figure 5.1.10. Stripline-Fed Crossed-Slot Radiator Developed by Teledyne Ryan Electronics

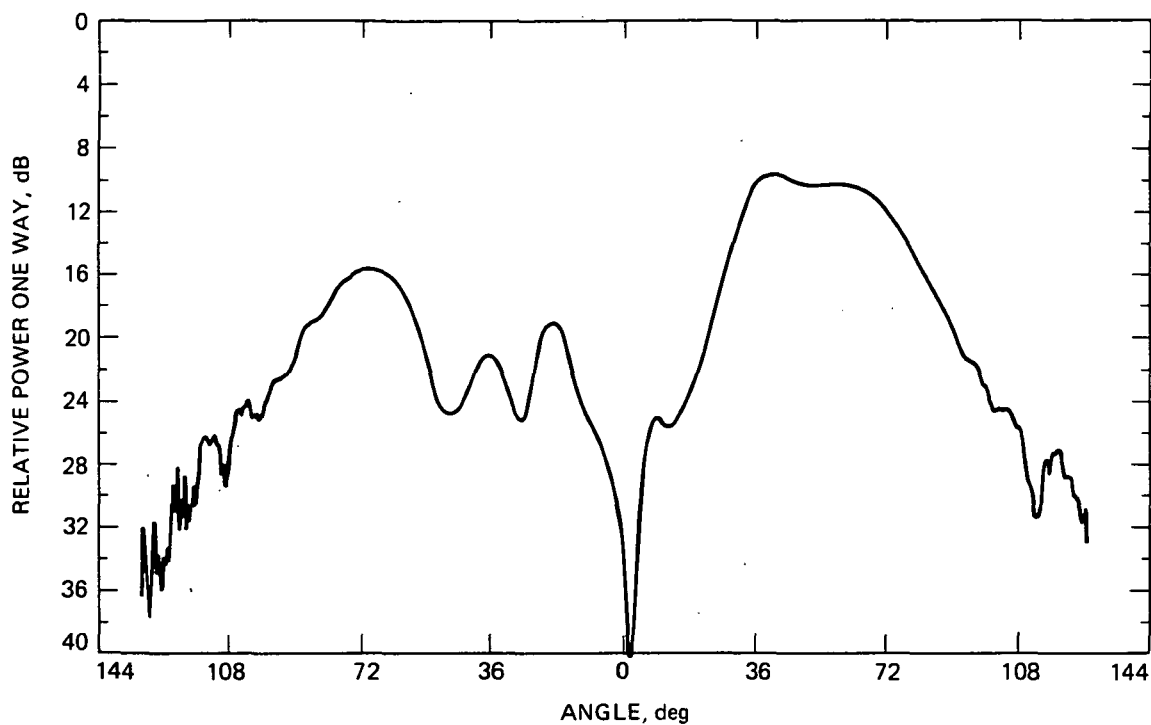


Figure 5.1.11. Typical Elevation Radiation Pattern of TRE Phased Array Antenna. $\theta_s = 30^\circ$ elevation, $\phi_s = 0^\circ$ azimuth.

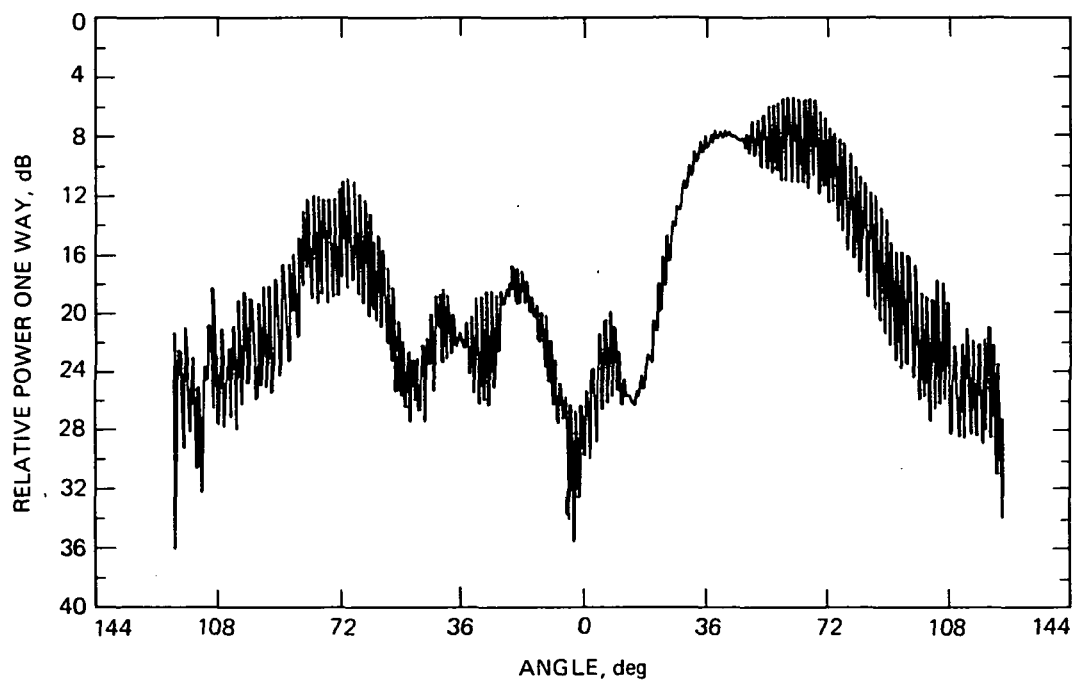


Figure 5.1.12. Typical Elevation Pattern Showing Axial Ratios for TRE Phased Array Antenna. $\theta_s = 30^\circ$ elevation, $\phi_s = 0^\circ$ azimuth.

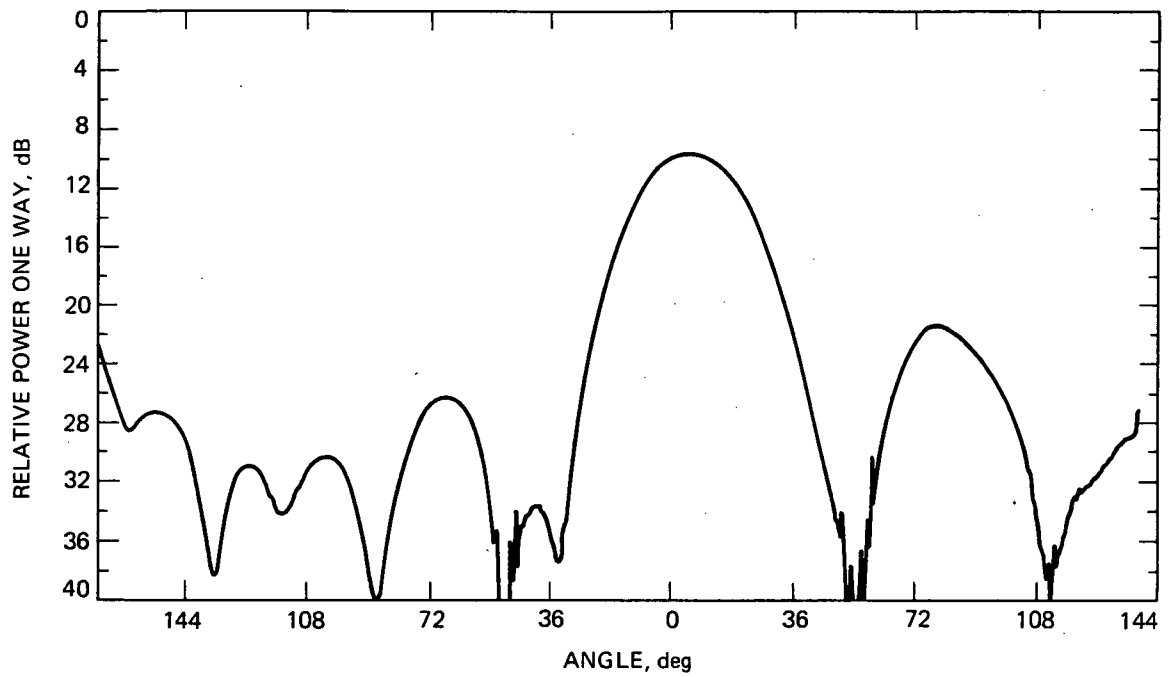


Figure 5.1.13. Typical Azimuth Radiation Pattern of TRE Phased Array Antenna. $\theta_s = 30^\circ$ elevation, $\phi_s = 0^\circ$ azimuth.

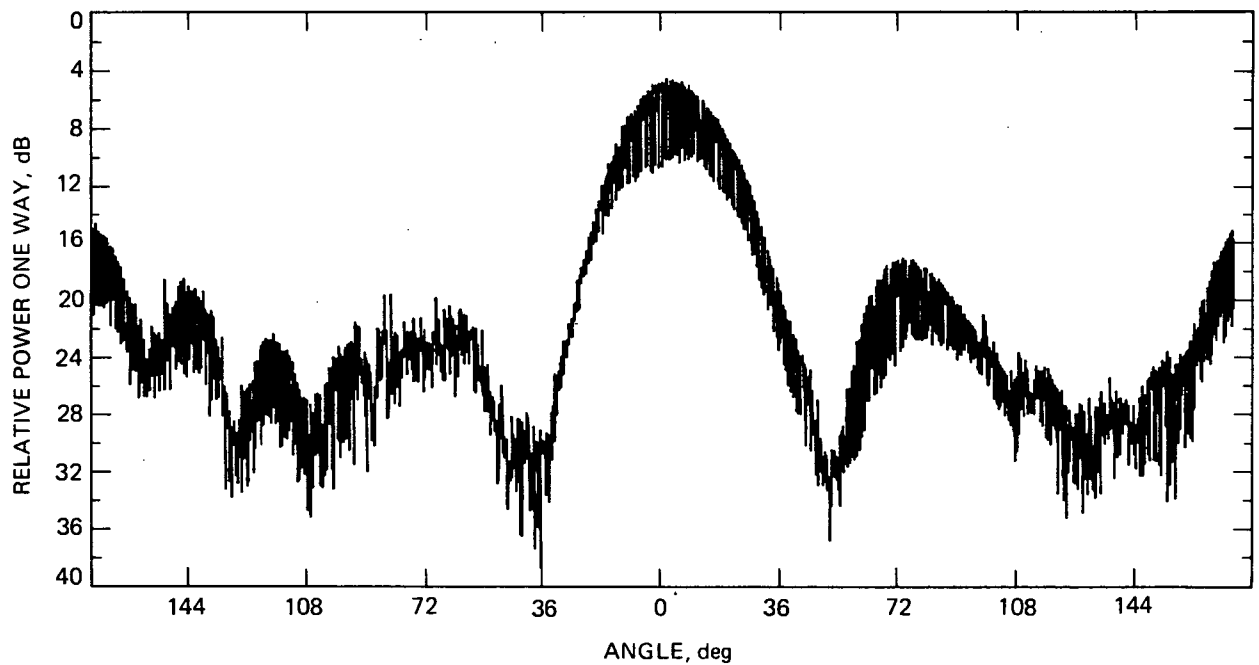


Figure 5.1.14. Typical Azimuth Pattern Showing Axial Ratios for TRE Phased Array Antenna. $\theta_s = 30^\circ$ elevation, $\phi_s = 0^\circ$ azimuth.

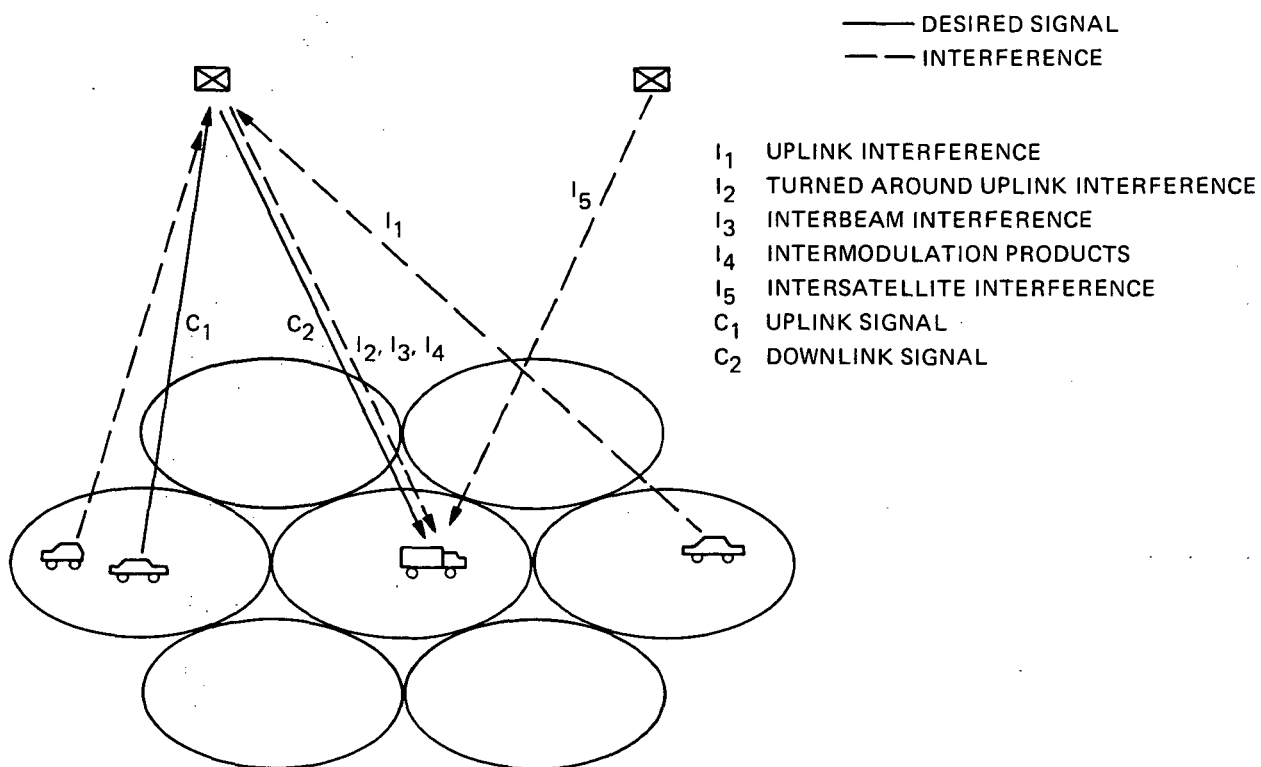


Figure 5.2.1. A Worst-Case Interference Scenario in MSS. Mobile-to-mobile links will pass through a gateway, but that does not generally alter the interference at L-band.

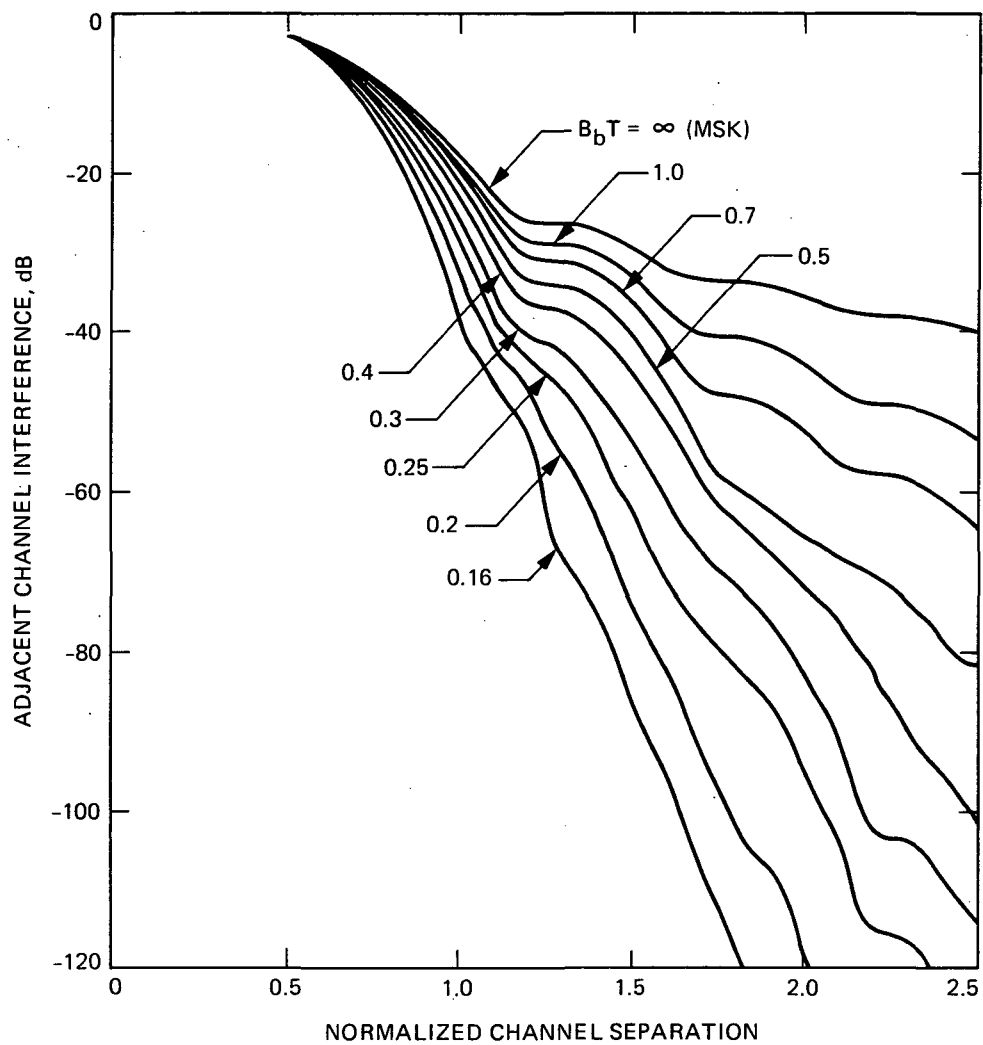


Figure 5.2.2. Adjacent Channel Interference for GMSK

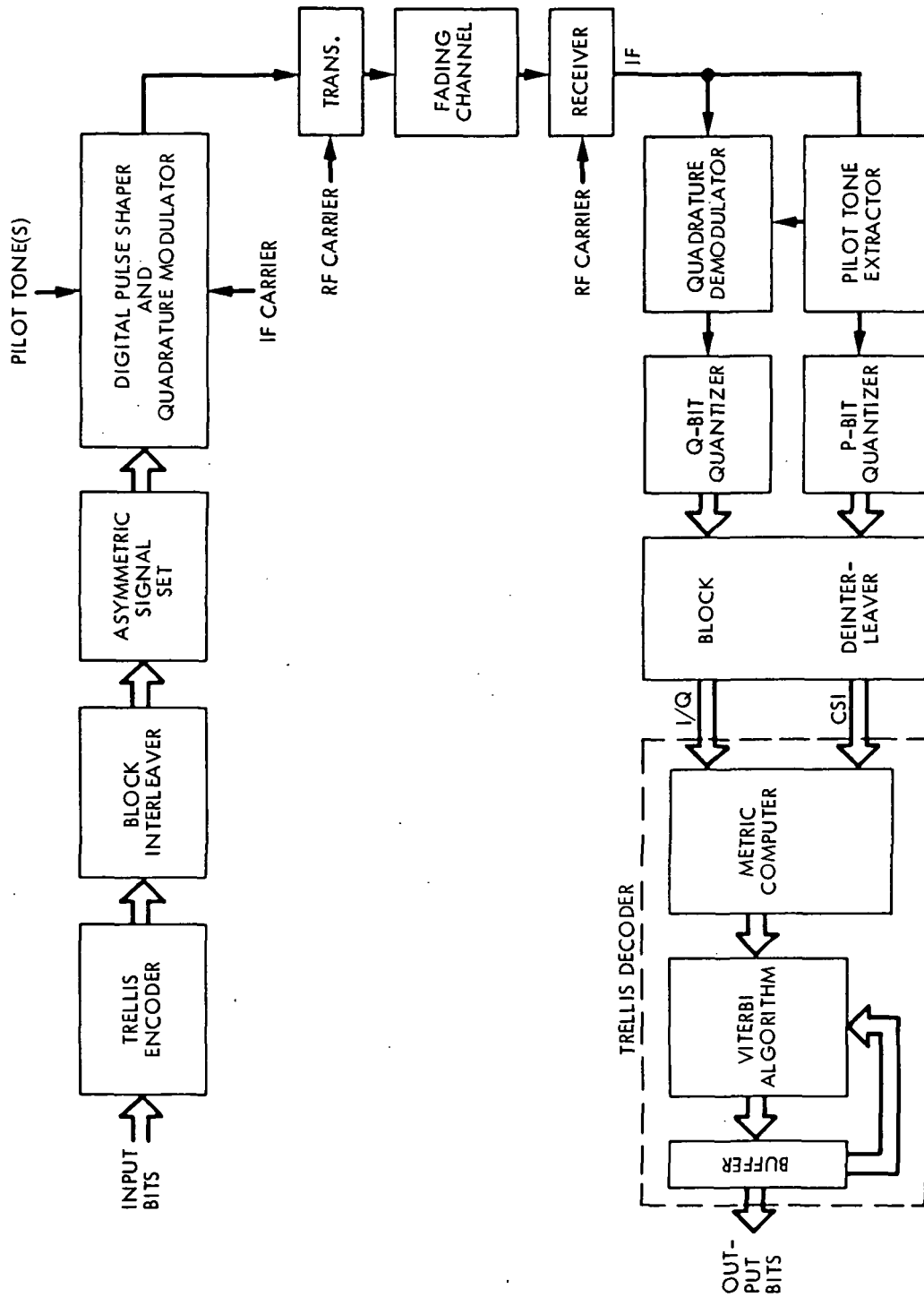


Figure 5.2.3. System Block Diagram for Coherent TCM/8PSK. CSI = Channel State Information.

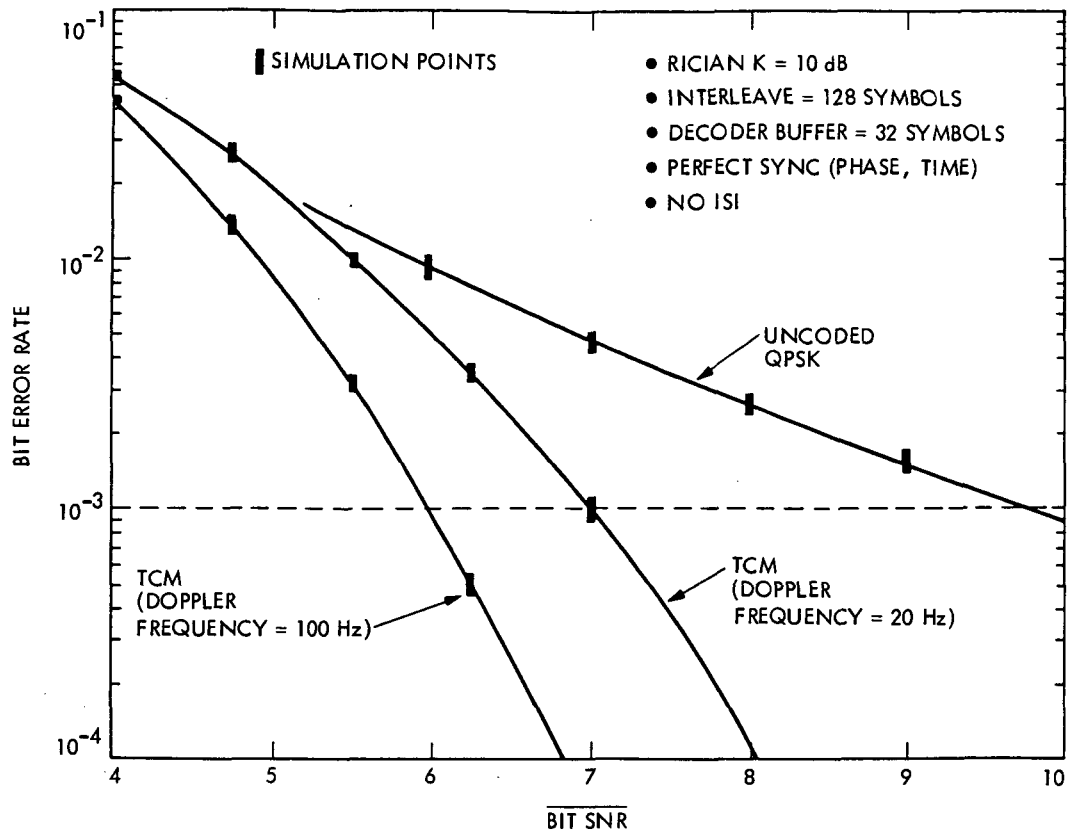


Figure 5.2.4. Performance of Rate 2/3, 16-State Trellis-Coded 8PSK Modulation (TCM/8PSK) Over Rician Fading Channel With CSI (Ideal Coherent Detection) and Interleaving

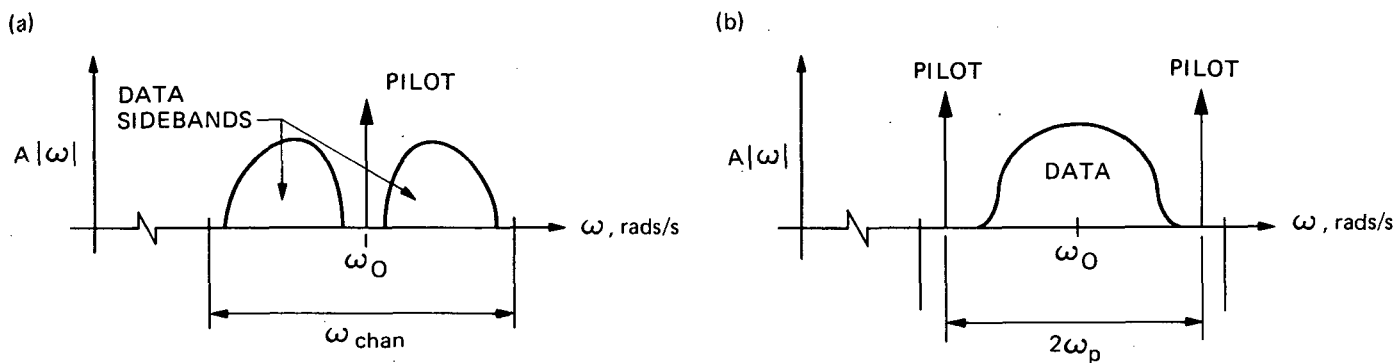


Figure 5.2.5. Two Versions of the Tone Calibrated Technique (TCT): (a) TCT Spectrum With Single Tone, and (b) DTCT Spectrum

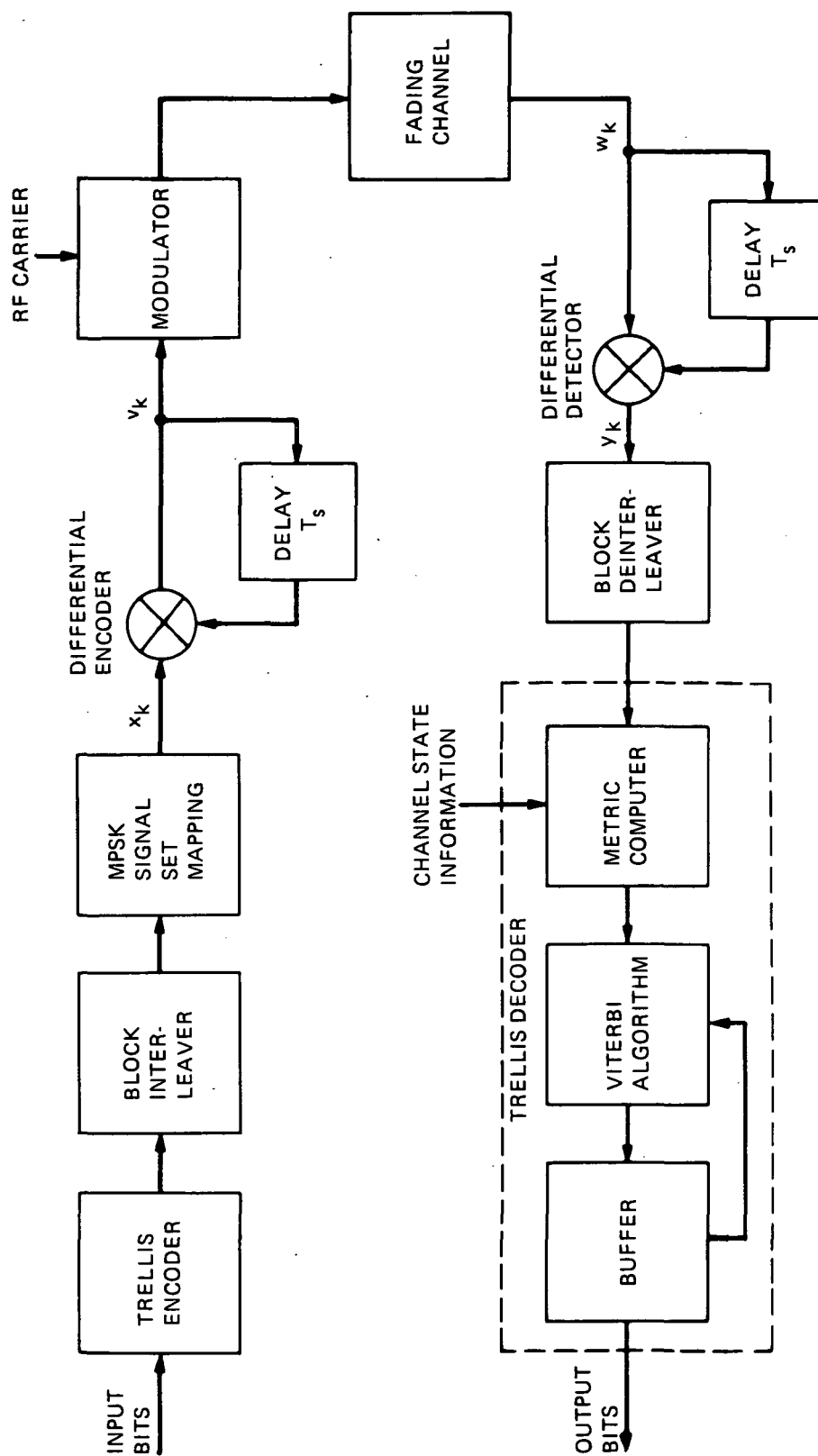


Figure 5.2.6. Block Diagram of Trellis-Coded MDPSK System

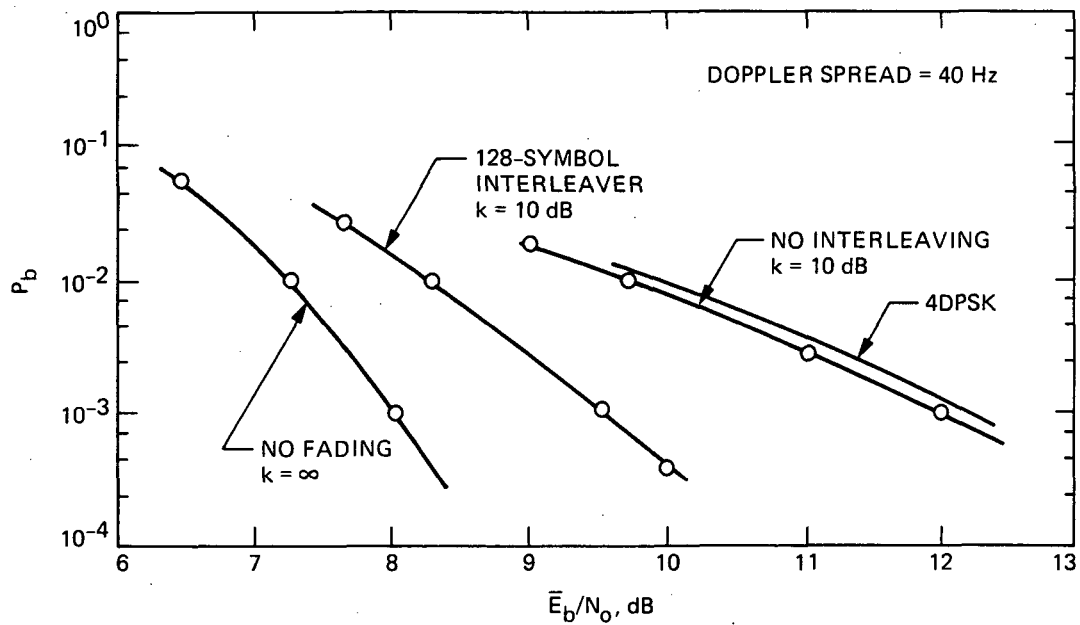


Figure 5.2.7. Simulation Results for Bit Error Rate Performance of Rate 2/3, 16-State Trellis-Coded 8DPSK (TCM/D8PSK)

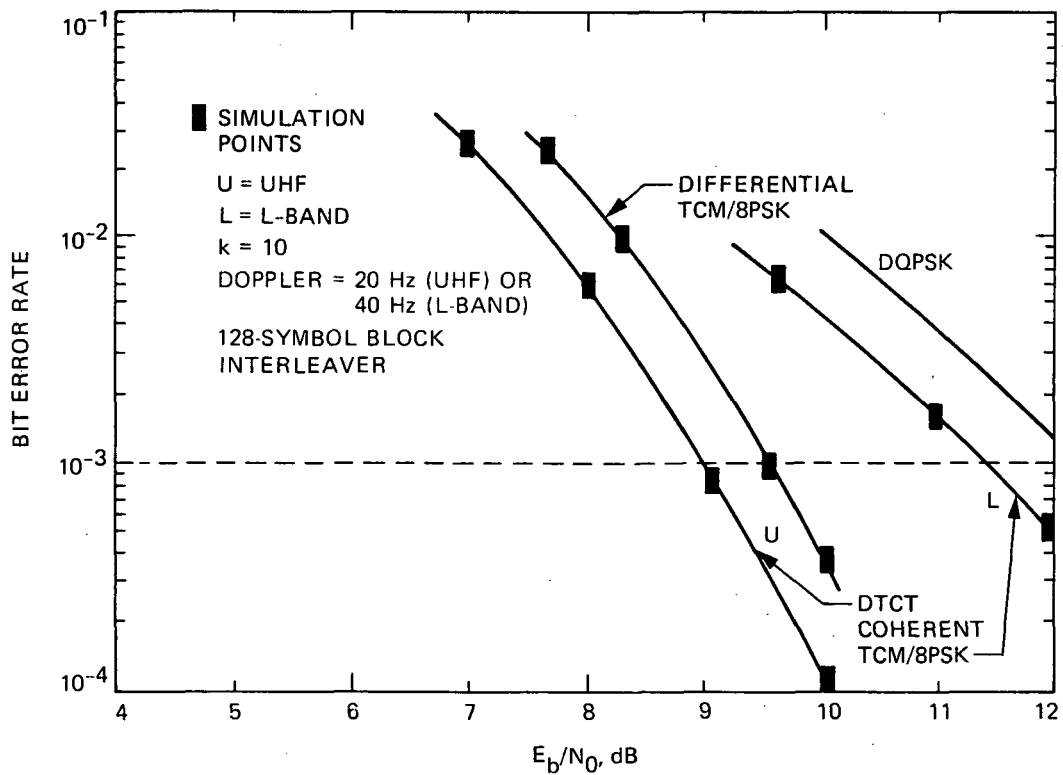


Figure 5.2.8. Comparison of TCM/D8PSK With Coherent TCM/8PSK (Using DTCT With Noisy Pilot) at UHF and L-Band.

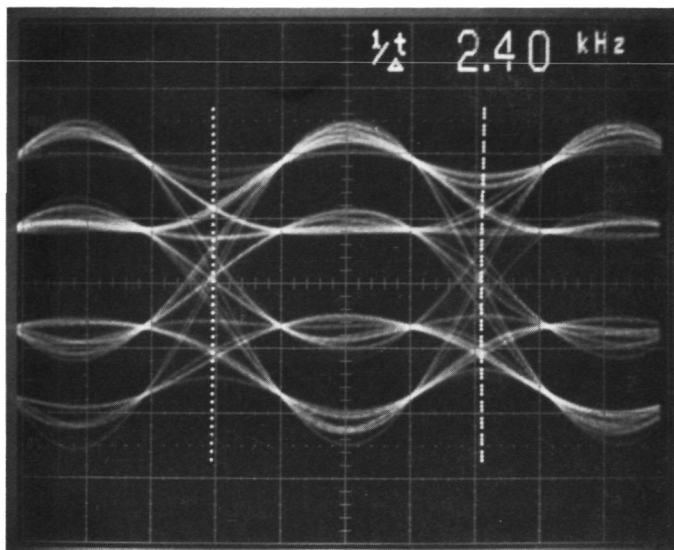


Figure 5.2.9. Eye Diagram of Root Raised-Cosine Pulse Shaping With 100% Excess Bandwidth

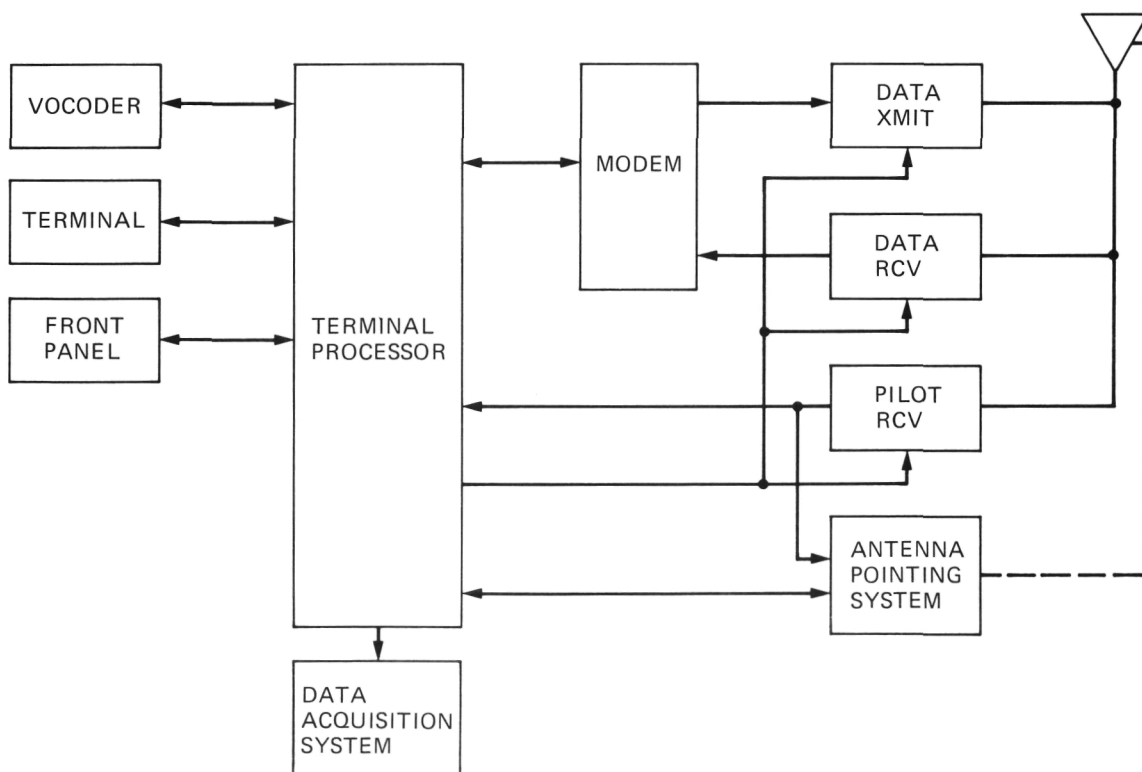


Figure 5.2.10. Mobile Terminal Block Diagram

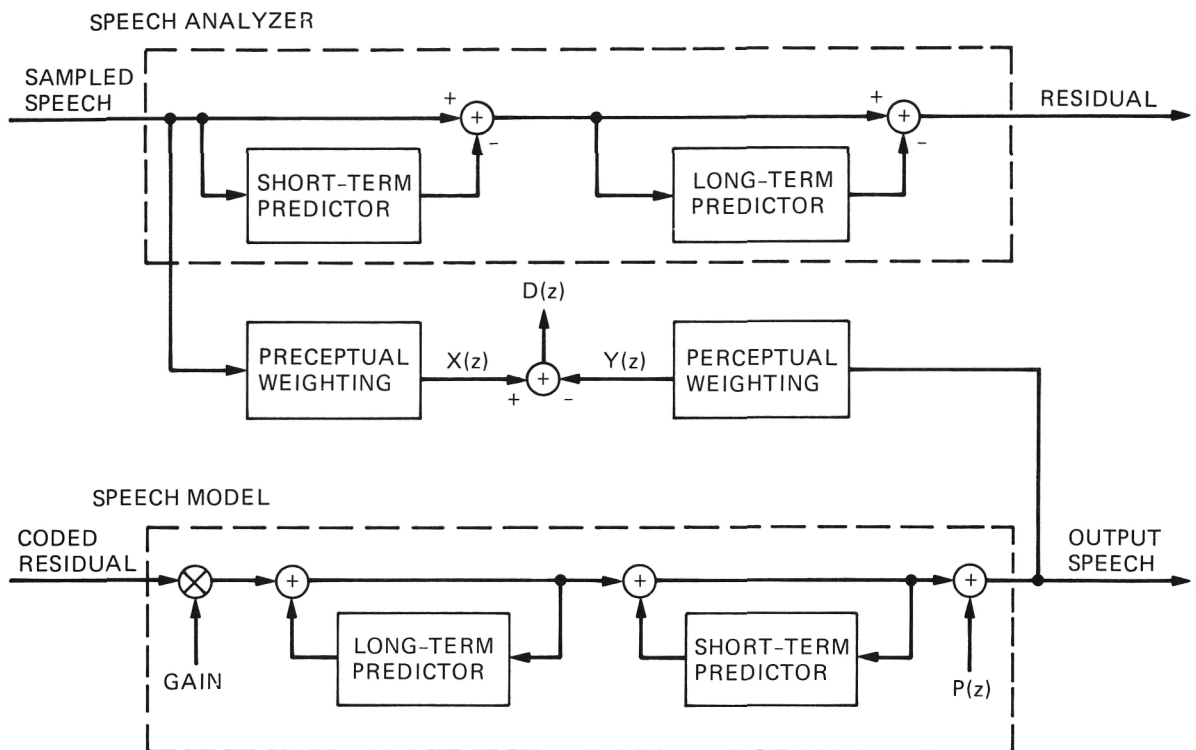


Figure 5.3.1. Model of LPC Speech Coders

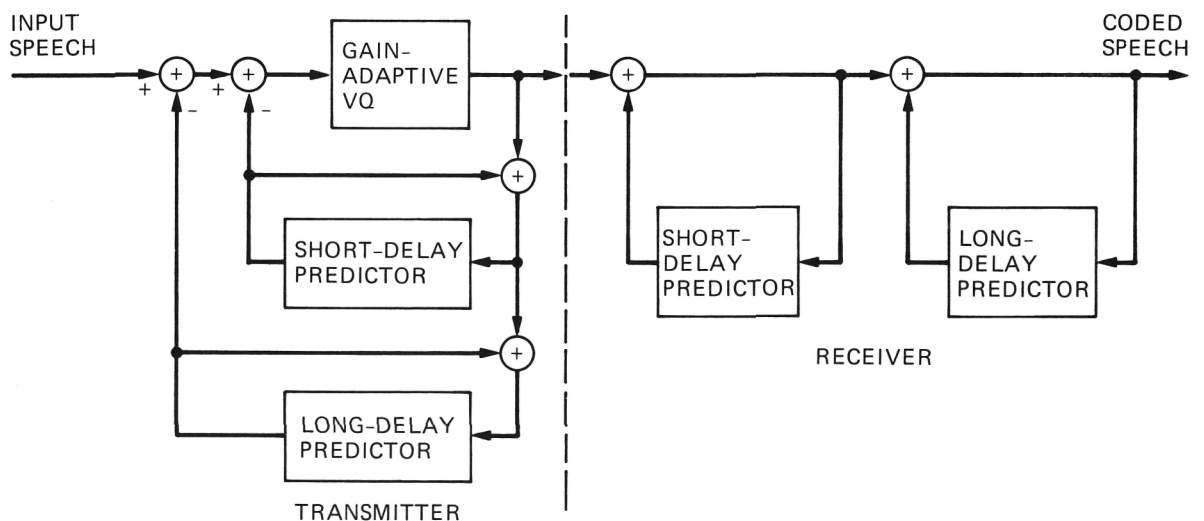


Figure 5.3.2. VAPC Functional Block Diagram

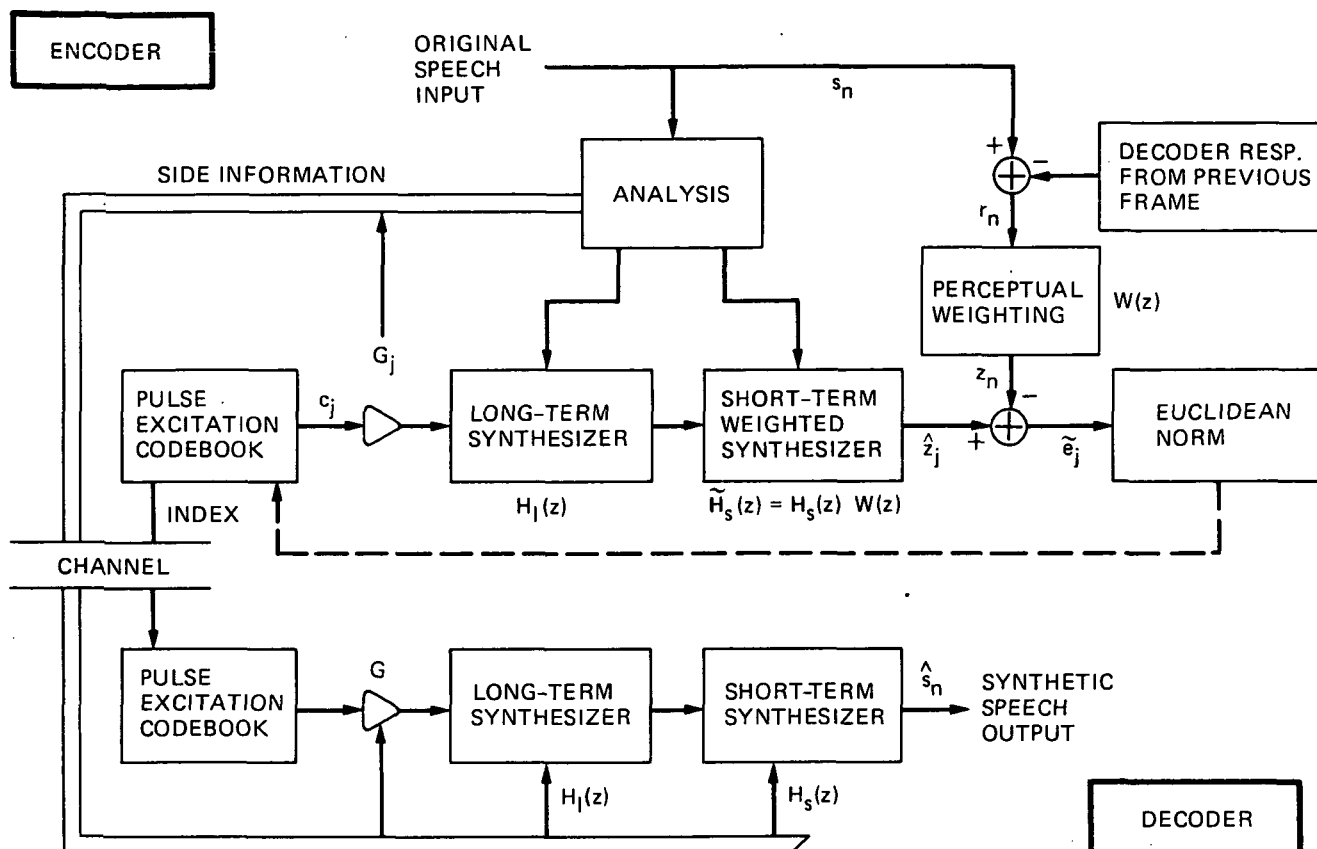


Figure 5.3.3. Block Diagram of VXC Speech Coder

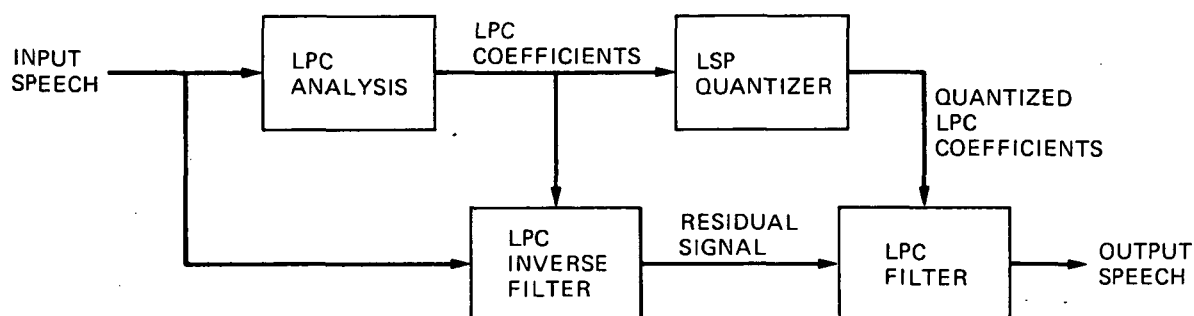


Figure 5.3.4. LSP Quantization System Concept Developed by GIT for the SEV

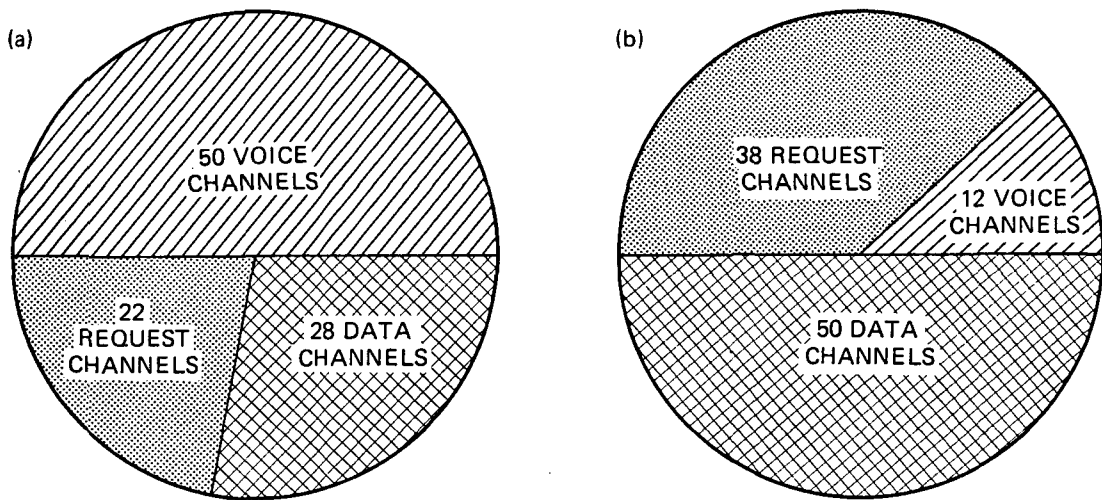


Figure 5.4.1. An Illustration of Channel Partitioning at Two Instants of Time: (a) This Partition Supports 25 Voice Calls per Minute and 3600 Data Messages per Minute, and (b) This Partition Supports 4 Voice Calls per Minute and 6600 Messages per Minute

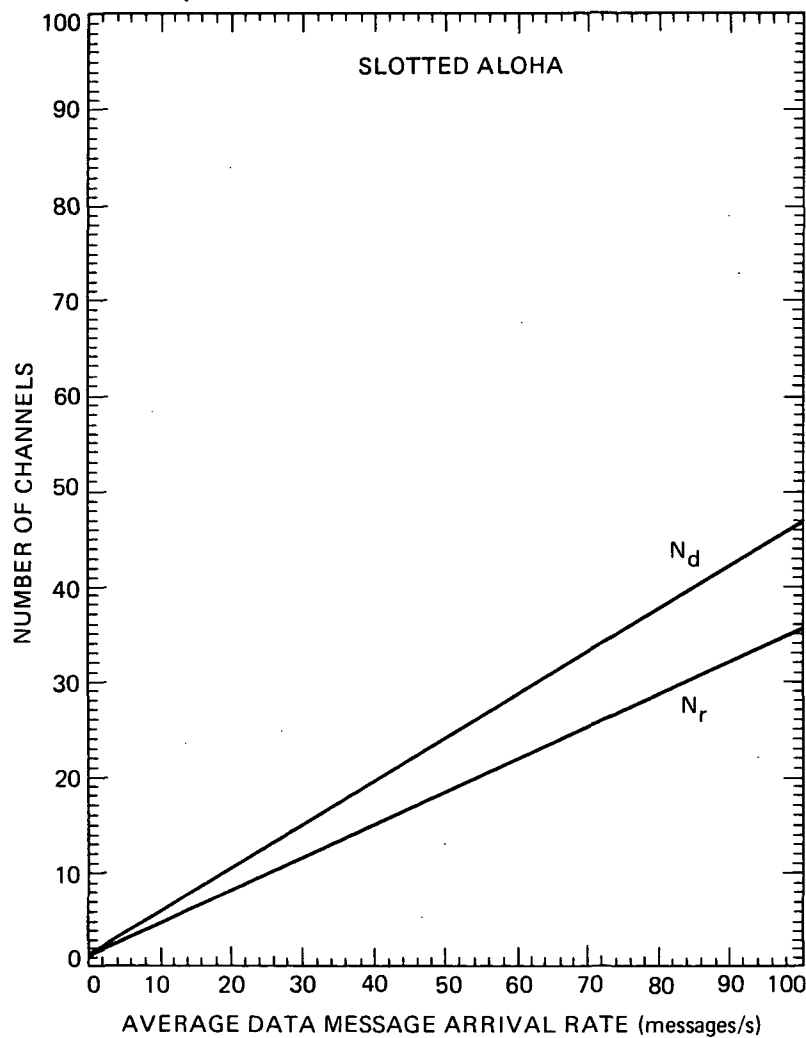


Figure 5.4.2. Number of Request Channels (N_r) and Data Channels (N_d) Versus Data Message Arrival Rate

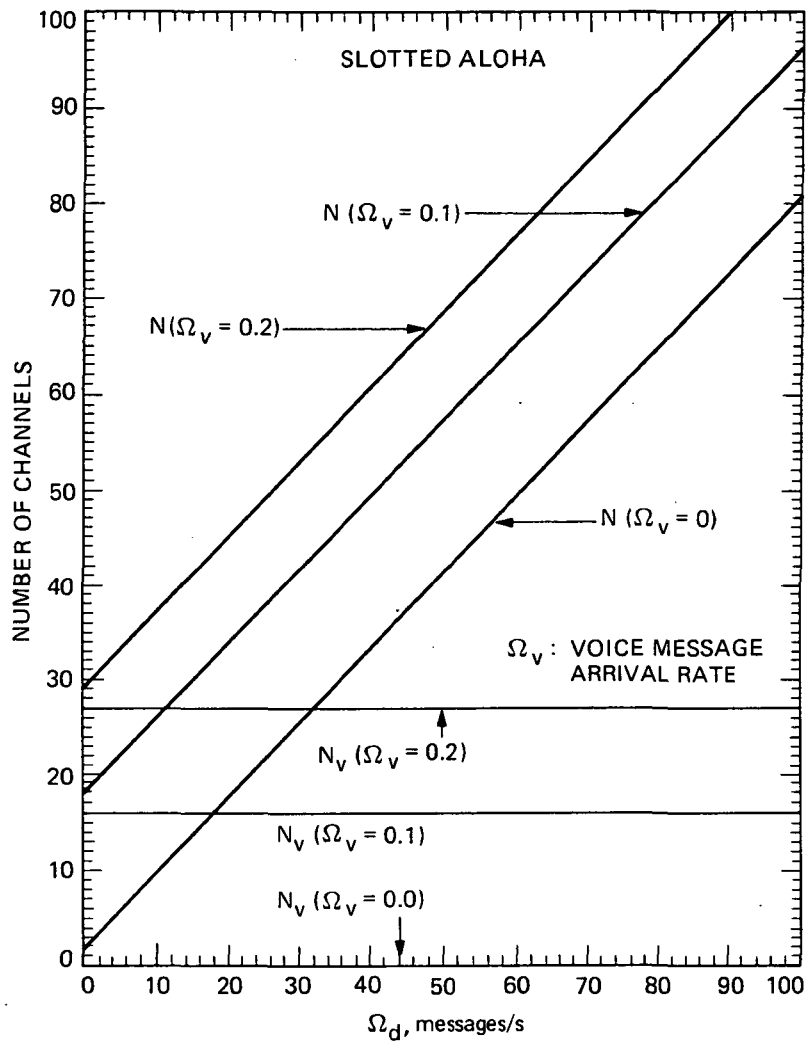


Figure 5.4.3. Number of Voice Channels (N_v) and Total Number of Channels (N) Versus Message Arrival Rate (Ω_d)

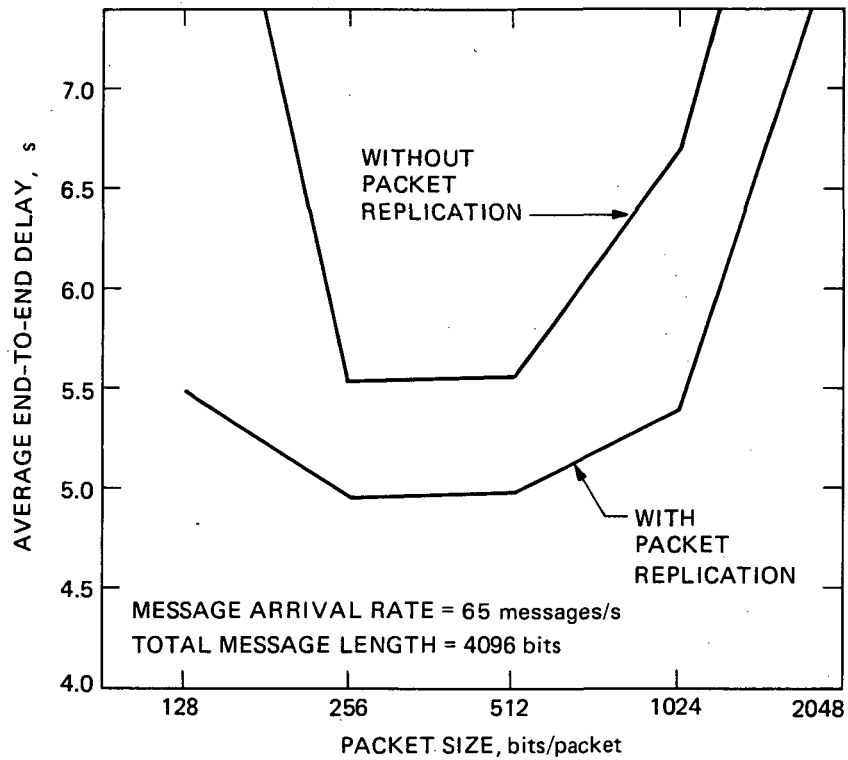


Figure 5.4.4. Average End-to-End Delay Versus Packet Size When Arrival Rate = 65 Messages/s

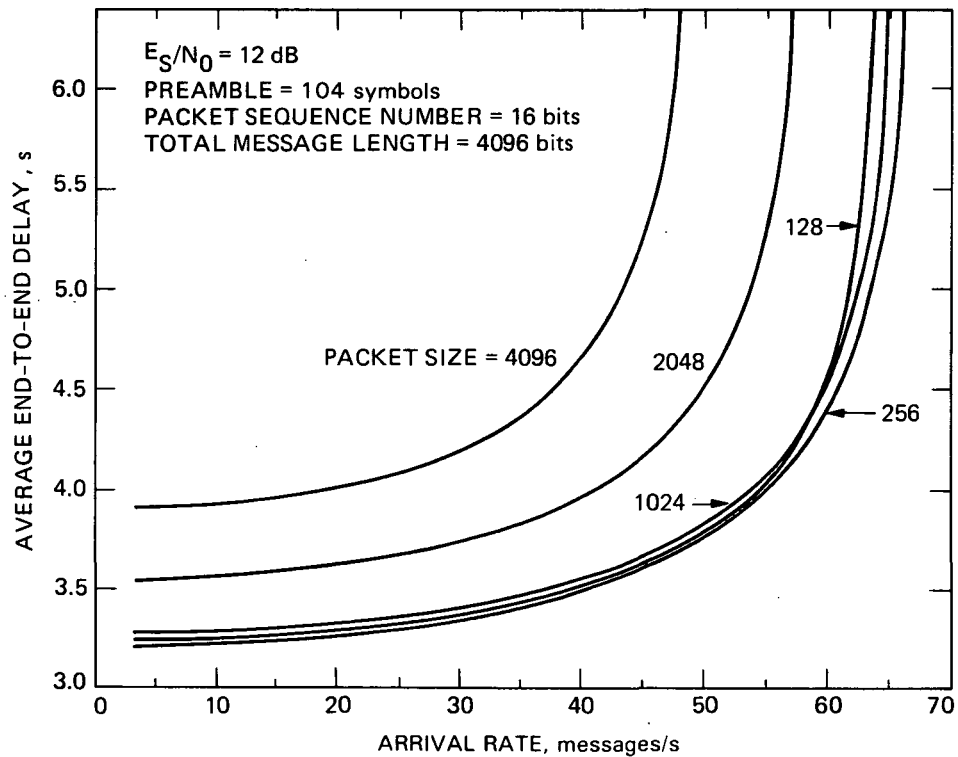


Figure 5.4.5. Average End-to-End Delay Versus Closed-End Traffic for Various Packet Sizes (Total Message Length = 4096 bits)

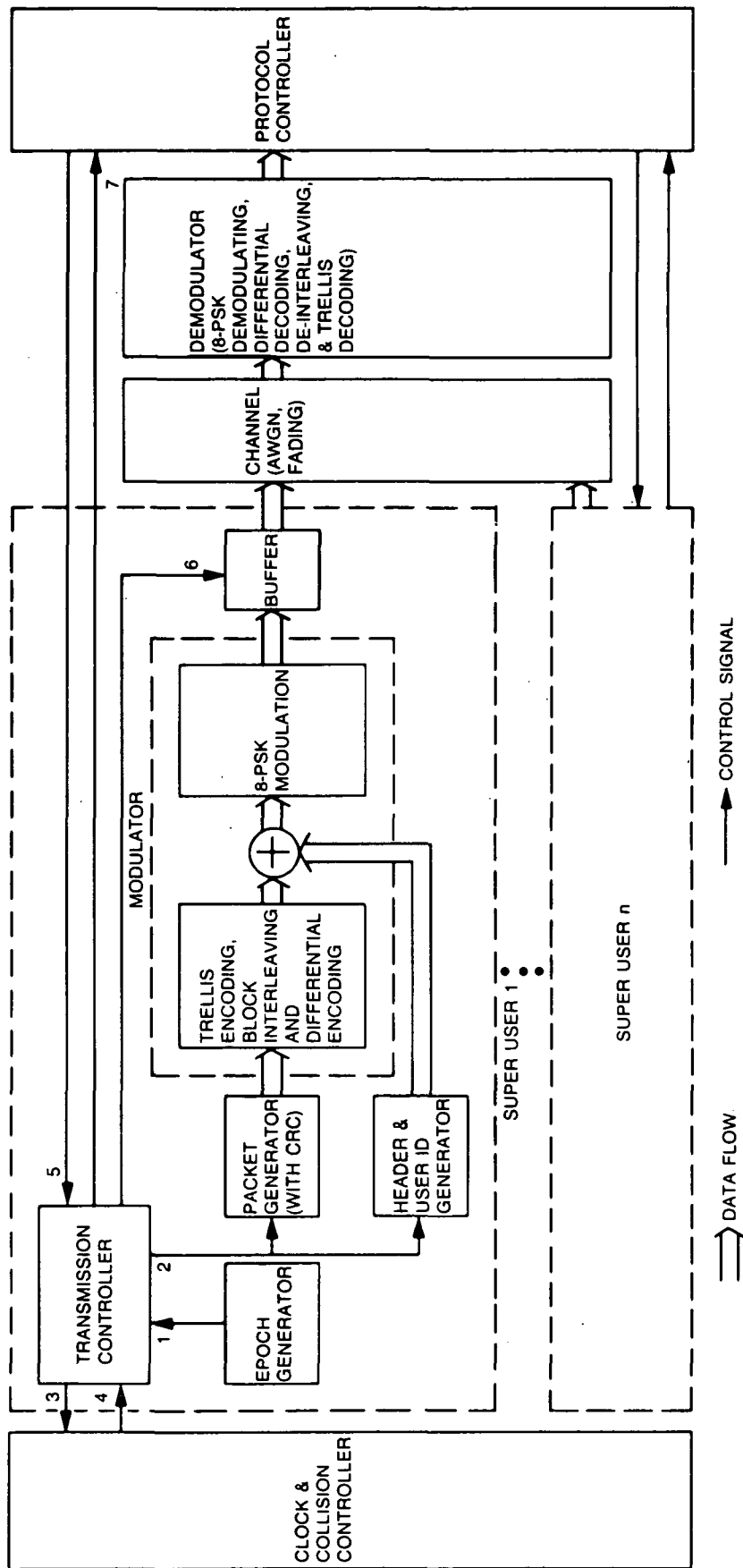


Figure 5.4.6. Block Diagram of the Simulator for the Request Channel of MSAT-X

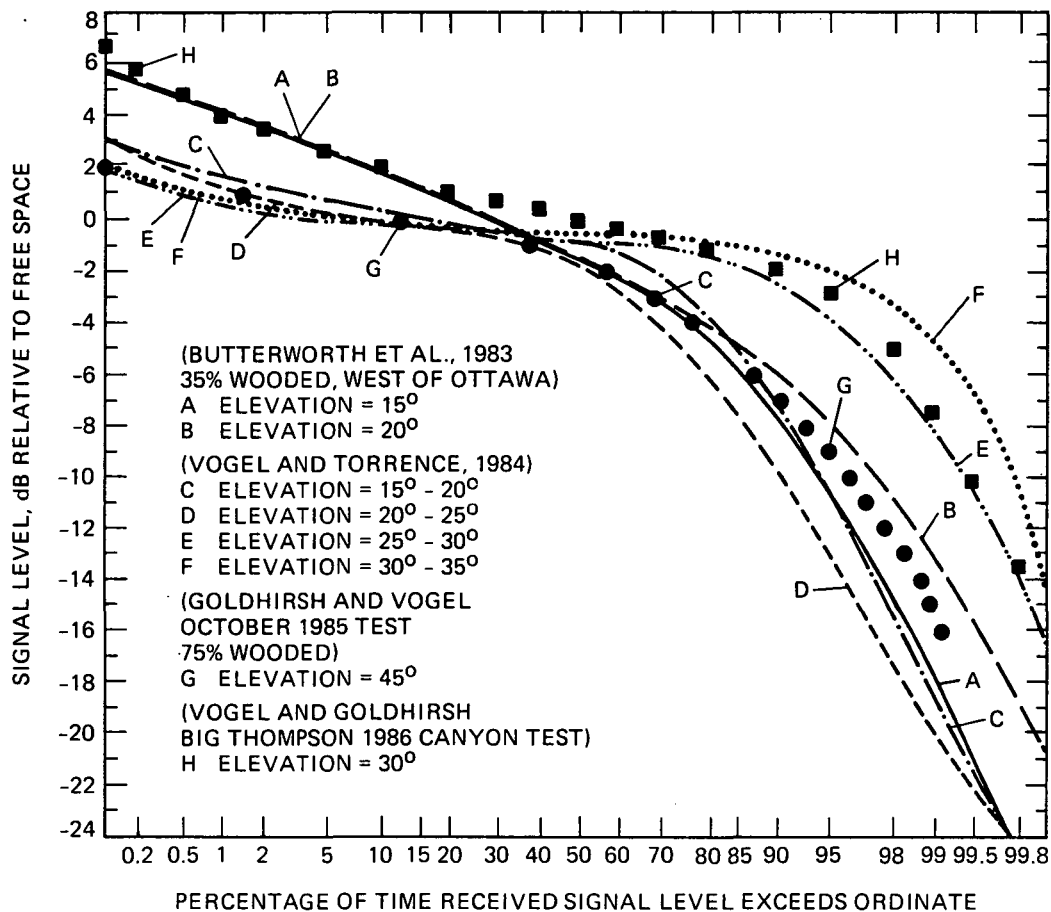


Figure 5.5.1. Cumulative Signal Level Distributions for Various Geographic Locations and Elevation Angles. See [Bostian, 1987] for references cited.

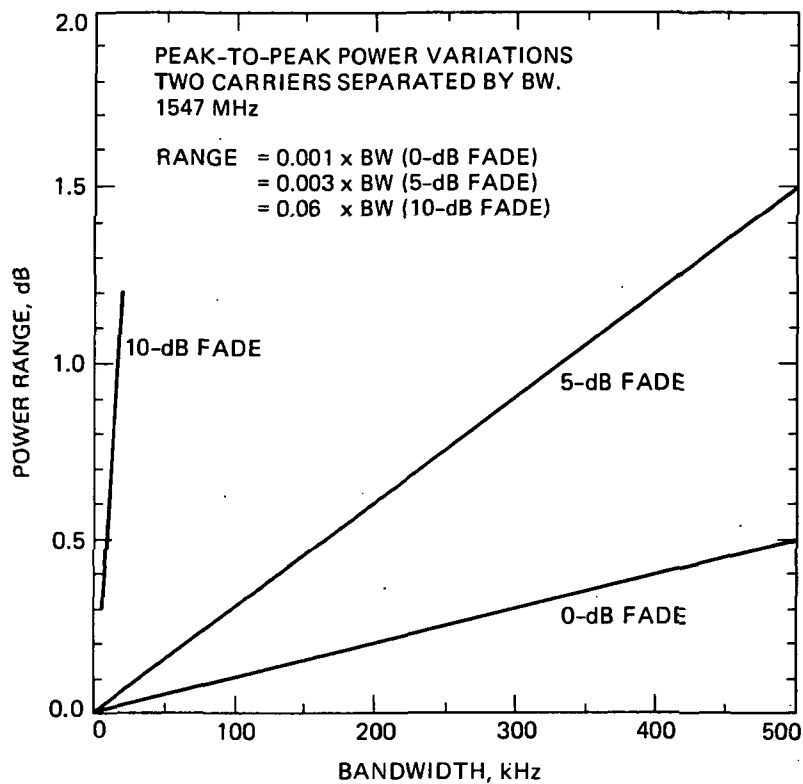


Figure 5.5.2. Predicted Peak-to-Peak Power Variation as a Function of Channel Bandwidth. (Bandwidth = 5 kHz for MSAT-X.)

SECTION 6

RESULTS OF MSAT-X: RECOMMENDED TECHNOLOGY UTILIZATION FOR MSS

6.1 INTRODUCTION

MSAT-X has been concerned with the development of ground segment technology to promote the realization of mobile satellite systems. In line with this, the focus here will be on arriving at the recommended manner of utilizing the developed ground segment technology. Inasmuch as an MSS is an integration of space and ground segments, fitting within an overall system architecture, it is necessary to deal with the space segment to ensure that the ground segment results are consistent with a realistic space segment.

The technology recommendations given below will be for an MSS based on the fundamental system concept arrived at by NASA, JPL, and their contractors as discussed in Section 4.1. At the outset, Section 6.2 will reiterate and elucidate this system concept. This is followed by a discussion of the spacecraft. The rationale behind the spacecraft assumptions is given, and how these spacecraft attributes relate to or impact the ground segment recommendations is clarified. This sets the stage for the main thrust of this section: an exposition of JPL's recommendations on how to utilize the ground segment technologies developed under MSAT-X to achieve the most efficient and viable MSS.

6.2 BASIC MSS ARCHITECTURE

The MSS proposed by JPL is a single-channel-per-carrier (SCPC) demand-assigned FDMA system. The perceived system will provide service to the contiguous United States (CONUS). Its space segment will consist of two geosynchronous satellites, separated by 35° orbital spacing. Each satellite will illuminate the entire CONUS, providing overlapped coverage. When medium-gain vehicle antennas are used, the 35° orbital spacing will be consistent with the inter-satellite isolation that these antennas can offer. MGAs could then enable the desired orbit reuse. The two-satellite architecture also provides for continued coverage when one of the satellites is eclipsed.

As discussed earlier, in Section 4.1, the proposed architecture relies on satellite antenna multibeam technology to effect frequency reuse. Although FDMA efficiently packs as many channels as possible in the limited spectrum of Figure 3.2.1 as permitted by interference considerations, frequency reuse is necessary to achieve the necessary MSS capacity. (This topic will be revisited in the following sections.)

To optimize the utilization of the very limited frequency spectrum at L-band (Figure 3.2.1), only the links between the satellites and the mobile terminals (in either direction) will be at L-band frequencies. The links between the satellites and gateway stations, base stations, or the NMC, collectively referred to as the backhaul links, will be at Ku-band frequencies. The satellites will be bent-pipe repeaters transponding from L-band to Ku-band or vice versa. There will be no direct L-band to L-band link. To avoid unnecessary congestion of the precious L-band spectrum, miscellaneous information exchanged between the NMC and fixed earth stations, e.g., a base station, could utilize a Ku-band to Ku-band cross-strap. Communications between mobile and fixed terminals will require one hop, while mobile-to-mobile communications will require two hops with a gateway station in the middle.

At the heart of the MSS architecture is the NMC. It oversees the network, controls its operation, and ensures the proper and efficient utilization of its resources. The NMC monitors the traffic and assigns channels according to the I-AMAP protocol, which dynamically partitions the channels between request, open-end, and closed-end links. The NMC also handles operational functions, such as billing.

Each link between a satellite and a mobile user will contain a data channel plus a shared pilot channel. The pilot is used as a reference by the antenna pointing system to aid the functions of satellite acquisition and tracking. In MSAT-X, all the channels are assigned a 5-kHz bandwidth. The challenge has been to transmit the highest quality voice possible, with the least power requirements attainable with a relatively inexpensive ground terminal and realistic present-day spacecraft, within this tight channel bandwidth. The challenges for any MSS will basically be the same, although

marketing considerations may demand the use of more than one bandwidth to support a wide variety of services. Whatever the eventual bandwidth(s) that will be used by an MSS operator, all technologies developed under MSAT-X are immediately applicable to an eventual MSS.

6.3 ON THE SPACE SEGMENT TO COMPLEMENT MSAT-X

Uncertainty relating to the space segment arises from the fact that the MSAT satellite(s) will depend on decisions made by the consortium of companies that will be developing the operational MSS. As mentioned earlier, agreement within the consortium on a variety of issues has not yet been achieved. Nevertheless, for MSAT-X purposes it is possible to make generic assumptions about the satellite(s) that should be valid for reasonable and expected choices of spacecraft. This is achieved by relying on present-day spacecraft technology and using designs that are consistent with a realistic state-of-the-art ground segment. This reflects the goal of obtaining the most efficient utilization of proven concepts while minimizing risk.

In a first-generation MSS, the satellite (or two satellites, if a two-satellite configuration is assumed for the first generation) would be designed using an existing commercial high-power communication satellite bus. A satellite would employ two deployable L-band communication antennas with a 4.2-m (14-ft) diameter. Although existing satellite buses are capable of deploying a larger antenna [Sue et al., 1985; Ford Aerospace, 1985; and RCA Astro Electronics, 1985], the selected antenna size represents approximately the upper limit that can be launched by the Shuttle without requiring unfurlable reflector technology. The antennas would be stowed during launch and deployed in orbit. One of these antennas would be used for reception of the L-band signals, while the other would be used for transmission. Separate transmit and receive antennas alleviate the problem of passive intermodulation which often exists in high-power communications satellites using a shared antenna for transmission and reception [Ford Aerospace, 1985, and Hoeber et al., 1986]. The gain of the L-band antenna is about 33.7 dB at 1.5 GHz and 34.3 dB at 1.6 GHz, and the corresponding 3-dB beamwidths are about 3.2°. The G/T of the satellite receiving system at L-band is 4 dB/K. (These figures

will be used later, in the link budgets of Section 6.4.2.) Four beams would be needed to illuminate the entire CONUS, as illustrated in Figure 6.3.1.

The satellite would be equipped also with a 0.4 m antenna to support the Ku-band communication link. This antenna, which has a 31.2-dB transmit gain and a 32.3-dB receive gain, produces a single beam covering the service area. The satellite receiving system at Ku-band has a corresponding G/T of 21 dB/K.

The MSS satellite would likely employ a high-power and a low-power transmitter in each beam in order to provide services to users with different mobile terminals. The high-power transmitter would serve the users with low-gain terminals, while the low-power transmitter would serve the users with medium-gain terminals. The separate-transmitter design alleviates the intermodulation and power-robbing problems associated with unequal carrier power amplification. The Ku-band and L-band power amplifiers could be implemented using solid-state devices and designed to operate at 5-dB backoff to reduce intermodulation products. The overall efficiency of the transmitters would be about 25%.

The realistic assumptions outlined in the above paragraphs will be reflected in the link power budgets to be given in Section 6.4.2. These budgets will tie together the space and ground segments for a conceived first-generation MSS. They will demonstrate the feasibility of the links, and lead into the system capacity results presented in Section 6.4.3.

6.4 TECHNOLOGY RECOMMENDATIONS FOR MSS

The technology recommendations presented in this section are based on the MSAT-X research performed at JPL. The evolution and results of the technology research have been summarized in Section 5. As mentioned above, in Section 6.2, the results of the technology research will be immediately applicable to any eventual MSS, particularly to an MSS with an architecture based on an SCPC FDMA concept as explained and advocated in Sections 4.1 and 6.2.

Because a consortium of U.S. companies will be developing the operational MSS, it is likely that, to accommodate the desires of the different participants, the eventual system may contain a mixing and matching of a variety of technologies. It is JPL's aim at this point to put forth what it believes is a consistent set of recommended ground segment technologies that, when integrated in the manner identified by JPL, would create a union more effective than the individual parts, with the result being an MSS that would most efficiently utilize its scarce resources and hence be most viable.

Since the thrust of MSAT-X has been ground segment technologies, the mobile terminal technologies are treated at some length in the following subsection. Again, since the mobile terminal is a part of an overall system, the mobile terminal technologies are quantitatively tied to the remainder of the MSS through the link budgets of Subsection 6.4.2 and the system capacity results of Subsection 6.4.3.

6.4.1 Mobile Terminal Technologies

In the five subsections to follow, the recommendations are given starting with the overall architecture for the mobile terminal. The architecture organizes the subsystems around a central processor. This is elucidated first. In the subsections that follow, the recommendations for the subsystems are given starting at the beginning of the link with the speech coder, then the modem, the transceiver, and finally the antenna. The issue of networking is addressed later, in Section 6.4.3.

6.4.1.1 Mobile Terminal Architecture. The mobile terminal consists of several subsystems linked together under the management of a central controller called the terminal processor. This is identified clearly in Figure 5.2.10. The figure depicts a modular design built around the terminal processor. Two strong reasons have made this architecture ideally suited to MSAT-X, and also make it the recommended approach for a mobile terminal in an operational MSS.

The first attractive feature is that the modular design easily supports the evolutionary development and upgrade of the different subsystem components such as the vocoder, modem, and transceiver. This modularity would easily allow for the substitution of subsystem options (different antennas, transceivers, vocoders, etc.) either to upgrade the system as technologies mature, or simply to fulfill the needs of the particular user. The change in interfaces would be handled mostly by modifying the software in the terminal processor (assuming that the appropriate controls on the hardware were exercised).

The second attractive feature in the architecture is the presence of the terminal processor acting, in essence, as the brain of the terminal, capable of combining information from the different subsystems it supervises and making global decisions. For example, if the modem senses the loss of signal while the pilot is still present, the terminal processor would interpret the event as a fade in the data channel and subsequently take appropriate action according to the length of the fade. By virtue of being the mobile terminal's master controller, the terminal processor becomes a central authority that coordinates diverse yet related functions such as pilot acquisition sequences and burst transmission timing for the slotted ALOHA scheme. It also serves as the primary human interface and carries out the requirements of the networking protocol.

6.4.1.2 Speech Coding. In a variety of mobile applications, both analog and digital voice have been suggested. Analog voice uses either FM or amplitude companded single sideband (ACSB). FM is spectrally inefficient and consequently unsuitable for MSS. ACSB needs a higher signal-to-noise ratio, but may generally degrade more gracefully than digital voice under reduced signal conditions. As pointed out in Section 5.3.1, digital voice has been viewed as a promising approach with major future potential for the MSS application. It has therefore been the choice adopted in MSAT-X.

The speech coders developed for MSAT-X and recently delivered have been designed with the fading channel in mind. Special frame synchronization features to handle outages are inherent in the vocoder designs. To date, the best speech quality has been obtained from the vector adaptive predictive

coding (VAPC) vocoder. This technique was developed at UCSB and implemented in a compact form using a customized DSP-32 board. (See Section 5.3, and for further detail see [SYSDOC, Section 4].) Preliminary results indicate that the speech quality, robustness, and suitability to the mobile environment is superior to that obtained from the self-excited vocoder developed at GIT.

Preliminary subjective testing has shown that the speech quality of the VAPC is "fair to good." The voice is natural-sounding, intelligible, and free of processor-induced anomalies such as bleeps. Although it does not yet meet the desired near-toll-quality, it is much superior to the 2400-bps "communication quality" speech obtainable by the standard LPC-10 vocoder, which actually sounds synthetic and suffers from loss of speaker identification.

A recommendation as to which speech coding scheme is definitely superior will be made at the end of the contracts. This will occur in late summer/early fall of 1988. As was previously noted, the preliminary results indicate that the VAPC algorithm developed by UCSB currently produces the best speech quality. With further refinement of the algorithm, true near-toll-quality speech may be attainable. Speech quality improvement is indeed an ongoing process. The refinement process, however, will eventually reach a point of diminishing return. Such a point has not yet been reached.

A development that is relevant to the MSAT-X speech coding effort is the study under way at the National Security Agency (NSA) which aims to evaluate a host of vocoders that have become available recently. Fourteen speech coders, which operate at 4800 bps and have been developed by institutions as prominent and diverse as AT&T, Motorola, Entropics, UCSB, and GIT, are being considered. A military-standard 4800-bps vocoder should soon emerge from this evaluation. The result will undoubtedly influence the broader recommendation that JPL will reach for a speech coding algorithm (or algorithms) most suited for the MSS environment. It is expected, however, that a speech coder such as the VAPC will exhibit overall performance superior to vocoders not specifically designed to handle fading outages.

6.4.1.3 Modulation/Coding. As discussed in Section 5.2, the choice for modulation and coding in MSAT-X had to evolve with MSAT-X. The necessity of using 4800-bps speech for near-toll-quality and the requirement to squeeze it through a 5-kHz bandwidth resulted in the abandonment of DMSK-type schemes suited for 2400 bps in 5 kHz for the more efficient combined modulation/coding. Extensive analytical research, aided by real-time simulation, showed that 16-state, rate 2/3 TCM 8PSK with interleaving is the scheme that can attain the required spectral efficiency (by using eight phasors) and power efficiency (by using trellis coding matched to the modulation). Moreover, with the obligatory shift to L-band from UHF, it has been concluded (see Section 5.2) that differential detection is superior to coherent detection (using some form of TCT). This was illustrated in Figure 5.2.8. The present baseline in MSAT-X has therefore become the 16-state, rate 2/3 trellis-coded differentially detected 8PSK (TCM/D8PSK for short). The best interleaving constrained by a 60-ms delay requirement (stemming from voice transmission) was found to be 128 8PSK symbols, 16 depth x 8 span, with a 32-symbol decoder buffer.

Since TCM/D8PSK is an innovative technique, a convincing argument comparing it to more established techniques becomes helpful in advocating it to the industry. This is done by first comparing the performance of TCM/D8PSK to that of DQPSK and GMSK. The comparison with DQPSK is fair because it has the same bandwidth as TCM/D8PSK for the same data rate. GMSK is included for historical reference. Table 6.4.1 gives this simple comparison of performance under typical MSS link conditions, but with no timing jitter or intersymbol interference (ISI) assumed. A 2.5-dB or more improvement is achieved by TCM/D8PSK over DQPSK under the stated conditions, and about 1 additional dB relative to DGMSK.

Obviously, on the real channel there will be ISI and timing jitter. This has been investigated at JPL on the hardware channel simulator and will also be tested in the field. Test results demonstrate a deviation within 1 dB from analysis/simulation for TCM/D8PSK on the Gaussian (AWGN) channel and the fading channel with $k = 10$ [Jedrey et al., 1988]. This is a remarkable result that demonstrates that TCM/D8PSK is not particularly sensitive to ISI and timing jitter, a common concern for 8-ary modulation

schemes. The square-root raised-cosine with 100% excess bandwidth pulse shaping discovered at JPL (see, for example, [Rafferty and Divsalar, 1988]) and used to achieve the combined features of ISI-free points and narrow spectrum is of critical importance here.

From all of the above, it is evident that the performance improvement over DQPSK and GMSK in the fading environment more than overshadows the slight increase in modem hardware complexity, which should not be of concern anyway, with today's integrated circuit and digital signal processor technologies. It therefore follows that the TCM/D8PSK baselined in MSAT-X (with its key design details) is JPL's recommendation for the modulation/coding scheme in MSS. It is also recommended that TCM/D8PSK be further demonstrated in the industry so that it will make the transition from a research environment to where it becomes commercially well established and readily implementable in an operational MSS.

6.4.1.4 Transceiver Capabilities. The transceiver requirements for an MSS represent a departure from the usual requirements for voice systems used in the communication industry. Instead of the customary use of wide bandwidth FM for voice, narrow-band digital voice is the recommended approach for MSS, as mentioned in Section 6.4.1.3. The transceiver for MSS also requires unique features; most notably, in addition to receiving the data channel, it has to receive and process the shared pilot signal transmitted from the satellite. The data and shared pilot channels occupy 5 kHz each, and the transceiver should be frequency agile, i.e., capable of selecting or tuning to the desired frequencies within the L-band frequencies of Figure 3.2.1. The receiver should also provide the pilot I and Q channel outputs (received pilot amplitude and phase information) to the steerable vehicle antenna.

The transceiver should also be capable of tracking the Doppler of the received pilot and preferably be capable of measuring it and correcting its transmitted pilot frequency. The modem in the mobile terminal requires a signal within 200 Hz of the channel center. The NMC plays the key role in correcting the major Doppler components. The NMC transmits precompensated pilot signals derived from a highly stable reference. These are used to calibrate the transponder, fixed stations, and mobile reference oscillators.

The result is correction of satellite motion and transponder oscillator drift, as well as correction of fixed station and mobile reference oscillator drifts. What remains is the contribution due to the motion of the vehicle, which can be up to 160 Hz. Depending on the implementation of the transceiver, the transmitted Doppler (on the return from the mobile terminal) may be double this amount, which is obviously undesirable.

A brass board transceiver with received Doppler tracking has been designed, implemented, and used in MSAT-X tests at JPL. Future plans call for including transmit Doppler correction and full frequency control by the terminal processor as per the architecture given above in Section 6.4.1.1 (Figure 5.2.10).

6.4.1.5 Vehicle Antennas. The vehicle antenna is a critical element in the MSS link. This is because it will have a significant impact on the economics of the operational MSS. Because of the inherent antenna performance/cost trade-off, the vehicle antenna will play a major role in determining the approach through which the capital investor will realize the return on his investment. Several key system issues are related to the vehicle antenna through the trade-off of the mobile terminal contribution versus the satellite contribution to the overall link performance. Some in the industry consortium, for example, feel that a very low cost vehicle antenna should be used in conjunction with spacecraft with higher EIRP. (Unfortunately, there is more than simple engineering performance to influence that choice of approach.) On the other hand, others feel that a more sound and less risky approach would utilize medium-gain vehicle antennas. This would basically make the user pay more in advance rather than per minute. The point to be accentuated here is the complexity of the vehicle antenna issue. With this in mind, JPL has adopted an approach that maintains as many viable options as possible. In the following paragraphs, JPL's impartial position based on technology research and engineering assessment is summarized.

As mentioned earlier (see, for example, Section 5.1), to alleviate the spacecraft power burden (and permit the use of a lower-risk spacecraft design), to enable orbit reuse, and to reduce the deleterious effects of

multipath, JPL views a medium-gain vehicle antenna as a necessity. It should be noted, however, that this does not preclude supplementary use of low-gain antennas, as will be pointed out next.

A user with a low-gain antenna (LGA) would have to pay more per minute of service and perhaps per month in service charges to account for the higher-power, and certainly more expensive, spacecraft. The extra cost is related to the differences in gain and G/T between the LGAs and MGAs. The difference in minimum gain is expected to be at least 4 to 5 dBic, and the difference in G/T at least 5 dB. This does not take into account the effects of multipath interference or sensitivity to background blackbody radiation, which could, in effect, reduce the G/T of an LGA significantly more than that of an MGA [Bell et al., 1988]. Ongoing testing will accurately determine these figures.

There are, in any event, two fundamental problems with using LGAs. The first is that an omni antenna illuminates all the geosynchronous arc over CONUS; hence, multi-satellite operation would not be possible in any frequency band used by the LGAs. (It would be very difficult to achieve the axial ratio required in that case to effect inter-satellite isolation.) The second problem, which is less severe, pertains to the performance in a multipath environment. In the following we will elaborate on these two issues.

An MSS based only on one spacecraft, i.e., with no orbit reuse, would probably not have sufficient capacity to ensure a viable system. (See Section 6.4.3.) It is unlikely that an MSS can be based solely on the use of LGAs--some hybrid with MGAs would be needed. This mixed mode of operation has its disadvantages, unfortunately. Separate spacecraft transmitters would likely be needed. A high-power transmitter would service the links with LGAs exclusively. This would avoid the problems of intermodulation and power robbing that would be experienced when different-level signals share the same high-power amplification. Even with separate transmitters, interference in a full-scale MSS would generally be increased due to a combination of two factors: a lack of directivity on the omni antennas, and increased intermodulation due to the likely need for higher, nonlinear amplification.

The second problem pertaining to LGAs is their performance in a multipath environment. Propagation results suggest that the link performance can be severely degraded due to multipath. By virtue of the LGAs' inherent radiation patterns, multipath would have a stronger degrading effect on LGAs than on MGAs. (Although the drop-off is similar by design on both antenna types, the LGAs have broader azimuthal beamwidths and thereby collect more energy from low elevation angles.) Actual voice link performance with an LGA may therefore be unacceptably poor in multipath environments. It should be noted, however, that the extent of this effect has not yet been established. Voice link performance will therefore need to be solidly established through field testing before LGAs become a real option.

Following the arguments of the above paragraphs, JPL recommends that medium-gain vehicle antenna technology be the dominant technology utilized in the MSS. Along with the choice of the MGA approach comes the choice of what kind of MGA to use. JPL believes that the MSS operator should offer all of the three options developed. The benefits of this are explored in what follows.

The mechanically steered, tilted linear array and the electronic phased array (TRE's design) have demonstrated performances that generally meet the MSS requirements (see Table 5.1.2). The phased array has a somewhat lower performance at low elevation angles and slightly less multipath rejection, but faster reacquisition. In addition, the planar mechanical array is expected to perform at least as well as the phased array of similar size, but at a cost about half that of the phased array (see Section 5.1). The trade-off is, therefore, mostly a cost-versus-conformity or appearance trade-off. For utility-type vehicles, the cheaper linear array is the obvious choice. For trucks, the linear array is the choice unless a conformal design would significantly enhance fuel efficiency for long distances. If the conformal design is desired, the planar mechanical array would probably be the choice. For passenger vehicles, the mechanical planar array may be a good alternative to the very attractive but quite expensive phased array. The phased array would probably be the choice when concealing the antenna becomes of primary importance, as with such agencies as the FBI and the CIA. It should be noted that reliability data with long-term testing may also have an impact on the

choice of the antenna and may depend on the user's environment. In conclusion, it is JPL's view that maintaining all the MGA options available has the potential of increasing the user base for the MSS.

6.4.2 Link Budgets

The link budgets given below serve the following purposes. First, they demonstrate that with reasonable space segment assumptions, the recommended system architecture and mobile terminal technologies lead to the desired link performance. Second, they provide insight into the contributions of MSS' different segments so that no part will be overdesigned. Third, they provide information needed for obtaining estimates of system capacity. The system capacity, in turn, leads to further insight into the efficacy of the ground segment technologies.

The budgets reflect the assumptions about the space segment outlined in Section 6.3. They also reflect the ground segment performance that has been demonstrated as explained throughout Section 5. For example, the 9.9-dBi vehicle antenna gain and the receiver G/T are consistent with the numbers provided in Table 5.1.2. Also, the required E_b/N_0 is consistent with the results of Figure 5.2.7 and accounts for the actual hardware losses observed in the experiments reported in Section 5.2.

It should be noted that the budgets of Tables 6.4.2 and 6.4.3 are still preliminary in nature. They are not intended to provide precise results or to reflect a firm straw-man design for the MSS. In that spirit, a simple noise contribution analysis is used to assess channel interference, and no preliminary tolerance values are given.

The most prominent observation to be made regards the margin available on the L-band links. The budgets indicate the availability of about 3 dB of margin. This number, although not intentionally provided as a fading margin, is adequate to provide protection in the event of moderate multipath fading (see Figure 5.5.1, curve H). It cannot, however, overcome deep fades or the effects of shadowing. This observation is in line with the well-accepted premise that the MSS is a line-of-sight system.

6.4.3 System Capacity

It is interesting, and, in fact, enlightening, to have at least a rough estimate of the system capacity based on the link budgets given above. This places in perspective the utilization of the MSS resources that result from the design and technology recommendations of MSAT-X.

Using the figure provided in the link budgets for the transmitted power per channel, with 25% HPA efficiency, and allowing for the power consumption by the K-band and other spacecraft subsystems, a rough estimate of the spacecraft power and weight requirements can be obtained [Sue et al., 1985]. A satellite of 5000-lb geostationary transfer orbit (GTO) mass and with 3 kW of spacecraft power can support a number of channels, in the range of 2000. The exact number depends on several factors, viz., the traffic mix, channel duty cycle, and service quality. For example, assuming that the service quality has a 2% blocking probability and a 3.2-s message delay, that the user traffic is one 90-s voice call or one 4096-bit data message per hour, and that 40% of the traffic is attributed to voice, the satellite would support 1929 channels. According to I-AMAP, these would be partitioned into 204 voice channels, 260 data channels, and 1465 reservation channels. (The seemingly large number of reservation channels can be reduced if the message delay requirement can be relaxed.) With this partitioning, a total of about 89,000 users could be accommodated by the satellite, corresponding to about 50 users per channel.

With about 2000 5-kHz channels per satellite, the required spectrum would be 10 MHz. Frequency reuse can be applied to achieve a reduction in the spectrum. However, only limited reuse is possible with the first-generation satellite beam layout shown in Figure 6.3.1. The outer (east and west) beams can use the same frequencies to reduce the overall spectral occupancy by a factor of 4/3. A look back at the spectrum allocations of Figure 3.2.1 and Table 3.2.1 then reveals that a first-generation MSS, based on the technologies of MSAT-X, would probably be either close to or not quite spectrum-limited. This indicates that the full utilization of the MSAT-X technologies will not occur until second-generation MSS satellites become available. These advanced spacecraft would utilize large multibeam antennas (say, 15 m at L-band). Those

antennas would alleviate any remaining power deficiency and concurrently permit a considerably larger number of channels per satellite. Hence, because they are both power- and bandwidth-efficient, the technologies developed under MSAT-X are well-suited to alleviating the power deficiencies of a first-generation MSS, as well as to resolving the spectrum limitations of later-generation mobile satellite systems.

Table 6.4.1. Comparison of the Performances of TCM/D8PSK, DQPSK, and Differential GMSK (DGMSK) Under Typical MSS Link Conditions (No ISI or Timing Jitter)

	E_b/N_o at $BER=1 \times 10^{-3}$ ($k = 10$; ~ 40 -Hz Doppler Spread)	Relative Bandwidth (BW) (Main Lobe; Also 99% BW)
DQPSK	12.2	1
DGMSK (BT = 0.5)	13	1.6
TCM/D8PSK (R = 2/3; 16-state 128 8PSK Symbol Interleaving)	9.5	1

Table 6.4.2. Forward (Ground-to-Mobile) Link Budget for BER = 1×10^{-3} (4800-bps TCM/D8PSK in 5 kHz;
Four Satellite-to-Mobile Beams)

Ground to Satellite						Satellite to Mobile					
PDF ^a	Design	Fav. ^a Tol. ^a	Adv. ^a Tol. ^a	Mean	Var. ^a (X0.01)	Design	Fav. Tol.	Adv. Tol.	Mean	Var. (X0.01)	
Transmitter Parameters											
(1) Transmit Power (dBW)	TRI	0.00	0.30	0.30	0.00	1.50	-1.00	0.30	-1.00	1.50	
(2) Transmit Circuit Loss (dB)	REC	-2.00	0.50	0.50	-2.00	8.33	-1.60	0.20	-1.60	1.33	
(3) Antenna Gain (dBi)	TRI	49.60	1.00	1.00	49.60	16.67	33.70	1.00	33.70	16.67	
(4) EIRP(DBW)		47.60			47.60		31.10		31.10		
(5) Pointing Loss (dB)	TRI	-1.00	0.50	0.50	-1.00	4.17	-0.10	0.05	-0.10	0.04	
Path Parameters											
(6) Space Loss (dB)		-206.90			-206.90		-188.31		-188.31		
Frequency (MHz/GHz)		13.20					15.52				
Range (km)		40,000					40,000				
(7) Atmospheric Attenuation (dB)	TRI	-1.50	0.20	0.20	-1.50	0.67	-0.10	0.02	-0.10	0.01	
(8) Edge of Beam Loss (dB)	TRI	-4.00	0.50	0.50	-4.00	4.17	-3.00	0.50	-3.00	4.17	
(9) Multipath Loss (dB)	GAU	0.00	0.00	0.00	0.00	0.00	0.00	0.00	0.00	0.00	
(10) Shadowing Loss (dB)	DEL	0.00	0.00	0.00	0.00	0.00	0.00	0.00	0.00	0.00	
Receiver Parameters											
(11) Polarization Loss (dB)	TRI	-0.50	0.20	0.20	-0.50	0.67	-0.50	0.20	-0.50	0.67	
(12) Antenna Gain (dBi)	TRI	32.30	0.50	0.50	32.30	4.17	9.90	0.50	9.83	6.06	
(13) Pointing Loss (dB)	TRI	0.00	0.00	0.00	0.00	0.00	-0.40	0.04	-0.40	0.03	
(14) Received Signal Power (dBW)		-134.00			-134.00		-151.41		-151.48		
[sum of (4) to (13)]											
(15) System Temperature (DBK)	GAU	28.28	0.40	0.49			25.28	0.49	0.46		
Circuit Loss (dB)		-1.50	0.20	0.20			-0.85	0.13	0.13		
Receiver NF (dB)		2.50	0.10	0.20			0.86	0.10	0.10		
External Antenna Temperature (K)		200.00	0.00	0.00			0.00	0.00	0.00		
Internal Antenna Temperature (K)		35.00	10.00	10.00							
Received N ₀ (dBW/Hz)	GAU	-200.32	0.40	0.49	-200.36	2.17	197.60	>>>>	>>>>	2.50	
[(15) - 228.6 dBW/Hz]											
Bandwidth (kHz)		5.00					5.00				
Channel Performance											
(17) Received C/N ₀ (dB · Hz)		66.31			66.36		51.91		51.82		
[(14) - (16)]											
(18) Effective C/N ₀ (dB · Hz)	GAU	63.63			63.65		51.09		51.02		
Overall C/I (dB)							23.46	1.00	23.46	11.11	
Interbeam Isolation							27.00	1.00	27.00		
Intersatellite Isolation							99.00	0.50	99.00		
Intermodulation Isolation	TRI	30.00	1.00	1.00	30.00	16.67	26.00	1.00	26.00		
Turnaround C/N ₀	GAU						63.63		63.65	59.17	
N ₀ (Up)/N ₀ (Required)		0.10			0.00		0.10		0.00		
Modem Loss (dB)		0.00			57.81		47.81		47.81		
Required C/N ₀ (dB · Hz)		57.81					11.00				
Required E _v /N ₀ (dB)											
(20) Performance Margin		5.82			5.84	0.77 (1σ)	3.28		3.21	1.02 (1σ)	

^aPDF = Probability Density Function; Fav. Tol. = Favorable Tolerance; Adv. Tol. = Adverse Tolerance; and Var. = Variance.

Table 6.4.3. Return (Mobile-to-Ground) Link Budget for BER = 1×10^{-3} (4800-bps TCM/D8PSK in 5 kHz;
Four Satellite-to-Mobile Beams)

Mobile to Satellite										Satellite to Ground			
PDF	Design	Fav. Tol.	Adv. Tol.	Mean	Var (X0.01)	Design	Fav. Tol.	Adv. Tol.	Mean	Var. (X0.01)			
Transmitter Parameters													
(1) Transmit Power (dBW)	TRI	2.00	1.00	2.00	16.67	-10.00	0.50	0.50	-10.00	4.17			
(2) Transmit Circuit Loss (dB)	REC	-1.35	0.18	-1.35	1.08	-1.50	0.20	0.20	-1.50	1.33			
(3) Antenna Gain (dBi)	TRI	7.80	1.00	7.80	16.67	31.20	0.50	0.50	31.20	4.17			
(4) EIRP (dBW)		8.45		8.45		19.70			19.70				
(5) [(1) + (2) + (3)]													
(5) Pointing Loss (dB)	TRI	-0.40	0.04	-0.40	0.03	0.00	0.00	0.00	0.00	0.00			
Path Parameters													
(6) Space Loss (dB)		-188.86		-188.86		-205.82			-205.82				
(6) Frequency (MHz/GHz)		1653.50				11.65							
(6) Range (km)		40,000				40,000							
(7) Atmospheric Attenuation (dB)	TRI	-0.20	0.02	-0.20	0.01	-1.30	0.20	0.20	-1.30	0.67			
(8) Edge of Beam Loss (dB)	TRI	-3.00	0.50	-3.00	4.17	-4.00	0.50	0.50	-4.00	4.17			
(9) Multipath Loss (dB)	GAU	0.00	0.00	0.00	0.00	0.00	0.00	0.00	0.00	0.00			
(10) Shadowing Loss (dB)	DEL	0.00	0.00	0.00	0.00	0.00	0.00	0.00	0.00	0.00			
Receiver Parameters													
(11) Polarization Loss (dB)	TRI	-0.50	0.20	-0.50	0.67	-0.50	0.20	0.20	-0.50	0.67			
(12) Antenna Gain (dBi)	TRI	34.30	1.00	34.30	16.67	48.90	1.00	1.00	48.90	16.67			
(13) Pointing Loss (dB)	TRI	-0.10	0.05	-0.10	0.04	-1.00	0.50	0.50	-1.00	4.17			
(14) Received Signal Power (dBW)		-150.31		-150.31		-144.02			-144.02				
(14) [sum of (4) to (13)]													
(15) System Temperature (dBK)	GAU	25.06	0.53	0.50		27.87	1.49	1.34					
(15) Circuit Loss (dB)		-0.60	0.20	0.20		-2.00	0.50	0.50					
(15) Receiver NF (dB)		0.86	0.10	0.10		2.50	0.50	0.50					
(15) External Antenna													
(15) Temperature (K)		170.00	0.00	0.00		50.00	0.00	0.00					
(15) Internal Antenna													
(15) Temperature (K)		35.00	10.00	10.00		35.00	9.90	9.90					
(16) Received N ₀ (dBW/Hz)	GAU	-203.54	0.53	0.50	-203.52	2.96	-200.73	1.49	1.34	-200.65			
(16) [(15) - 228.6 dBW/Hz]										22.29			
(16) Bandwidth (kHz)		5.00				5.00							
Channel Performance													
(17) Received C/N ₀ (dB · Hz)		53.23		53.21		56.71			56.64				
(17) [(14) - (16)]													
(18) Effective C/N ₀ (dB · Hz)	GAU	52.88		52.86		51.08			51.05				
(18) Overall C/I (dB)	TRI	27.00	1.00	27.00	16.67	26.00	1.00	1.00	26.00	11.11			
(18) Interbeam Isolation													
(18) Intersatellite Isolation													
(18) Intermodulation Isolation													
(18) Turnaround C/N ₀	GAU	0.70		0.00		26.00	1.00	1.00	26.00	75.61			
(18) N ₀ (Up)/N ₀ (Required)						52.88			52.86				
(18) Modem Loss (dB)		0.00		0.00		0.70			0.00				
(19) Required C/N ₀ (dB · Hz)		49.36		49.36		47.81			47.81				
(19) Required E _b /N ₀ (dB)						11.00							
(20) Performance Margin		3.52		3.50	0.87 (1σ)	3.27			3.24	1.20 (1σ)			

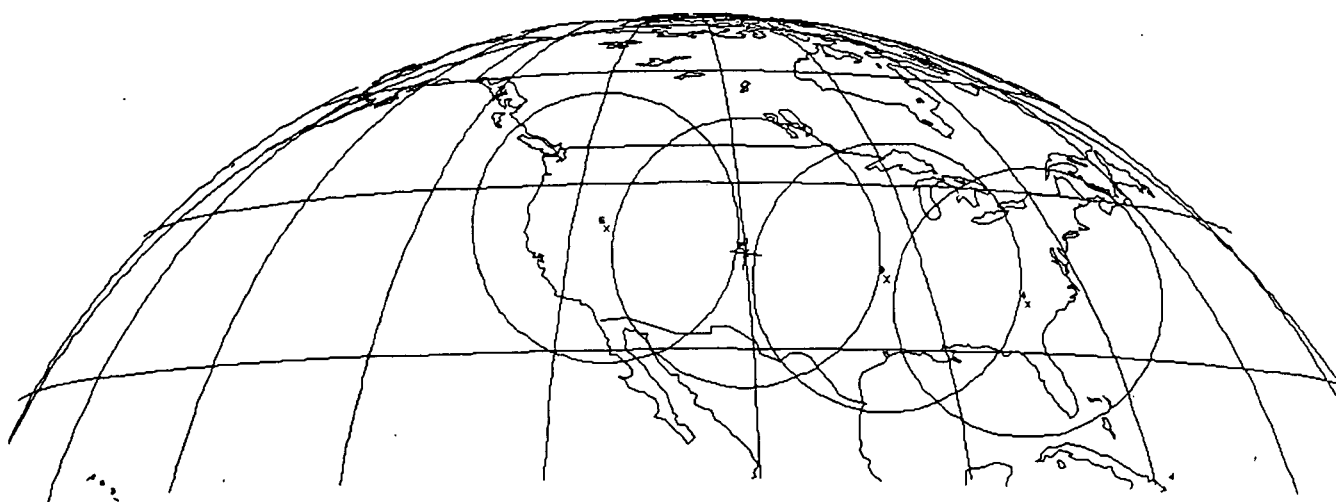


Figure 6.3.1. Multibeam Coverage of CONUS by First-Generation MSS Satellite

SECTION 7
REFERENCES

Ball Aerospace Corporation, "Concepts and Cost Trade-Off for Land Vehicle Antenna in Satellite Mobile Communications," Boulder, Colorado, July 1984.

D. Bell and F. M. Naderi, "Mobile Satellite Communications--Vehicle Antenna Technology Update," American Institute of Aeronautics and Astronautics (AIAA) Space System Technology Conference, San Diego, California, June 1986.

D. Bell et al., "MSAT-X Antennas Noise Temperature and System G/T," to appear in MSAT-X Quarterly No. 16 (JPL 410-13-16), Jet Propulsion Laboratory, Pasadena, California, July 1988.

J. Berner, "PiFEx Tower 1 Results," Proceedings of NAPEX XI, held on June 19, 1987, at the Virginia Polytechnic Institute and State University, Blacksburg, Virginia, JPL Internal Document D-4647, Jet Propulsion Laboratory, Pasadena, California, August 31, 1987.

J. Berner and R. Winkelstein, "Antenna Pointing System," MSAT-X Quarterly No. 13 (JPL 410-13-13), Jet Propulsion Laboratory, Pasadena, California, January 1988.

C. Bostian, "Propagation Studies Related to LMSS," Proceedings of NAPEX XI, held on June 19, 1987, at the Virginia Polytechnic Institute and State University, Blacksburg, Virginia, JPL Internal Document D-4647, Jet Propulsion Laboratory, Pasadena, California, August 31, 1987.

C. Cheetham, "The Terminal Processor: The Heart of the Mobile Terminal," MSAT-X Quarterly No. 12 (JPL 410-13-12), Jet Propulsion Laboratory, Pasadena, California, October 1987.

J. H. Chen et al., "Speech Coding for the Mobile Satellite Experiment," ICC 1987, Communications Research Laboratory (CRL), U.C. Santa Barbara (UCSB), 1987.

Cubic Corporation, "Trade-Off Between Land Vehicle Antenna Cost and Gain for Satellite Mobile Communications," MSAT-X Report No. 103, Jet Propulsion Laboratory, Pasadena, California, August 1984.

F. Davarian, "Channel Simulation to Facilitate Mobile Satellite Communications Research," IEEE Transactions on Communications, Vol. COM-35, January 1987.

F. Davarian et al., "DMSK: A Practical 2400-bps Receiver for the Mobile Satellite Service," JPL Publication 85-51 (MSAT-X Report No. 111), Jet Propulsion Laboratory, Pasadena, California, June 15, 1985.

D. Divsalar, "JPL's Mobile Communication Channel Software Simulator," Proceedings of the Propagation Workshop in Support of MSAT-X, JPL Internal Document D-2208, Jet Propulsion Laboratory, Pasadena, California, January 1985.

D. Divsalar and M. K. Simon, "Trellis Coded Modulation for 4800 to 9600 bps Transmission Over a Fading Satellite Channel," JPL Publication 86-8, Jet Propulsion Laboratory, Pasadena, California, June 1, 1986.

R. F. Emerson, "Clock Synchronization Requirement for Mobile Terminals," JPL Interoffice Memorandum, MSAT-X: 331-85 (JPL internal document), Jet Propulsion Laboratory, Pasadena, California, January 21, 1985.

J. Flanagan et al., "Speech Coding," IEEE Transactions on Communications, Vol. COM-27, April 1979.

Ford Aerospace and Communications Corporation, "Spacecraft Configuration Study for the Second Generation Mobile Satellite System," Final Report, prepared under contract to the Jet Propulsion Laboratory, Pasadena, California, January 1985.

General Electric Corporation (GE), "Mobile Radio Alternative Systems Study--Vol. 3: Satellite/Terrestrial (Hybrid) Systems Concepts," GE Technical Report, prepared for NASA Lewis Research Center, Cleveland, Ohio, June 1983.

Georgia Institute of Technology, "Development, Design, Fabrication, and Evaluation of a Breadboard Speech Compression System at 4800 BPS," ninth quarterly progress report submitted to the Jet Propulsion Laboratory, Pasadena, California, by the School of Engineering, Georgia Institute of Technology, Atlanta, Georgia, June 5, 1987.

C. Hoeber et al., "Passive Intermodulation Product Generation in High Power Communications Satellites," AIAA 11th Communication Satellite Systems Conference, San Diego, California, March 1986.

J. Huang, "L-Band Phased Array Antennas for Mobile Satellite Communications," 37th IEEE Vehicular Technology Conference, Tampa, Florida, June 1987a.

J. Huang, "Production Costs of MSAT Conformal Phased Array Antennas," MSAT-X Quarterly No. 11 (JPL 410-13-11), Jet Propulsion Laboratory, Pasadena, California, July 1987b.

V. Jamnejad, "A Mechanically Steered Monopulse Tracking Antenna for PiFEx: Overview," MSAT-X Quarterly No. 13 (JPL 410-13-13), Jet Propulsion Laboratory, Pasadena, California, January 1988a.

V. Jamnejad, "A Mechanically Steered Monopulse Tracking Antenna for PiFEx: RF System Design," MSAT-X Quarterly No. 13 (JPL 410-13-13), Jet Propulsion Laboratory, Pasadena, California, January 1988b.

T. C. Jedrey and N. E. Lay, "The Implementation of a 4800 bps Trellis Encoded 8-DPSK Modem," MSAT-X Quarterly No. 12 (JPL 410-13-12), Jet Propulsion Laboratory, Pasadena, California, October 1987.

T. C. Jedrey et al., "An All-Digital 8-DPSK TCM Modem for Land Mobile Satellite Communications," International Conference on Acoustics, Speech, and Signal Processing (ICASSP), New York City, New York, April 1988.

Jet Propulsion Laboratory, MSAT-X Quarterly No. 13 (JPL 410-13-13), Special Issue on PiFEx Tower-1 Experiments, Pasadena, California, January 1988.

Jet Propulsion Laboratory, "SYSDOC (MSAT-X Technical Documentation)," JPL Internal Document (in preparation), Pasadena, California.

J. P. McGeehan and A. J. Bateman, "Phase-Locked Transparent Tone-in-Band (TTIB): A New Spectrum Configuration Particularly Suited to the Transmission of Data Over SSB Mobile Radio Networks," IEEE Transactions on Communications, Vol. COM-32, January 1984.

K. Murota and K. Hirade, "GMSK Modulation for Digital Mobile Radio Telephony," IEEE Transactions on Communications, Vol. COM-29, No. 7, July 1981.

F. Naderi (editor), "Land Mobile Satellite Service (LMSS): A Conceptual System Design and Identification of the Critical Technologies," JPL Publication 82-19, Part II, Jet Propulsion Laboratory, Pasadena, California, February 15, 1982.

F. Naderi et al., "NASA's Mobile Satellite Communications Program: Ground and Space Segment Technologies," Proceedings of the 35th Annual International Astronautics Federation Congress, Lausanne, Switzerland, October 1984.

W. Rafferty and D. Divsalar, "Modulation and Coding With Doppler Estimation for Land Mobile Satellite Channels," IEEE International Conference on Communications, Philadelphia, Pennsylvania, June 1988.

RCA Astro Electronics, "Spacecraft (Mobile Satellite) Configuration Design Study," Final Report, prepared under contract to the Jet Propulsion Laboratory, Pasadena, California, June 1985.

Rensselaer Polytechnic Institute (RPI), "A Study of Transparent Tone in Band Modulation for Binary PSK Signalling," Interim Report, Troy, New York, February 1, 1988.

A. Salmasi et al., "Land Mobile Satellite Service (LMSS) Channel Simulator: An End-to-End Hardware Simulation and Study of the LMSS Communications Links," JPL Publication 84-12, Jet Propulsion Laboratory, Pasadena, California, May 1, 1984.

Signatron, Inc., "MSAT-X Networking System Study Final Report--Vol. 1: A Feasibility Assessment of I-AMAP," JPL Document 9950-1198, Jet Propulsion Laboratory, Pasadena, California, June 8, 1985.

M. K. Simon and D. Divsalar, "The Performance of Trellis Coded Multilevel DPSK on a Fading Mobile Satellite Channel," JPL Publication 87-8, Jet Propulsion Laboratory, Pasadena, California, June 1, 1987.

M. K. Simon and D. Divsalar, "Open Loop Frequency Synchronization of MDPSK With Doppler," IEEE International Conference on Communications, Seattle, Washington, June 1988.

M. K. Sue et al., "Second-Generation Mobile Satellite System: A Conceptual Design and Trade-Off Study," JPL Publication 85-58, Jet Propulsion Laboratory, Pasadena, California, June 1, 1985.

TRW, "Mobile Communications Satellite System," TRW Technical Report, Vol. 2, prepared for NASA Lewis Research Center, Cleveland, Ohio, April 11, 1983.

G. Ungerboeck, "Channel Coding With Multilevel/Phase Signals," IEEE Transactions on Information Theory, Vol. IT-28, No. 1, January 1982.

W. Vogel and J. Goldhirsh, "Multipath Measurements at L-Band and UHF in Mountainous Terrain for Land-Mobile Satellite System," Proceedings of NAPEX XI, held on June 19, 1987, at the Virginia Polytechnic Institute and State University, Blacksburg, Virginia, JPL Internal Document D-4647, Jet Propulsion Laboratory, Pasadena, California, August 31, 1987.

W. Vogel and U. S. Hong, "Measurement and Modeling of Land Mobile Satellite Propagation at UHF and L-Band," Proceedings of NAPEX XI, held on June 19, 1987, at the Virginia Polytechnic Institute and State University, Blacksburg, Virginia, JPL Internal Document D-4647, Jet Propulsion Laboratory, Pasadena, California, August 31, 1987.

C. C. Wang and T. Y. Yan, "Performance Analysis of an Optimal File Transfer Protocol for Integrated Mobile Satellite Services," Globecom 1987, Tokyo, Japan, 1987a.

C. C. Wang and T. Y. Yan, "A Simulator for the MSAT-X Request Channel," MSAT-X Quarterly No. 12 (JPL 410-13-12), Jet Propulsion Laboratory, Pasadena, California, October 1987b.

R. Winkelstein, "Antenna Acquisition Timing Using a Noncoherent Signal Detection Process," MSAT-X Quarterly No. 11 (JPL 410-13-11), Jet Propulsion Laboratory, Pasadena, California, July 1987.

K. Woo, "Low Gain and Steerable Vehicle Antennas for Communications With Land Mobile Satellite," IEEE National Telesystems Conference, Galveston, Texas, November 1982.

K. Woo, "Ground Vehicle Antenna Development for Land Mobile Satellite Service," 1984 International Symposium Digest, IEEE AP-S International Symposium, Boston, Massachusetts, June 1984.

T. Y. Yan and F. M. Naderi, "A Proposed Architecture for a Satellite-Based Mobile Communications Network: The Lowest Three Layers," IEEE International Conference on Communications, Toronto, Canada, 1986.

T. Y. Yan and C. C. Wang, "On the Bandwidth Utilization and Capacity of Demand Assigned Protocols for the Integrated Mobile Satellite Services," IEEE Globecom, New Orleans, Louisiana, 1985.